EXPLODING QCD

enumeration and computation of QCD processes

Petros D. Draggiotis
University of Nijmegen, Nijmegen, the Netherlands
petros@sci.kun.nl

Contents

Introduction **1**

1 Introduction **1**

2 Elements of QCD **3**
2.1 Introduction 3
2.2 Quantum ChromoDynamics 3
2.3 Hadron-hadron collisions 9
2.4 The Schwinger-Dyson equation 11
2.5 Large Hadron Collider 13

3 Counting in QCD **15**
3.1 Introduction 15
3.2 Diagram counting 15
3.2.1 Single-field theories 15
3.2.2 QED-like theories 18
3.2.3 Asymptotics by saddle-point methods 21
3.2.4 QCD: a closer look 30
3.3 Process counting 34
3.3.1 Arrangement of the initial states and final states 34
3.3.2 Counting of the final states 36
3.3.3 Gluonic contributions 38
3.3.4 Asymptotic results 40
3.3.5 Distinct amplitudes 43
3.4 Appendix A: Asymptotic form of $H_m(x)$ 49
3.5 Appendix B: Distinct processes revisited 52

4 Colour connections and antennas **55**
4.1 Introduction . . . 55
4.2 Colour generation . . . 56
4.3 Appendix: Colour Traces . . . 60

5 The battle for phase space integration: SARGE versus RAMBO **63**
5.1 Introduction . . . 63
5.2 The adversaries . . . 64
5.2.1 At first there was ...RAMBO . . . 64
5.2.2 SARGE...the Challenger . . . 65
5.3 The Confrontation . . . 68

6 The Recursive Equations for QCD **75**
6.1 Introduction . . . 75
6.2 Building the amplitude . . . 78
6.2.1 Iteration of the SD equation . . . 78
6.2.2 Computational complexity . . . 85
6.2.3 Colour treatment . . . 86
6.2.4 Helicity treatment . . . 89
6.2.5 The Fermi sign function . . . 90
6.3 Appendix: The complete recursion relations . . . 92

7 Jets **93**
7.1 Introduction . . . 93
7.2 Jet kinematics . . . 93
7.3 Hadron scattering . . . 94
7.4 Flavor treatment . . . 102
7.5 Jet production rates . . . 104

Bibliography **113**

List of publications **117**

Chapter 1

Introduction

Perturbation theory is the best tool we have for calculations in QCD. However the increasing accuracy of measurements in modern day colliders, has pushed perturbation theory to the limits of its capacity. The need to know quantities such as cross sections for a large number of particles involved (typically > 6 produced particles) has made analytic calculations increasingly difficult. This is mainly due to the factorial growth of Feynman graphs involved in the calculation (in the order of millions and even billions of graphs).

In the past 20 years many methods have been developed both analytical and numerical to deal with the problem. Analytical methods involve analytic approximations (like the Special Helicities method, `SPHEL`), and methods with influence from supersymmetry and string theories. There are also methods half analytic, half approximate in nature like the `NJETS` algorithm. It is the purpose of this thesis to present a new numerical procedure for the computation of cross section in QCD which is devoid of the use of Feynman graphs. It is based on an iteration of field equations stemming from the Schwinger-Dyson equation for the lowest order (tree-level) in perturbation theory.

In Chapter 2 we present an brief introduction in the workings of the non-abelian $SU(3)$ field theory, commonly refered to as QCD, which is the fundamental language that best describes strong interactions, up to date. We state the underlying principles and use them to describe the collision of hadrons. We also introduce the Schwinger-Dyson equation, on which much of the algorithm for the computation of QCD amplitudes is based. Finally we describe the Large Hadron Collider, the future accelerator that carries the prospect of the discovery of new physics in the new millenium.

Chapter 3 deals with counting. It is an attempt to enumerate the number of

Feynman graphs for a particular scattering process and the enumeration of all of those processes relevant for the production of jets in a collider (numbers that turn out to be enormous). Exact results are presented as well as approximate, in the form of asymptotic estimates by painstakingly analyzing the structure of the Schwinger-Dyson equation for several theories including QCD.

The non-abelian nature of QCD results in a rich color structure of the theory. Attempts to manage and simplify the complicated color structure of amplitudes are presented in Chapter 4. Several ways to simplify the color structure of QCD for numerical purposes are decribed here as well as some exact results.

Numerical computation of cross sections leans heavily on the integration of phase space. Chapter 5 introduces `SARGE`, a new algorithm for Monte Carlo integration of phase space that is more efficient than existing algorithms, due to the fact that it takes into account the non-trivial phase space structure of QCD amplitudes.

The core of the algorithm for numerical computation of amplitudes is in Chapter 6. There we describe the iterative building of the amplitude, along with ways to treat the helicity and the color. Fermi statistics between identical fermions are also introduced using a carefully defined function.

This algorithm is put to the test in the final chapter of this thesis, Chapter 7. Comparisons and plots are presented that prove the usefulness of the numerical procedure. Also a numerical treatment of quark flavors is discussed.

Chapter 2

Elements of QCD

2.1 Introduction

Quantum ChromoDynamics is the theory of strong interactions. Ever since it was formulated, more than 30 years ago, it has been a field of active research, due to the inherent complexity and richness of the theory. With new and powerful colliders at our disposal in the very near future it will be possible to examine various aspects of the theory in high accuracy and this in turn requires tools to study the theory in more detail. This chapter is no more than a reminder of the best things that make QCD a highly successful theory for the description of the hadron world. We will briefly review the gauge symmetry that underlies the Lagrangian formulation and asymptotic freedom (Sect.2.2), hadron collisions (Sect.2.3) and a discussion of the Schwinger-Dyson (Sect.2.4). Finally we end with some facts about the LHC.

2.2 Quantum ChromoDynamics

Abelian gauge symmetry If we consider the Lagrangian for a free electron field $\psi(x)$

$$\mathcal{L}_0 = \bar{\psi}(x)(i\gamma^\mu \partial_\mu - m)\psi(x) \tag{2.1}$$

we can clearly see that it has a *global* $U(1)$ symmetry corresponding to the invariance of the theory under a phase change

$$\begin{aligned} \psi(x) &\rightarrow \psi'(x) = e^{-i\alpha}\psi(x) \\ \bar{\psi}(x) &\rightarrow \bar{\psi}'(x) = e^{i\alpha}\bar{\psi}(x) \end{aligned} \tag{2.2}$$

We want to turn this into a *local* symmetry by making the phase α depend on the space-time position, i.e. $\alpha(x)$. So we construct a theory that is invariant under

$$\begin{aligned} \psi(x) &\rightarrow \psi'(x) = e^{-i\alpha(x)}\psi(x) \\ \bar{\psi}(x) &\rightarrow \bar{\psi}'(x) = e^{i\alpha(x)}\bar{\psi}(x) \end{aligned} \tag{2.3}$$

The complication now is that the transformed derivative term in (2.1)

$$\begin{aligned} &\bar{\psi}(x)\partial_\mu\psi(x) \rightarrow \\ &\bar{\psi}'(x)\partial_\mu\psi'(x) = \bar{\psi}(x)\partial_\mu\psi(x) - i\bar{\psi}(x)\partial_\mu\alpha(x)\psi(x) \end{aligned} \tag{2.4}$$

spoils the invariance because the second term. We need to define a 'new' derivative, a *gauge-covariant derivative* D_μ to replace ∂_μ, so that

$$D_\mu\psi(x) \rightarrow [D_\mu\psi(x)]' = e^{-i\alpha(x)}D_\mu\psi(x) \tag{2.5}$$

This can be done by defining

$$D_\mu\psi = (\partial_\mu + ieA_\mu)\psi \tag{2.6}$$

where e is a free parameter which will eventually be identified with the electromagnetic coupling constant. We have also introduces a new field $A_\mu(x)$. The Langrangian now becomes

$$\mathcal{L}_0 = \bar{\psi}(x)i\gamma^\mu(\partial_\mu + ieA_\mu(x))\psi(x) - m\bar{\psi}(x)\psi(x) \tag{2.7}$$

The new field $A_\mu(x)$ has the transformation

$$A_\mu(x) \rightarrow A'_\mu(x) = A_\mu(x) + \frac{1}{e}\partial_\mu\alpha(x) \tag{2.8}$$

To make the gauge field a true dynamical variable we need to add to the Lagrangian a kinetic term involving its' derivatives. Such a term that is renormalizable (dimension equal to four) and invariant under the local symmetry is

$$\mathcal{L}_A = -\frac{1}{4}F^{\mu\nu}F_{\mu\nu}, \quad F_{\mu\nu} = \partial_\mu A_\nu - \partial_\nu A_\mu \tag{2.9}$$

Combining everything together we arrive at the *QED* Langrangian

$$\mathcal{L}_{QED} = \bar{\psi}(x)i\gamma^\mu D_\mu\psi(x) - m\bar{\psi}(x)\psi(x) - \frac{1}{4}F^{\mu\nu}F_{\mu\nu} \tag{2.10}$$

Non-abelian gauge symmetry The symmetry (2.3) considered above is called *Abelian* because $U(1)$ is an abelian group. We can generalize the previous discussion to the case where non-abelian groups are concerned. In particular the symmetry can be extended to the case of the $SU(N)$ group. Suppose we now have a number of fermion fileds, $\psi_i,\ i = 1, \ldots, p$, interacting with a number of vector fields $A^\mu_a,\ a = 1, \ldots, r$. We shall denote the spinor fields collectively under a single column $\boldsymbol{\psi}$. We generalize the transformation (2.3) to

$$\boldsymbol{\psi}(x) \to \boldsymbol{\psi}'(x) = e^{-ig\boldsymbol{T}\cdot\Lambda(x)}\boldsymbol{\psi}(x), \quad \boldsymbol{T}\cdot\Lambda(x) = \sum_a \boldsymbol{T}_a\Lambda_a(x) \tag{2.11}$$

where $\boldsymbol{T}_a$ are $p\times p$ matrices, that are the generators of $SU(N)$ and act on the column vector $\boldsymbol{\psi}(x)$, $\Lambda_a(x)$ are arbitrary functions of x and g is eventually going to be the coupling constant. The $SU(N)$ generators satisfy the commutation relations

$$[T_a, T_b] = if_{abc}T_c \tag{2.12}$$

where f_{abc} are the structure constants of $SU(N)$. By analogy to (2.6) we define a covariant derivative

$$D^\mu\boldsymbol{\psi} = \left(\partial^\mu + ig\boldsymbol{T}\cdot\boldsymbol{A}^\mu\right)\boldsymbol{\psi} \tag{2.13}$$

The vector fields $\boldsymbol{A}^\mu$ transform as

$$A^\mu_a \to A^\mu_a + \partial^\mu\Lambda_a + gf_{abc}\Lambda_b A^\mu_c \tag{2.14}$$

A gauge invariant Lagrangian for the gauge fields is constructed in the same way as in the QED case

$$\begin{aligned}\mathcal{L}_A &= -\frac{1}{4}F^{\mu\nu}_a F_{\mu\nu\,a}\\ F^{\mu\nu}_a &= \partial^\mu A^\nu_a - \partial^\nu A^\mu_a - gf_{abc}A^\mu_b A^\nu_c\end{aligned} \tag{2.15}$$

Putting it all together, the $SU(N)$ gauge invariant Lagrangian is

$$\mathcal{L}_{SU(N)} = \bar{\psi}(x)(i\gamma^\mu D_\mu - m)\psi(x) - \frac{1}{4}F^{\mu\nu}_a F_{\mu\nu\,a} \tag{2.16}$$

Chromodynamics is the $SU(3)$ nonabelian gauge theory of colour charge. The fermions which carry colour charge are the *quarks* $\psi_A,\ A = 1, 2, 3$ and they come in six flavours u, d, s, c, b, t. The gauge bosons, which also carry colour, are the *gluons*

$A^\mu_a,\ a = 1, \ldots, 8$. The group $SU(3)$ has an infinite number of irreducible respresentations. Quarks, antiquarks and gluons are assigned to the representations $\mathbf{3}, \mathbf{3}^*, \mathbf{8}$ respectively. The group generators T_a of the previous section, are for $SU(3)$ $T_a = \lambda_a/2$. For the fundamental representation they have the matrix representations

$$\lambda_1 = \begin{pmatrix} 0 & 1 & 0 \\ 1 & 0 & 1 \\ 0 & 0 & 0 \end{pmatrix} \quad \lambda_2 = \begin{pmatrix} 0 & -i & 0 \\ i & 0 & 1 \\ 0 & 0 & 0 \end{pmatrix} \quad \lambda_3 = \begin{pmatrix} 1 & 0 & 0 \\ 0 & -1 & 0 \\ 0 & 0 & 0 \end{pmatrix}$$
$$\lambda_4 = \begin{pmatrix} 0 & 0 & 1 \\ 0 & 0 & 0 \\ 1 & 0 & 0 \end{pmatrix} \quad \lambda_5 = \begin{pmatrix} 0 & 0 & -i \\ 0 & 0 & 0 \\ i & 0 & 0 \end{pmatrix} \quad \lambda_6 = \begin{pmatrix} 0 & 0 & 0 \\ 0 & 0 & 1 \\ 0 & 1 & 0 \end{pmatrix}$$
$$\lambda_7 = \begin{pmatrix} 0 & 0 & 0 \\ 0 & 0 & -i \\ 0 & i & 0 \end{pmatrix} \quad \lambda_8 = \frac{1}{\sqrt{3}} \begin{pmatrix} 1 & 0 & 0 \\ 0 & 1 & 0 \\ 0 & 0 & -2 \end{pmatrix}$$

These are called the Gelmann matrices and are normalized as

$$Tr\{t^a t^b\} = \frac{1}{2}\delta^{ab} \tag{2.17}$$

They are also *traceless*. The Langrangian for QCD is (2.16) but once we try to quantize it we start to run into trouble. To see the problem lets consider the Langrangian without fermions

$$\mathcal{L} = -\frac{1}{4} F^{\mu\nu}_a F_{\mu\nu\ a} \tag{2.18}$$

We try to quantize it in the canonical formalism, so we construct canonical momenta Π^a_μ conjugate to the fields A^a_μ, regard them as operators and set up canonical commutation relations between A^a_μ and Π^a_μ. The momentum conjugate to A^a_μ is

$$\Pi^a_\mu = \frac{\partial \mathcal{L}}{\partial \dot{A}^{\mu a}} = -F^a_{0\mu} \tag{2.19}$$

where $\dot{A}^{\mu a} = \partial_0 A^{\mu a}$. The canonical commutation relations would then be

$$[A^a_\mu(x), \Pi^a_\nu(y)]_{x_0=y_0} = i\delta^{ab} g_{\mu\nu} \delta^3(\mathbf{x} - \mathbf{y}) \tag{2.20}$$

Setting $\mu = \nu = 0$ and $a = b = 1$ we get $[A^1_0(x), \Pi^1_0(y)]_{x_0=y_0} = i\delta^3(\mathbf{x} - \mathbf{y})$. On the other hand from (2.19) we see that $\Pi^a_0(y) = 0$. There is an inconsistency with the commutation relation and this shows that the simple-minded canonical quantization

does not work for gauge theories. The difficulty lies in the fact that in the gauge invariant Langrangian, the field A^a_μ has the freedom of gauge tranformations (2.14). One way of getting rid of the difficulty is to eliminate the gauge freedom by putting constraints on the field. One covariant constraint would be the Lorentz condition $\partial^\mu A^a_\mu = 0$. By this constraint the arbitrariness of the field due to gauge freedom is elliminated. We can add this condition in the Langrangian by using a Langrange multiplier

$$\lambda(\partial^\mu A^a_\mu)^2 \tag{2.21}$$

It is customary to write $\lambda = -1/2\xi$ and the QCD Langrangian now is

$$\mathcal{L}_{QCD} = \bar{\psi}(x)(i\gamma^\mu D_\mu - m)\psi(x) - \frac{1}{4}F^{\mu\nu}_a F_{\mu\nu\ a} - \frac{1}{2\xi}(\partial^\mu A^a_\mu)^2 \tag{2.22}$$

The new term added is called the *gauge fixing* term. Physical predictions based on this Langrangian should be independent of ξ. Two popular choices for the gauge fixing constant are $\xi = 1$ (Feynman gauge) and $\xi \to 0$ (Landau gauge). From this Langrangian we can read off the expressions for the gluon and fermion propagators and the couplings between the fields. For the gluon 3-vertex and 4-vertex in particular we have:

$$V^{\mu\nu\lambda}(P, p_1, p_2) = f^{abc}[g^{\mu\nu}(P - p_1)^\lambda + g^{\nu\lambda}(p_1 - p_2)^\mu + g^{\lambda\mu}(p_2 - P)^\nu] \tag{2.23}$$

$$\begin{aligned} G^{\mu\nu\lambda\rho}_{abcd} &= f^{xac}f^{xbd}\left(g^{\mu\nu}g^{\lambda\rho} - g^{\mu\rho}g^{\nu\lambda}\right) \\ &+ f^{xad}f^{xbc}\left(g^{\mu\nu}g^{\lambda\rho} - g^{\mu\lambda}g^{\nu\rho}\right) \\ &+ f^{xab}f^{xcd}\left(g^{\mu\lambda}g^{\nu\rho} - g^{\mu\rho}g^{\nu\lambda}\right) \end{aligned} \tag{2.24}$$

Running of the strong coupling constant When computing observables to a certain degree of accuracy, we must include in the calculation not only the lowest order in the coupling constant in the pertubation series but also higher orders in $\alpha_s = g^2/4\pi$. This is done by including loop diagrams in addition to the tree calculation. But usually loop diagrams are inherently infinite and a 'regularization' procedure must be followed so that meaningful quantities can be obtained. This process of *renormalization*, as it is called, in not only relevant when we encounter infinite-valued diagrams. In fact renormalization is always necessary since the parameters that appear in the classical Langrangian- denoted as *bare* parameters- are meaningful only to a completely free theory. Intaractions will always modify the values of these parameters and after all the full interacting theory is what is measured

in the laboratory. The coupling constant of QCD, being such a parameter, will be modified by interactions, and this introduces a dependence of α_s on the scale, that is the energy Q^2 at which it is measured in an experiment. This dependence can be made explicit by studying loop corrections to the coupling of quarks to gluons, and gluons to themselves. To the lowest order the *running* of the coupling constant, that is the dependence on the scale, is [Ellis et al., 1996]:

$$\alpha_s(Q^2) = \frac{12\pi}{(33 - 2n_f)\log(Q^2/\Lambda^2)} \tag{2.25}$$

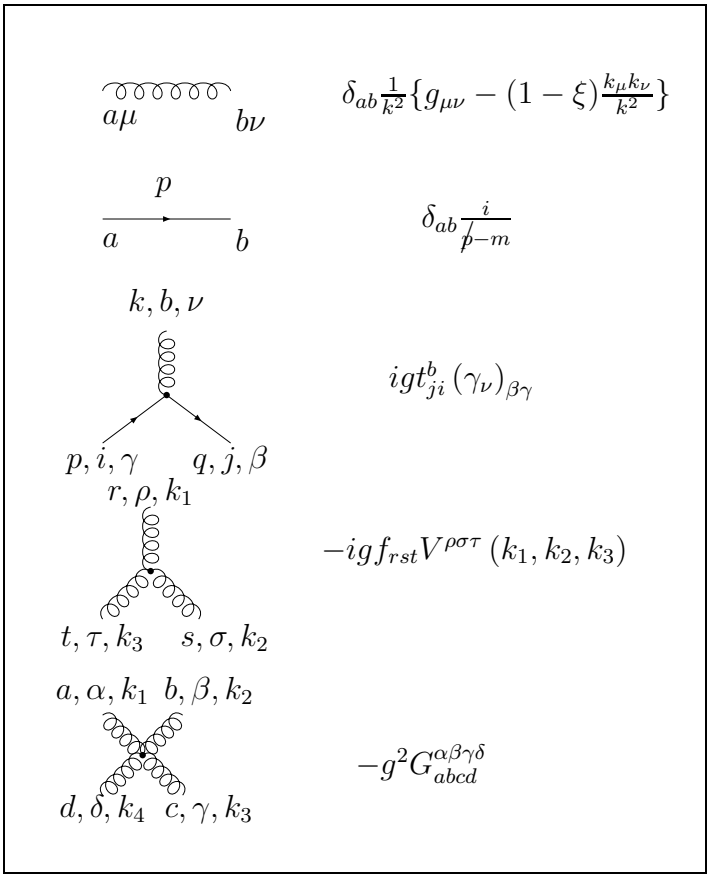

Propagators and couplings of the fields in QCD

where n_f is the number of flavours. By looking at the running of α_s we see that it has a remarkable property: the coupling constant decreases with increasing energy. This property is called *asymptotic freedom* and is of great important in QCD. It allows us to continue to use perturbation theory at high energies because the coupling becomes

'weak' and quarks and gluons behave like almost free particles. When the energy is decreasing the coupling becomes stronger, quarks and gluons tend to bind inside hadrons and perturbation theory is no longer applicable. The scale at which this breakdown of perturbation occurs is indicated by Λ. The behaviour of QCD at high energies is totally different from QED. The running of the electromagnetic coupling $\alpha = e^2/4\pi$ would be:

$$\alpha(Q^2) = \frac{3\pi}{\log(\Lambda^2/Q^2)} \tag{2.26}$$

At high energy this becomes stronger, which indicates the infinite range of electromagnetic forces.

2.3 Hadron-hadron collisions

The high energy interactions of hadrons are described by the QCD *improved parton model* [**?**]. In this model a hard scattering process between two hadrons is the result of an interaction between the quarks and the gluons that are the constituents of the incoming hadrons. The process can be viewed graphically in Fig.2.1 Two partons interact with momentum fractions x_1 and x_2 from the initial hadron momenta P_1, P_2. A parton of virtuality equal to the collision energy $\sqrt{\hat{s}}$ is formed which then fluctuates into quarks, antiquarks and gluons. By the uncertainty principle, this fluctuation occurs at a distance scale of $1/Q$, $Q = \sqrt{\hat{s}}$, and if Q is large the production rate for this short-distance process is predicted by perturbation theory. This is because at the energy scale Q the force that controls the interaction between partons is propotional to $\alpha_s(s)$, therefore it is weak and perturbation theory is valid [Ellis et al., 1996].

Subsequently other partons are radiated and quarks and gluons form themselves into hadrons like $D^0, K^+, K^0, \pi^+, \pi^-$ etc. This process is called *hadronization*. Hadronization occurs at a much later time caracterized by $1/\Lambda$ where Λ is the scale in α_s, (2.25) i.e the scale at which the coupling becomes strong. By now we have entered the realm of non-pertubative effects. But so much time has passed since the original parton creation that the hadronizaton phase cannot significantly affect the total hadron production rate.

The cross section for this scattering process can be written as

$$\sigma(s) = \sum_{ij} \int_0^1 dx_1 dx_2 \int d\Phi f_i(x_1) f_j(x_2) \frac{d\hat{\sigma}_{ij}}{d\Phi}(x_1, x_2, \hat{s}) \tag{2.27}$$

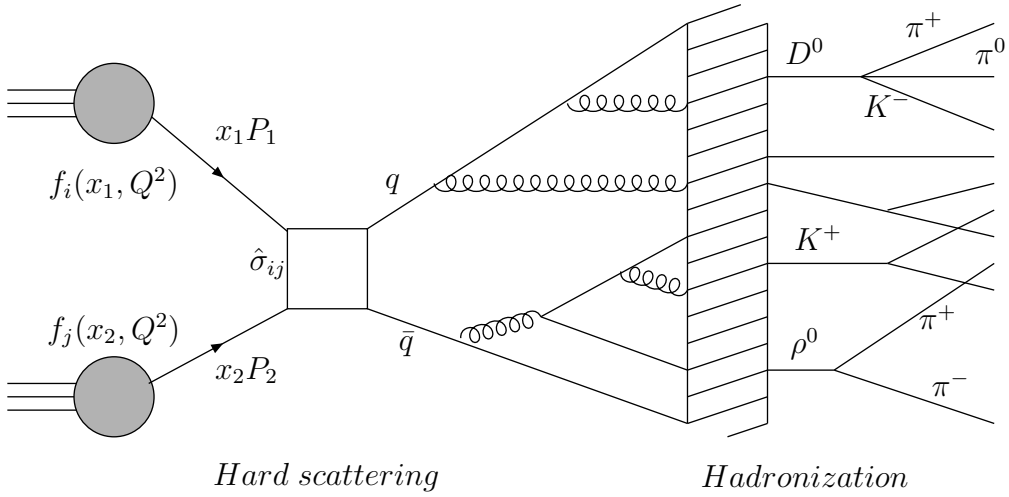

Figure 2.1: Hadron-hadron collision, showing the hard scattering and the hadronization phase.

The momenta of the partons which participate in the hard interaction are $p_1 = x_1P_1$ and $p_2 = x_2P_2$. The functions $f_i(x)$ represent the density of quarks and gluons carrying a fraction x of the hadron momentum and are defined at a factorization scale μ. The short distance differential cross section between partons of types i and j is denoted by $\frac{d\hat{\sigma}_{ij}}{d\Phi}$. Averaging (summation) over the degrees of freedom (helicity, colour etc.) of the initial (final) states is implied. $d\Phi$ denotes the phase space element. The sum is over all partonic subprocesses. For a two-to-two parton subprocess, for example, it includes the processes in the following table.

The hard scattering part of hadron collisions is the part that we are dealing with in this work. In later chapters we will describe an algorithm that allows us to do calculations with parton subprocesses that include not only the two particle final state shown in Table 2.1 but an arbitrary number of final state partons. Analytic answers exist for up to four final partons but are quite hard to obtain and even more so for multiparton final state because the number of Feynman graphs becomes extremely large.

The hadronization phase is an active field of research. Since this belongs to the nonperturbative realm of QCD there is still a limited understanding of the process. There exist models that describe hadronization, with a varying degree of success, like the *independent fragmentation model*, the *string model* and the *cluster model* [Ellis et al., 1996] and several software codes like `HERWIG` [Corcella and et al., 2001].

Process	$\sum\|M\|^2/g^4$
$qq' \to qq'$	$\frac{4}{9}\frac{s^2+u^2}{t^2}$
$q\bar{q} \to q'\bar{q}'$	$\frac{4}{9}\frac{t^2+u^2}{s^2}$
$q\bar{q} \to q\bar{q}$	$\frac{4}{9}\left(\frac{s^2+u^2}{t^2}+\frac{t^2+u^2}{s^2}\right)-\frac{8}{27}\frac{u^2}{st}$
$q\bar{q} \to gg$	$\frac{32}{27}\frac{t^2+u^2}{tu}-\frac{8}{3}\frac{t^2+u^2}{s^2}$
$gg \to q\bar{q}$	$\frac{1}{6}\frac{t^2+u^2}{ty}-\frac{3}{8}\frac{t^2+u^2}{s^2}$
$gq \to gq$	$-\frac{4}{9}\frac{s^2+u^2}{su}+\frac{u^2+s^2}{t^2}$
$gg \to gg$	$\frac{9}{2}\left(3-\frac{tu}{s^2}-\frac{su}{t^2}-\frac{st}{u^2}\right)$

Table 2.1: The matrix element squared for massless partons $p_1 + p_2 \to p_3 + p_4$. The notation is $s = (p_1 + p_2)^2$, $t = (p_1 - p_3)^2$, $u = (p_1 - p_4)^2$. The spin and colour degrees of freedom are averaged(summed) over initial(final) states [Ellis et al., 1996]

Hadronization is outside the scope of this work.

2.4 The Schwinger-Dyson equation

Using different techniques, Schwinger and Dyson ([Dyson, 1949] [Schwinger, 1951]) derived independently functional equations for the Green functions as a consequence of the field equations, i.e. the specific structure of the dynamical Lagrangian. When properly renormalized these equations maybe used as an alternative tool to perturbation theory. A closer look reveals that the system involves an infinite hierarchy of equations. For simplicity we take a Euclidean field theory in zero dimensions, i.e. we consider a universe with only one point ϕ [Kleiss, 2000]. We denote the action of this theory with $S(\phi)$. All the information about this model is contained in the momenta of the distribution, or the *Green's functions*:

$$G_p \equiv < \phi^p >= N \int d\phi \; \phi^p e^{-S(\phi)} \tag{2.28}$$

where N is the normalisation. We can combine all the Green's functions in one object, namely the generating function, as follows:

$$Z(J) = \sum_{p \geq 0} G_p \frac{J^p}{p!} = N \int d\phi \; e^{-(S(\phi) - J\phi)} \tag{2.29}$$

This is the so called path integral of the theory, which in our simple case is just an ordinary integral in one variable. We can derive a differential equation for $Z(J)$ by

using the standard identity that the integral of a derivative is zero:

$$\int d\phi \frac{d}{d\phi} \equiv 0 \tag{2.30}$$

If we act this identity on $Z(J)$ we get:

$$\begin{aligned} 0 &= \int d\phi \frac{d}{d\phi}\, e^{-S(\phi)+J\phi} \\ &= \int d\phi \{-S'(\phi) + J\}\, e^{-S(\phi)+J\phi} \end{aligned} \tag{2.31}$$

where the prime denotes differentiation with respect to the argument. This can be rewritten as:

$$S'\left(\frac{d}{dJ}\right) Z(J) = JZ(J) \tag{2.32}$$

This is called the *Schwinger-Dyson equation* and it allows us to construct the whole set of connected diagrams. For example for a theory with a $\phi^3 + \phi^4$ interaction,

$$S(\phi) = \frac{1}{2}\mu\phi^2 + \frac{1}{3!}\lambda_3\phi^3 + \frac{1}{4!}\lambda_4\phi^4 \tag{2.33}$$

the equations is:

$$\mu Z'(J) + \frac{1}{2}\lambda_3 Z''(J) + \frac{1}{6}\lambda_4 Z'''(J) = JZ(J) \tag{2.34}$$

When we return to the 4-dimensional world the SD equation is no longer a 'simple' differential equation but becomes a functional equation since the fields are now operators. The generating function for QCD is (neglecting ghost terms)

$$Z[J,\eta,\bar{\eta}] = \int [DA][D\psi][D\bar{\psi}] \exp\{iS + \int d^4x \left(A^a_\mu J^{a\,\mu} + \bar{\psi}\eta + \bar{\eta}\psi\right)\} \tag{2.35}$$

where $S(A,\psi,\bar{\psi}) = \int d^4x \mathcal{L}$ is the QCD action and $J,\eta,\bar{\eta}$ are the source terms for the gauge boson and the fermion fields respectively. The SD equation is now

$$\{\frac{\delta}{\delta A^{\mu a}(x)} S(\frac{1}{i\delta J}, \frac{1}{i\delta\bar{\eta}}, -\frac{1}{i\delta\eta}) + J^a_\mu(x)\} Z[J,\eta,\bar{\eta}] = 0 \tag{2.36}$$

for the gluon field, with similar equations for the fermion fields.

LHC General Parameters	
Energy at collision	7 TeV
Dipole field at 7 TeV	8.33 Tesla
Luminosity	$10^{34} cm^{-2} s^{-1}$
Luminosity lifetime	10 h
Number of particles per bunch	1.1 10^{11}
Circumference	27 Km

Table 2.2: Design performance parameters of LHC. Taken from *http://lhc-new-homepage.web.cern.ch /lhc-new-homepage/*

2.5 Large Hadron Collider

The CERN Large Hadron Collider (LHC) is presently under construction and will start operation in 2007. This machine will be installed in the existing LEP tunnel and will provide pp collisions and heavy-ion collisions (e.g. $Pb - Pb$). When running in the pp mode, the CoM energy will be 14 TeV, which is a factor of about seven larger than at the present machine with the highest CoM energy (the Tevatron collider at Fermilab) and the design luminosity will be $10^{34} cm^{-2} s^{-1}$, which is a factor of 100 larger than at previous machines (LEP, Tevatron). Such luminosity and CoM energy will allow searches for new particles to be performed up to masses of ~ 5 TeV [Gianotti, 1999].

The LHC is an unprecedented project, not only in terms of performance, but also in terms of cost, complexity and size of the experiments and human effort (more than 4000 physicists are involved in the project). It will be dedicated to the study of some important physics which are briefly described below.

- *Understand the origin of particle masses* Although the success of the Standard Model (SM) has been tremendous with precision at the level of 0.1 % by the LEP, SLC and Tevatron experiments, some aspects of the theory are still obscure. In particular the origin of the masses and the mass hierarchy of leptons, quarks and gauge bosons is not yet understood. Moreover, the Higgs boson, the scalar particle that is believed to give masses to the particles through the Symmetry Breaking mechanism still eludes experimental verification. The current lower limit for the mass of the Higgs is ~ 120 GeV.

- *Physics beyond the SM* There are several reasons to believe that the SM is not the final word to an ultimate theory of interactions. First of all, as already

mentioned, the Higgs Mechanism has little physical justification and radiative corrections to the Higgs mass lead to infinities. There are hints the coupling constants of electromagnetic, weak and strong interactions unify into a single coupling constant at an energy scale of $\sim 10^{19}$ GeV. This leads one to believe in new physics beyond the realm of SM. There are indications of these from Grand Unified Theories (GUTs) and Supersymmetry, which predict new physics at an energy scale ($\sim$ TeV) accesible to the LHC.

- *Answers to open questions* There are many issues that LHC could help clarify. Are quarks elementary particles? Are there additional families of quarks, leptons and gauge bosons? What is the origin of asymmetry between matter and antimatter in the universe? What is the origin of QCD confinement?

- *Precision measurements* Any observed deviation from the SM is a possible signal for new physics, so measuring properties of particles with the highest possible precision is an important issue.

A brief description of LHC is shown in the table 2.2 The following experiments are planned to attend the LHC:

- ALICE This is a general-purpose heavy-ion detector designed to study the physics of strongly interacting matter and the quark-gluon plasma in nucleus-nucleus collisions

- ATLAS This is a general-purpose experiment for recording proton-proton collisions

- CMS is a general purpose proton-proton detector designed to run at the highest luminosity at the LHC

- LHCb This detector is designed to study CP violation and other rare phenomena in decays of hadrons with heavy flavours, in particular B mesons

Chapter 3

Counting in QCD

3.1 Introduction

With the growing complexity of scattering amplitudes that are becoming amenable to calculation, especially as we probe higher and higher energies, the question of the number of contributiong Feynman graphs becomes of interest in its own right. As we will explore in this chapter, even the enumeration of tree graphs is a non-trivial question. The number of diagrams of QCD amplitudes increases very rapidly with the number of external legs. In [Argyres et al., 1992] the number of graphs for theories with a single, self-interacting scalar field was studied, and a method derived to estimate the asymptotic number of tree graphs for the $1 \to n$ amplitude for large n was described, improving on earlier estimates [Kuijf, 1991, Voloshin, 1992]. Another issue then arises, that of summing the contributions of all possible QCD processes to a given multi-jet final state. In this chapter we shall address these questions. We start at section 2 with counting the number of graphs and estimating asymptotic results for large number of external legs and for different theories, from the simple scalar field one, to the full QCD case. In section 3 we move on to determine exact and asymptotic results for the number of processes, given the number of jet products.

3.2 Diagram counting

3.2.1 Single-field theories

The enumeration of tree diagrams in a given theory is simpler than that of general diagrams with loops, in the sense that for tree diagrams symmetry factors do not

occur: indeed, at present the counting of topologically distinct higher-order diagrams appears almost hopeless. Since diagrams can be counted by simply replacing all propagators and vertices by unity, the counting problem becomes equivalent to solving the Schwinger-Dyson (SD) equation for a simple zero-dimensional Euclidean theory. To set the stage, let us consider such a theory, with a single self-interacting scalar field φ and a Euclidean action

$$S(\varphi) = \frac{1}{2}\varphi^2 - V(\phi) \quad , \quad V(\varphi) = \frac{1}{3!}\varphi^3 + \frac{1}{4!}\varphi^4 + \cdots \tag{3.1}$$

where $V(\phi)$ collects all higher-point interactions according to whether they are present in the theory or not. Note that the minus sign and the factorials in front of the interaction terms ensure that all vertices are precisely unity. Let us denote by $a(n)$ the number of tree diagrams entering in the $1 \to n$ amplitude, and by $\phi(z)$ its generating function:

$$\phi(z) \equiv \sum_{n\geq 1} \frac{z^n}{n!} a(n) \quad . \tag{3.2}$$

This generating function, then, obeys the algebraic Schwinger-Dyson equation

$$\phi(z) = z + V'(\phi(z)) \quad , \tag{3.3}$$

where double-counting is avoided by the factorials in front of the terms in the interaction potential: for instance, in pure φ^3 theory the Schwinger-Dyson equation, translated back in terms of $a(n)$, reads

$$a(n) = \delta_{n,1} + \frac{1}{2} \sum_{n_{1,2}\geq 1} \frac{n!}{n_1! n_2!} a(n_1) a(n_2) \delta_{n,n_1+n_2} \quad . \tag{3.4}$$

Obtaining the exact number of graphs for given n is simply a matter of algebraically iterating Eq.(3.3) up to the appropriate order in powers of z, which is a trivial task for any halfway decent computer algebra system. We show the number of diagrams for various number of external lines N and for ϕ^3 and $\phi^3 + \phi^4$ interactions, in the table.

For the asymptotic result, however, we have to employ more. The asymptotic form of $a(n)$ is of course given by the singularity structure of $\phi(z)$ as a function of z. Now, $\phi(z)$ cannot have poles for finite z if $V(\varphi)$ is a finite polynomial, since the SD equation cannot then be satisfied. The singularities must therefore be branch points. Let us write z as a function of ϕ:

$$z = F(\phi) \equiv \phi - V'(\phi) \quad . \tag{3.5}$$

N	ϕ^3	$\phi^3+\phi^4$
4	3	4
5	15	25
6	105	220
7	945	2,485
8	10,395	34,300
12	654,729,075	5,348,843,500
13	13,749,310,575	140,880,765,025
14	316,234,143,225	4,063,875,715,900

We now look for that value of ϕ (and z) for which the definition of $\phi(z)$ becomes ambiguous, *i.e.* where a branch cut starts. Such points ϕ_0 will be situated where $d\phi/dz$ diverges, or

$$\frac{dF(\phi)}{d\phi} = 0 \quad \text{at } \phi = \phi_0 \ . \tag{3.6}$$

To each of these roots corresponds a value $z_0 = F(\phi_0)$, and that z_0 which lies closest to the origin determines the leading asymptotic behaviour. We can then make an expansion around the appropriate value of ϕ_0:

$$z = F(\phi_0) + \frac{1}{2}F''(\phi_0)(\phi-\phi_0)^2 + \cdots \ , \tag{3.7}$$

and we can read off the approximate form of $\phi(z)$ in the neighbourhood of the singular point:

$$\phi(z) \sim \phi_0 - \left(1 - \frac{z}{F(\phi_0)}\right)^{1/2} \sqrt{\frac{-2F(\phi_0)}{F''(\phi_0)}}. \tag{3.8}$$

The expansion of the square-root form,

$$\sqrt{1-x} = 1 - \sum_{n\geq 1} \frac{(2n-2)!x^n}{n!(n-1)!2^{2n-1}} \sim \sum_n \frac{x^n}{n^{3/2}\sqrt{4\pi}} \ , \tag{3.9}$$

where we indicate its asymptotic form, then tells us that the asymptotic form of $a(n)$ is given by

$$a(n) \sim \frac{n!}{n^{3/2}} C^n D \quad , \quad C = \frac{1}{F(\phi_0)} \quad , \quad D = \sqrt{\frac{-F(\phi_0)}{2\pi F''(\phi_0)}} \ . \tag{3.10}$$

Two points are in order here. If it should happen that F'' vanishes together with F', we might have to look for a cube-root branch point rather than a square-root one: we have never yet encountered this case. Secondly, it is possible, as for instance in pure φ^4 theory, that there are several z_0 values equally far from zero. In that case we have to add the asymptotic contributions from every such point, and this is the mechanism by which in pure φ^4 theory even values of n become forbidden.

Some results are collected in the the following table, for theories in which all interactions from φ^3 up to and including φ^M are present.

M	C	D
3	2.00000	.282095
4	2.50804	.191409
5	2.57845	.178231
6	2.58755	.175794
7	2.58859	.175393
8	2.58868	.175336
9	2.58869	.175331
∞	2.58869	.175329

The last theory, with potential $V(\varphi) = \exp(\varphi) - \varphi - 1$, is interesting in that it establishes an upper bound on the number of tree graphs in any single-field theory. Equivalently, it gives the number of graphs arising from an effective action after tadpole renormalization.

3.2.2 QED-like theories

We now turn to the more complicated case where fermionic fields are also present: we then have fermions, antifermions, and bosons. The simplest case is that of QED with a single fermion type. The action is then given by

$$S(\varphi, \chi, \bar{\chi}) = \frac{1}{2}\varphi^2 + \bar{\chi}\chi - \bar{\chi}\chi\varphi \ , \tag{3.11}$$

where χ denotes the fermion and $\bar{\chi}$ the antifermion field. We now have three amplitudes, depending on the incoming line, and we have the following generating func-

tions:

$$\begin{aligned}
\phi(z,x,\bar{x}) &= \sum_{n_{0,1,2}\geq 0} \frac{z^{n_0}x^{n_1}\bar{x}^{n_2}}{n_0!n_1!n_2!} a(\varphi \to n_0\varphi, n_1\chi, n_2\bar{\chi}) \quad , \\
\psi(z,x,\bar{x}) &= \sum_{n_{0,1,2}\geq 0} \frac{z^{n_0}x^{n_1}\bar{x}^{n_2}}{n_0!n_1!n_2!} a(\chi \to n_0\varphi, n_1\chi, n_2\bar{\chi}) \quad , \\
\bar{\psi}(z,x,\bar{x}) &= \sum_{n_{0,1,2}\geq 0} \frac{z^{n_0}x^{n_1}\bar{x}^{n_2}}{n_0!n_1!n_2!} a(\bar{\chi} \to n_0\varphi, n_1\chi, n_2\bar{\chi}) \quad ,
\end{aligned} \tag{3.12}$$

and coupled SD equations:

$$\phi = z + \psi\bar{\psi} \quad , \quad \psi = x + \phi\psi \quad , \quad \bar{\psi} = \bar{x} + \phi\bar{\psi} \quad . \tag{3.13}$$

These can be readily expressed in ϕ alone:

$$\psi = \frac{x}{1-\phi} \quad , \quad \bar{\psi} = \frac{\bar{x}}{1-\phi} \quad , \tag{3.14}$$

and

$$\phi = z + \frac{\xi}{(1-\phi)^2} \quad , \quad \xi = x\bar{x} \quad . \tag{3.15}$$

The combination ξ implies, of course, conservation of fermion number, and we see that it suffices to determine ϕ as a function of z and ξ, except for processes without any external bosons. Again, combined expansion in powers of ξ and z is trivial by iterating Eq.(3.15). Some results are shown in the table that follows where N is the number of external legs, ℓ is the number of fermion pairs. Note that we take into account ony one fermion type.

ℓ	N=6	N=7	N=8	N=9	N=10	N=11	N=12	N=13
1	24	120	720	5,040	40,320	362,880	3,628,800	39,916,800
2	40	240	1,680	13,440	120,960	1,209,600	13,305,600	159,667,200
3	36	252	2,016	18,144	181,440	1,995,840	23,950,080	311,351,040
4	–	–	1,728	17,280	190,080	2,280,960	29,652,480	415,134,720
5	–	–	–	–	158,400	2,059,200	28,828,800	432,432,000
6	–	–	–	–	–	–	23,587,200	377,395,200

For the asymptotic behaviour we now have to study a two-variable problem. We do this by momentarily keeping z fixed, and considering the singularity of ϕ in terms of ξ:

$$\xi = F_z(\phi) = (1-\phi)^2(\phi - z) \quad , \quad F_z'(\phi) = (1-\phi)(1+2z-3\phi) \quad . \tag{3.16}$$

The singularity, parametrized by z, must be again of branch-point type, and is situated at

$$\phi_0 = \frac{1+2z}{3} \quad , \quad F_z(\phi_0) = \frac{4}{27}(1-z)^3 \quad , \quad F''_z(\phi_0) = -2(1-z) \ , \tag{3.17}$$

so that the asymptotic behaviour for high powers of ξ is given by

$$\phi_z(\xi) \sim \sum_n \frac{1}{n^{3/2}\sqrt{27\pi}} \frac{(27/4)^n}{(1-z)^{3n-1}} \xi^n \ . \tag{3.18}$$

This immediately gives the behaviour with powers of z as well. Expanding the form $(1-z)^{-3n+1}$,

$$\phi(\xi, z) \sim \sum_{n,k} \xi^n z^k \frac{(27/4)^n}{\sqrt{27\pi}} \frac{(3n-2+k)!}{k!(3n-2)!n^{3/2}} \ , \tag{3.19}$$

gives for the number of graphs, by comparing with (3.12)

$$a(\varphi \to k\varphi, n\chi\bar{\chi}) \sim \frac{(27/4)^n}{\sqrt{27\pi}} \frac{(3n-2+k)!n!^2}{(3n-2)!n^{3/2}} \ . \tag{3.20}$$

The goodness of this asymptotic result, when compared with the exact enumeration, does not depend on k but only on n: the exact result is 1.3644356 times the approximate one for $n = 1$, which ratio decreases to 1.0244771 for $n = 10$ and to 1.0120180 for $n = 20$. This k-independence is related to the fact that we have here the exact Taylor expansion of the pole around $z = 1$: when we use Stirling's approximation for the factorials, a dependence on k is introduced.

We may extend our discussion to the case of more fermions. If we introduce f fermion flavours, each flavour j will have its own generating functions ψ_j and $\bar{\psi}_j$, with variables x_j and $\bar{x}_j$: but ϕ will still be described by Eq.(3.15), with the sole redefinition

$$\xi = x\bar{x} \to \xi = \sum_{j=1}^{f} x_j \bar{x}_j \ . \tag{3.21}$$

The amplitude therefore becomes, upon multinomial expansion:

$$\begin{aligned} a(\varphi \to k\varphi, n_1\chi_1\bar{\chi}_1, n_2\chi_2\bar{\chi}_2, \ldots, n_f\chi_f\bar{\chi}_f) \\ \sim \frac{(27/4)^n}{\sqrt{27\pi}} \frac{(3n-2+k)!n!n_1!n_2!\cdots n_f!}{(3n-2)!n^{3/2}} \ . \end{aligned} \tag{3.22}$$

For theories in which the various fermion types have the same type of vertices, this is the general way in which one goes from the single-fermion to the multi-fermion case, and therefore we shall only consider the single-fermion case in the following.

The next simplest case is that where we allow a φ^3 self-interaction for the boson in addition to the $\varphi\chi\bar{\chi}$ vertex. The analog of Eq.(3.15) is then

$$\phi = z + \frac{1}{2}\phi^2 + \frac{\xi}{(1-\phi)^2} \quad , \tag{3.23}$$

so that

$$F_z(\phi) = (1-\phi)^2(\phi - \frac{1}{2}\phi^2 - z) \tag{3.24}$$

The equation $F_z'(\phi)$ now has two roots, leading however to the same result: with $\phi = 1 - \Phi$ and $z = 1/2 - \zeta$, the singularity condition reads $\Phi^2 = \zeta$, and the form of ϕ close to the singularity reads

$$\phi \sim \sum_n \frac{2^{n-2}}{n^{3/2}\sqrt{\pi}} \frac{1}{\zeta^{2n-1/2}} \quad . \tag{3.25}$$

In turn, this gives the asymptotic form

$$a(\phi \to k\phi, n\chi\bar{\chi}) \sim \frac{2^{3n+k-5/2}}{n^{3/2}\sqrt{\pi}} \frac{(2n+k-3/2)!n!^2}{(2n-3/2)!} \quad . \tag{3.26}$$

Again, the goodness of the approximation is independent of k, and the ratio exact/approximate reads 1.253314137 for $n = 1$, 1.019251423 for $n = 10$, and 1.009498692 for $n = 20$.

3.2.3 Asymptotics by saddle-point methods

It is tempting to extend the reasoning of the previous section to more complicated cases. This is, however, dangerous because of the following reason. In finding the singularity we have first to solve $F_z'(\phi_0) = 0$ to find ϕ_0 as a function of z, and then to determine the coefficient of z^k in $1/F_z(\phi_0(z))^m$, where m is a large number. In principle, this is then again determined by the precise nature of the singularity of this form, that is, the behaviour of $F_z(\phi_0(z))$ close to a root. If z_0 is this root, we can generally write

$$F_z(\phi_0(z)) = A(z_0 - z)^p \left(1 + B(z_0 - z) + \mathcal{O}\left((z_0 - z)^2\right)\right) \quad , \tag{3.27}$$

for some positive p. Naively making the expansion around $z = z_0$ gives then

$$\begin{aligned}
&\frac{1}{F_z(\phi_0(z))^m} \sim \frac{1}{A^m(z_0-z)^{pm}} - \frac{mB}{A^m(z_0-z)^{pm-1}} + \cdots \\
= &\sum_k \frac{1}{A^m z_0^{pm}} \left(\frac{z}{z_0}\right)^k \left[\frac{(pm+k-1)!}{k!(pm-1)!} - mBz_0 \frac{(pm+k-2)!}{k!(pm-2)!} + \cdots\right] \\
= &\sum_k \frac{1}{A^m z_0^{pm}} \left(\frac{z}{z_0}\right)^k \frac{(pm+k-1)!}{k!(pm-1)!} \left[1 - Bz_0 \frac{m(pm-1)}{(pm+k-1)} + \cdots\right] \quad . \qquad (3.28)
\end{aligned}$$

The correction term is *not* small for generic large m and k values, but only becomes small in the 'super-asymptotic' limit $k \gg m^2 \gg 1$, which is too asymptotic to interest us here.

The most efficient way to determine the high-k behaviour appears to be the following. Let us rewrite the relation between ϕ_0 and z:

$$F'_z(\phi) = 0 \Rightarrow G(\phi) = z \quad . \qquad (3.29)$$

For instance, in the 'QED+φ^3' case considered above, we have $G(\phi) = 2\phi - \phi^2 - 1/2$. The form of the coefficient $c_{n,k}$ of $\xi^n z^k n^{-3/2}$ is then given by a (counter-clockwise) Cauchy integral around $z = 0$:

$$c_{n,k} \sim \frac{1}{2i\pi} \oint dz \, \frac{1}{z^{k+1}} \frac{1}{F_z(\phi)^n} \sqrt{\frac{-F_z(\phi)}{2\pi F''_z(\phi)}} \quad , \quad G(\phi) = z \quad . \qquad (3.30)$$

We can readily transform this into a loop integral for ϕ:

$$\begin{aligned}
c_{n,k} \quad \sim \quad & \frac{1}{2i\pi} \oint d\phi \, \frac{G'(\phi)}{G(\phi)^{k+1} H(\phi)^n} \sqrt{\frac{-H(\phi)}{2\pi H_2(\phi)}} \quad , \\
& H(\phi) = F_{G(\phi)}(\phi) \quad , H_2(\phi) = F''_{G(\phi)}(\phi) \quad . \qquad (3.31)
\end{aligned}$$

Note that, in the definition of H_2, the substitution $z = G(\phi)$ must be made *after* the differentiation. The only tricky point is to determine which of the various roots of $G(\phi) = 0$ should be chosen to integrate around. Note that this question *can* be answered unambiguously: if worst comes to worst, one can simply check the result against the exact enumeration for largish values of n and k. Having found the point around which to do the ϕ integral, we then proceed to deform the integration contour into a pair of integrals parallel to the imaginary axis. The upwards integral ('main'

integral) is chosen to run over the saddle point $\hat{\phi}$, situated on the real axis and given by

$$K'(\hat{\phi}) = 0 \quad , \quad K(\phi) \equiv -n \log H(\phi) - k \log G(\phi) \quad . \tag{3.32}$$

In many cases $\hat{\phi}$ can actually be given as a function of n and k in closed form. The downwards integral ('return' integral) is chosen to run over another saddle point. In the cases we have studied, we have always found that the values of $H(\phi)$ and $F(\phi)$ in the saddle point of the return integral are larger (in absolute value) than those for the saddle point of the main integral, so that the contribution of the return integral is exponentially suppressed with respect to the main integral. The result, therefore, is

$$c_{n,k} = \frac{1}{2\pi} \frac{G'(\hat{\phi})}{G(\hat{\phi})^{k+1} H(\hat{\phi})^n} \sqrt{\frac{-H(\hat{\phi})}{H_2(\hat{\phi}) K''(\hat{\phi})}} \quad . \tag{3.33}$$

The final asymptotic estimate for the number of tree graphs with $k+1$ external bosons and $2n$ fermions/antifermions can therefore be written as follows:

$$\begin{aligned} & a(\varphi \to k\varphi, n\chi\bar{\chi}) \sim (n-1)!^2 k! C_1^n C_2^{k+1} D \quad , \\ & C_1 = 1/H(\hat{\phi}) \quad , \\ & C_2 = 1/G(\hat{\phi}) \quad , \\ & D = \frac{n^{1/2} G'(\hat{\phi})}{2\pi} \sqrt{\frac{-H(\hat{\phi})}{H_2(\hat{\phi}) K''(\hat{\phi})}} \quad . \end{aligned} \tag{3.34}$$

The numbers C_1, C_2 and D only depend on the ratio k/n.

As a first check, we redo the QED case with one fermion flavour. Here, $G(\phi) = (3\phi - 1)/2$ so that we must integrate around $\phi = 1/3$. There is only a single saddle point $\hat{\phi} = (n+k)/(3n+k)$. Since $\hat{\phi} > 1/3$ and main integral is indeed upwards, and the return integral can be moved out to infinity. The result for $c_{n,k}$ is nothing but the Stirling approximation of the 'exact' result.

The next case is that of 'QED+φ^3'. The equation $G(\phi) = 0$ has two roots, $1 \pm \sqrt{1/2}$, of which $1 - \sqrt{1/2}$ is on the appropriate Riemann sheet. This can be seen from the fact that the saddle point $\hat{\phi} = (2n + k - \sqrt{2n^2 + nk})/(2n + k)$ is to the right of this root, and has a positive value for $G'(\hat{\phi})$: choosing the other possible saddle point (with a + sign before the square root) leads to a negative $G'(\hat{\phi})$ and

consequently a negative asymptotic estimate. Again, the saddle-point result boils down to the Stirling approximation of the 'exact' one.

A more complicated case is that of QED with a pure φ^4 interaction added. The SD equation for this is:

$$\phi = z + \frac{1}{6}\phi^3 + \frac{\xi}{(1-\phi)^2} \tag{3.35}$$

We find

$$\begin{aligned}
\xi = F_z(\phi) &= (1-\phi)^2(\phi - z - \frac{1}{6}\phi^3) \ , \\
G(\phi) &= -\frac{5}{12}\phi^3 + \frac{1}{4}\phi^2 + \frac{3}{2}\phi - \frac{1}{2} \ , \\
G'(\phi) &= -\frac{1}{4}(5\phi^2 - 2\phi - 6) \ , \\
H(\phi) &= \frac{1}{4}(1-\phi)^3(2-\phi^2) \ , \\
H_2(\phi) &= \frac{1}{2}(1-\phi)(5\phi^2 - 2\phi - 6) \ .
\end{aligned} \tag{3.36}$$

Note that the roots of H_2 are also roots of H or G': this is a general occurrence. The main-integral saddle point $\hat{\phi}$ is a root of the equation

$$(5n+3k)\phi^3 - 3(n+k)\phi^2 - 6(3n+k)\phi + 6(n+k) = 0 \ . \tag{3.37}$$

By standard methods, we can find the three roots of this equation:

$$\begin{aligned}
\hat{\phi}_r &= \frac{1}{5n+3k}\left[2(31n^2+30nk+7k^2)^{1/2}\sin\left\{\frac{2r\pi}{3} - \frac{1}{3}u\right\} + n + k\right] \ , \\
u &= \arcsin\left(\frac{29n^3+75n^2k+63nk^2+17k^3}{(31n^2+30nk+7k^2)^{3/2}}\right) \ ,
\end{aligned} \tag{3.38}$$

with $r = 0, 1, 2$. The choice $r = 0$ interpolates smoothly between .325259493 for $k/n = 0$ and 1 for $n/k = 0$, and this turns out to be the correct saddle point. The singularity structure of the integrand is as follows: there are poles of order $k+1$ at the three roots of G, -1.788306912, .3252594930, and 2.063047419. There is a pole of order $3n-1$ at 1, and poles of order n at $\pm\sqrt{2}$. With the standard convention that the square root branch cut lies along negative real values, there are cuts along the real ϕ axis from $-\sqrt{2}$ to $(1-\sqrt{31})/5 \sim -.9135528726$ and from $(1+\sqrt{31})/5 \sim 1.313552873$

to $\sqrt{2}$. The return integral can be taken to cross the real axis at -.9135528726, where $H = 2.041476117$ and $G = -1.344004635$. The saddle-point values for the main integral are always smaller than these in absolute value, confirming the above statement that the return integral may safely be neglected.

The more relevant case of QCD is treated in the same manner. We have now for the SD equation

$$\phi = z + \frac{1}{2}\phi^2 + \frac{1}{6}\phi^3 + \frac{\xi}{(1-\phi)^2} \tag{3.39}$$

By iterating Eq.(3.39) we get the exact number of graphs. Some results are shown in the next table where N is the number of external legs and ℓ is the number of (identical) fermion pairs. For the asymptotic result we have

ℓ	N=8	N=9	N=10	N=11	N=12	N=13
0	34,300	559,405	10,525,900	224,449,225	5,348,843,500	140,880,765,025
1	15,495	231,280	4,016,775	79,603,720	1,773,172,275	43,864,374,400
2	8,040	113,650	1,875,720	35,432,530	754,334,280	17,877,362,650
3	4,362	59,424	946,050	17,258,640	355,273,170	8,151,299,520
4	2,400	31,896	494,880	8,796,600	176,474,400	3,947,643,000
5	–	–	263,400	4,593,600	90,357,000	1,981,324,800
6	–	–	–	–	47,073,600	1,016,341,200

$$\begin{aligned}
\xi = F_z(\phi) &= (1-\phi)^2(\phi - z - \frac{1}{2}\phi^2 - \frac{1}{6}\phi^3) \ , \\
G(\phi) &= -\frac{5}{12}\phi^3 - \frac{3}{4}\phi^2 + 2\phi - \frac{1}{2} \ , \\
G'(\phi) &= \frac{1}{4}(4-5\phi)(2+\phi) \ , \\
H(\phi) &= \frac{1}{4}(1-\phi)^3(2-2\phi-\phi^2) \ , \\
H_2(\phi) &= -\frac{1}{2}(1-\phi)(4-5\phi)(2+\phi) \ ,
\end{aligned} \tag{3.40}$$

and $\hat{\phi}$ solves

$$(5n+3k)\phi^3 + 3(3n+k)\phi^2 - 12(2n+k)\phi + 6(n+k) = 0 \ ; \tag{3.41}$$

$\log_{10}(k/n)$	C_1	C_2	D
-3.0	8.143	4155.	.0002929
-2.5	8.157	1316.	.0005196
-2.0	8.217	417.5	.0009172
-1.5	8.389	133.6	.001594
-1.0	8.961	43.78	.002640
-0.5	10.89	15.40	.003802
0	18.00	6.452	.003882
0.5	48.97	3.666	.0002183
1.0	197.2	2.833	.0006782
1.5	836.8	2.599	.0001506
2.0	3141.	2.535	.00002913
2.5	10660.	2.516	.000005336
3.0	34530.	2.511	.0000009583

Table 3.1: The non-universal constants C_1, C_2 and D for QCD-like theory

this root can be written as

$$\begin{aligned} \hat{\phi} &= \frac{1}{5n+3k}\left[2(13k^2+49n^2+50nk)^{1/2}\sin\left(\frac{1}{3}u\right)-3n-k\right] \quad , \\ u &= \arcsin\left(2\frac{141n^3+225n^2k+123nk^2+23k^3}{(13k^2+49n^2+50nk)^{3/2}}\right) \quad . \end{aligned} \tag{3.42}$$

The singularity structure resembles that of the previous case: poles of order $k+1$ at the three values -3.343142188, .2853836802, and 1.257758508; a pole of order $3n-1$ at 1, and poles of order n at $-1-\sqrt{3}\sim -2.732050808$ and at $-1+\sqrt{3}\sim .7320508076$; and branch cuts running from $-1-\sqrt{3}$ to -2 and from $-1+\sqrt{3}$ to 4/5. The loop-integration contour is situated around .2853836802 and $\hat{\phi}$ moves smoothly from this value upwards to .7320508076 as k/n increases from 0 to infinity. The saddle point for the return integral is at $\phi=-2$, where $H=27/2$ and $G=-25/6$, again always considerably bigger than $H(\hat{\phi})$ and $G(\hat{\phi})$. This allows for the complete determination of $C_{1,2}$ and D: the value of $\hat{\phi}$ is given by Eq.(3.42), and

$$\begin{aligned} K''(\phi) &= n\frac{5\phi^4+12\phi^3+2\phi^2-36\phi+20}{(2-2\phi-\phi^2)^2(1-\phi)^2} \\ &\quad +3k\frac{25\phi^4+60\phi^3+54\phi^2-204\phi+156}{(5\phi^3+9\phi^2-24\phi+6)^2} \quad . \end{aligned} \tag{3.43}$$

In table 3.1 we present the non-universal quantities C_1, C_2 and D for various ratios k/n. As expected, the accuracy of the asymptotic approximation improves uniformly if n and k grow with a fixed ratio. In table 3.2 we collect some results, where we have of course only those values for which both n and k are integers, and have iterated the exact generating function up to $n+k = 29$. The accuracy is actually quite reasonable even for moderate values of n and k.

n	$k = n/3$	$k = n/2$	$k = 2n/3$	$k = n$	$k = 3n/2$	$k = 2n$	$k = 3n$
1						1.019	1.003
2		.9904		1.010	1.010	1.007	.9995
3	.9709		.9999	1.006		1.004	.9993
4		.9927		1.004	1.004	1.003	.9994
5				1.003		1.002	.9995
6	.9837	.9946	.9992	1.002	1.003	1.002	.9995
7				1.002		1.001	.9996
8		.9958		1.002	1.002	1.001	
9	.9888		.9993	1.001		1.001	
10		.9966		1.001	1.001		
11				1.001			
12	.9915	.9971	.9994	1.001			
13				1.001			
14		.9975		1.001			
15	.9932		.9995				
16		.9978					
17							
18	.9943	.9980					
19							
20							
21	.9951						

Table 3.2: The ratio between asymptotic and exact results for QCD

We may also consider a theory where φ^p bosonic self-interactions occur for every

p. We simply list the results:

$$\begin{aligned}
\phi &= z + \exp(\phi) - \phi - 1 + \frac{\xi}{(1-\phi)^2} \quad , \\
\xi &= (1-\phi)^2(\phi - z - \exp(\phi) + \phi + 1) \quad , \\
G(\phi) &= 3\phi - \frac{1}{2}\phi\exp(\phi) - \frac{1}{2}\exp(\phi) \quad , \\
G'(\phi) &= 3 - \exp(\phi) - \frac{1}{2}\phi\exp(\phi) \quad , \\
H(\phi) &= \frac{1}{2}(-1+\phi)^3\,(-2+\exp(\phi)) \quad , \\
H_2(\phi) &= -(-1+\phi)\,(-6+2\exp(\phi)+\phi\exp(\phi)) \quad , \\
0 &= \exp(\hat{\phi})((n+k)\hat{\phi} + n - k) - (6n+2k)\hat{\phi} + 2k \quad , \\
K''(\phi) &= n\frac{12 - 10\exp(\phi) + 3\exp(2\phi) - 4\phi\exp(\phi) + 2\phi^2\exp(\phi)}{(-2+\exp(\phi))^2(-1+\phi)^2} \\
&\quad + k\frac{(6\phi\exp(\phi) + \exp(2\phi) + 6\phi^2\exp(\phi) + 36 - 24\exp(\phi))}{(-6\phi + \phi\exp(\phi) + \exp(\phi))^2} \quad . \qquad (3.44)
\end{aligned}$$

The Riemann sheet structure of the function G is of course much more complicated in this case, but fortunately the relevant saddle point is the simplest solution on the real axis, again interpolating smoothly between the appropriate zeroes of H and G. In table 3.3, we give the non-universal quantities as a function of k/n. These numbers are qualitatively quite similar to that for QCD. The accuracy of the approximation appears to be almost identical to that of the QCD case.

Another interesting case is that of scalar QED, where we have an additional $\varphi^2\chi\bar{\chi}$ interaction term. The SD equations now become more complicated:

$$\psi = x + \psi(\phi + \phi^2/2) \quad , \quad \bar{\psi} = \bar{x} + \bar{\psi}(\phi + \phi^2/2) \quad , \quad \phi = z + (1+\phi)\psi\bar{\psi} \quad , \qquad (3.45)$$

so that

$$\phi = z + \frac{\xi(1+\phi)}{(1-\phi-\phi^2/2)^2} \quad . \qquad (3.46)$$

$\log_{10}(k/n)$	C_1	C_2	D
-3.0	8.150	2000.	.0002904
-2.5	8.170	1250.	.0005151
-2.0	8.224	384.6	.0009093
-1.5	8.396	135.1	.001580
-1.0	8.977	44.05	.002614
-0.5	10.91	15.53	.003753
0	17.99	6.494	.003797
0.5	48.08	3.731	.002092
1.0	184.5	2.907	.0006325
1.5	729.9	2.681	.0001372
2.0	2564.	2.618	.00002613
2.5	8333.	2.591	.000004754
3.0	20000	2.584	.0000008515

Table 3.3: The non-universal constants C_1, C_2 and D for a ϕ^p theory

Following the same steps as before, we find

$$\begin{aligned} G(\phi) &= \frac{-2+9\phi^2+4\phi^3+6\phi}{3(2+2\phi+\phi^2)} \ , \\ G'(\phi) &= \frac{4(\phi^2+2\phi+4)(1+\phi)^2}{3(2+2\phi+\phi^2)^2} \ , \\ H(\phi) &= \frac{(2-2\phi-\phi^2)^3}{12(2+2\phi+\phi^2)} \ , \\ H_2(\phi) &= \frac{(\phi^2+2\phi+4)(-2+2\phi+\phi^2)}{2+2\phi+\phi^2} \ ; \end{aligned} \tag{3.47}$$

the main-integral saddle point is a solution of

$$(4n+k)\phi^3+3(3n+k)\phi^2+6n\phi-2(n+k)=0 \ , \tag{3.48}$$

and reads

$$\begin{aligned} \hat{\phi} &= \frac{1}{4n+k}\left[2(k^2+4nk+n^2)^{1/2}\sin\left(\frac{\pi+u}{3}\right)-3n-k\right] \ , \\ u &= \arcsin\left(\frac{n(3k^2+18nk+25n^2)}{(k^2+4nk+n^2)^{3/2}}\right) \ . \end{aligned} \tag{3.49}$$

Finally, we also need

$$K''(\phi) = \frac{4n(84\phi^2 + 26\phi^4 + 6\phi^5 + \phi^6 + 24 + 56\phi + 64\phi^3)}{(-2 + 2\phi + \phi^2)^2(2 + 2\phi + \phi^2)^2} + \frac{8k(36 + 320\phi^2 + 371\phi^4 + 205\phi^5 + 72\phi^6 + 16\phi^7 + 2\phi^8 + 148\phi + 432\phi^3)}{(2 + 2\phi + \phi^2)^2(-2 + 9\phi^2 + 4\phi^3 + 6\phi)^2}. \tag{3.50}$$

The results for the non-universal constants are given in the following table. The

$\log_{10}(k/n)$	C_1	C_2	D
-3.0	9.671	4189.	.1731E-5
-2.5	9.690	1326.	.5466E-5
-2.0	9.756	420.2	.1721E-4
-1.5	9.970	133.7	.5371E-4
-1.0	10.66	43.18	.1627E-3
-0.5	13.06	14.55	.4459E-3
0	23.03	5.510	.8568E-3
0.5	85.11	2.667	.6268E-3
1.0	805.8	1.776	.1574E-3
1.5	.1526E5	1.496	.2247E-4
2.0	.4021E6	1.407	.2542E-5
2.5	.1197E8	1.379	.2647E-6
3.0	.3712E9	1.370	.2681E-7

Table 3.4: The non-universal constants C_1, C_2 and D for scalar QED theory

non-universal constants appear to vary much more rapidly as a function of k/n than in the case of QCD. The accuracy of the asymptotic estimate, however, is essentially the same.

3.2.4 QCD: a closer look

Let us take a closer look at the case of QCD. We would like to count the number of 4-vertices and study the probability distribution of the number of 4-vertices and compare it to the total number of diagrams. For simplicity we take the case of purely gluonic amplitudes. The generating function satisfies the third order equation:

$$\phi = x + \frac{1}{2}\phi^2 + \frac{z}{6}\phi^3 \tag{3.51}$$

where z is a parameter, the powers of which carry the information about 4-vertices. Following the procedure detailed in the previous section we write

$$x = F(\phi) = \phi - \frac{1}{2}\phi^2 - \frac{z}{6}\phi^3 \tag{3.52}$$

$$F'(\phi) = 1 - \phi - \frac{z}{2}\phi^2 \tag{3.53}$$

$$F''(\phi) = -1 - z\phi \tag{3.54}$$

We see that putting $z = 1$ we recover the expressions for the total number of diagrams in the QCD case we studied in the previous section. We can use (3.10) to obtain the asymptotic form for the number of diagrams with n external legs and m 4-vertices. We shall write everything in terms of ϕ keeping in mind that it is a function of z and x. To this end we need $F(\phi_0)$ and $F''(\phi_0)$, where ϕ_0 is the root of (3.53). We find (we drop the '0' subscript with the understanding that ϕ is really ϕ_0)

$$z = -2\frac{\phi - 1}{\phi^2} \tag{3.55}$$

$$F(\phi(z)) = -\frac{1}{6}\phi\,(\phi - 4) \tag{3.56}$$

$$F''(\phi(z)) = \frac{\phi - 2}{\phi} \tag{3.57}$$

The asymptotic result is:

$$a(n; \phi(z)) \sim \frac{n!}{n^{3/2}}\frac{\sqrt{3}}{6}\sqrt{\frac{\phi^2(\phi-4)}{\pi(\phi-2)}}\left(\frac{-6}{\phi(\phi-4)}\right)^n \tag{3.58}$$

We define the propability distribution $\pi(m)$ of the 4-vertices as:

$$P(z) = \sum_{m\geq 0}\pi(m)z^m \tag{3.59}$$

where $P(z)$ is the normalized distribution of z:

$$P(z) = \frac{a(n; z)}{a(n; 1)} \tag{3.60}$$

Since we are working in terms of ϕ we define the normalization of P as $a(n; \phi(z = 1))$. For $z = 1$ we get $\phi = -1 + \sqrt{3}$ and we have for $P(\phi)$:

$$P(\phi) = \sqrt{\frac{3}{18 - 8\sqrt{3}}}\left(\frac{\sqrt{3}-1}{\sqrt{3}+5}\right)^n\sqrt{\frac{\phi^2(\phi-4)}{(\phi-2)}}\left(\frac{-22}{\phi(\phi-4)}\right)^n \tag{3.61}$$

We can evaluate $\pi(m)$ by using the Cauchy integral, from (3.59)

$$\pi(m) = \frac{1}{2\pi i}\oint dz \frac{P(z)}{z^{m+1}} = \frac{1}{2\pi i}\oint d\phi\, 2\frac{\phi-2}{\phi^3}\,\frac{P(z(\phi))}{z(\phi)^{m+1}} \tag{3.62}$$

We write this as

$$\frac{1}{2\pi i}\oint d\phi\, e^{n\sigma(\phi)}\tau(\phi)^{1/2} \tag{3.63}$$

where

$$\sigma(\phi) = \ln\left(\frac{-22}{\phi(\phi-4)}\right) - \mu\ln\left(-2\frac{\phi-1}{\phi^2}\right) \tag{3.64}$$

$$\tau(\phi) = \frac{(\phi-2)(\phi-4)}{(\phi-1)^2} \tag{3.65}$$

and $\mu = m/n,\ 0 \le \mu < \frac{1}{2}$. We evaluate this integral by using saddle-point approximation. The first derivative of $\sigma(\phi)$ and it's root are:

$$\sigma'(\phi) = \frac{(2-2\phi-4\mu+\mu\phi)(\phi-2)}{\phi(\phi-1)(\phi-4)}$$

$$\sigma'(\hat{\phi}) = 0 \to \hat{\phi} = 2\frac{2\mu-1}{\mu-2}$$

Expanding $\sigma(\phi)$ up to second order and putting it to the exponent at the integrand we have

$$\begin{aligned}\pi(\mu) &\sim \frac{1}{2\pi i}\int_{-i\,\infty}^{+i\,\infty}\tau(\phi)^{1/2}\; e^{n\sigma(\hat{\phi})+\frac{n}{2}(\phi-\hat{\phi})^2\sigma''(\hat{\phi})} \\ &\sim \frac{1}{\sqrt{2\pi n\sigma''(\hat{\phi})}}\tau(\hat{\phi})^{1/2}e^{n\sigma(\hat{\phi})}\end{aligned} \tag{3.66}$$

The asymptotic form of $\pi(\mu)$ is not very informative but we include it for completeness

$$\begin{aligned}\pi(\mu) \sim\ & \frac{6}{\sqrt{\pi}\sqrt{18-8\sqrt{3}}}\left(\frac{\sqrt{3}-1}{\sqrt{3}+5}\right)^n\sqrt{\frac{2\mu-1}{n\mu(\mu-2)^3}}\left(-\frac{3}{2}\frac{\mu(\mu-2)}{(2\mu-1)^2}\right)^{-n\mu} \\ & \left(-\frac{11}{6}\frac{\mu^2-4\mu+4}{2\mu-1}\right)^n\end{aligned} \tag{3.67}$$

The exact probability distribution of 4 vertices can be obtained by iterating the functional equation for ϕ. This results in a series in x with coefficients that are polynomials in z. Picking out the right powers of z we can compute $\pi(\mu)$. A comparison of the asymptotic estimate with the exact result is shown in Fig. 3.1 for different numbers of external legs $N = 10, 20, 80, 100$.

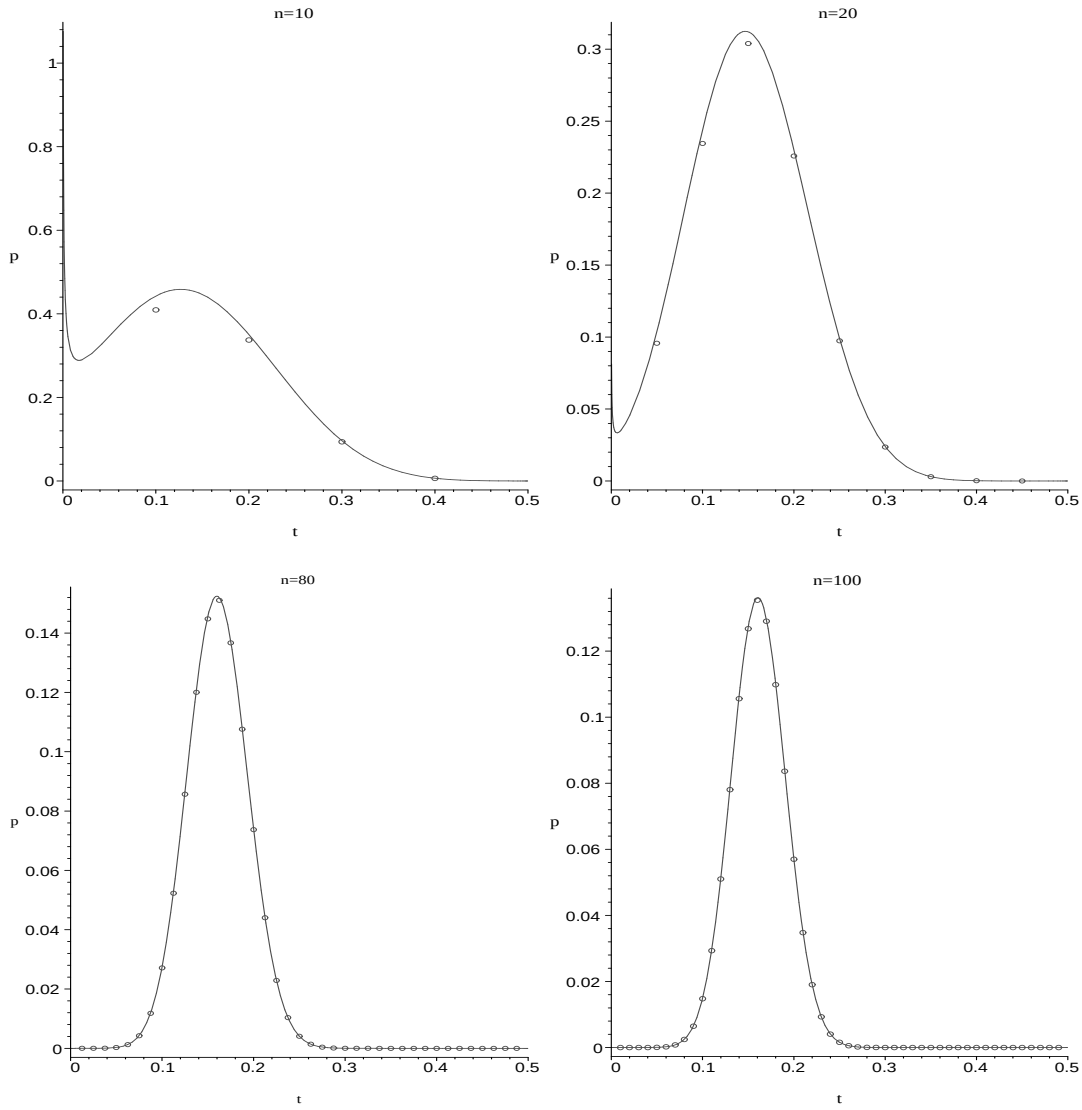

Figure 3.1: Probability distribution of the number of 4-vertices for a small number of of external legs, $N = 10, 20$ and a large number, $N = 80, 100$ in terms of t where $t = m/N$. The circles give the exact result obtained by expanding in terms of z. The line is the asymptotic estimate.

3.3 Process counting

Having counted all the diagrams that contribute in a particular process, we now move one step further. In jet production, what one sees as an end product is just the number of jets. Specific information about the processes involved is not observed but rather one assumes that all relevant process contribute. This is because in hadron-hadron collision, for example, the constituents are quarks and gluons scattering among each other giving a large number of different scattering amplitudes. In this section we concern ourselves with the question of the number of processes that are relevant for the production of a number of jets.

Under the assumption that the various (anti)quark types and gluons cannot be distinguished experimentally, and that all these parton types are (essentially) massless, the only information experimentally available about any given event is the configuration of the observed momenta. We shall denote such an event by its momenta as follows:

$$p_1 + p_2 \quad \rightarrow \quad q_1 + q_2 + q_3 + \cdots + q_n \quad ,$$

where n outgoing partons/jets are observed. To obtain the total probability density for this event in phase space, one has to consider all possible $2 \rightarrow n$ QCD amplitudes[1],viewed here as functions of $2 + n$ momentum arguments, and assign the observed momenta to these arguments in all possible ways without double counting. Note that, due to the composite nature of the incoming hadrons, also the initial state may require more than one assignment: for instance, a quark-gluon initial state $q(p_1)g(p_2)$ is to be counted as distinct from $q(p_2)g(p_1)$, whereas of course the purely gluonic initial state $g(p_1)g(p_2)$ is counted only once. Similarly, if the final states contains m quarks of a certain type, a corresponding factor $1/m!$ has to be applied. In what follows we shall denote the number of (essentially) massless quarks in the final state by f, so that $f = 4$ at relatively low momenta where the b quark might be identifiable, $f = 5$ typically for QCD studies at the LHC, and f would be 6 at some future multi-hundred TeV collider. The number of flavours contributing appreciably in the initial state is denoted by j, so that $j = 3$ would be appropriate if the charm quark structure function can be neglected, and $j = 4$ if it is included. We shall, however, keep to general j and f as much as possible.

3.3.1 Arrangement of the initial states and final states

The various possibilities for the initial states are:

[1]Of course, squared and spin/colour-summed and -averaged in the usual way.

- $\boldsymbol{gg}$ Obviously, there is only one possibility for the initial state. The final state can be anything so there are n partons in the final state.
- $\boldsymbol{q_i\bar{q}_i}$ If we have j flavours then there are $2j$ possibilities for the initial state and n partons to be distributed in the final state.
- $\boldsymbol{gq_i}$, $\boldsymbol{g\bar{q}_i}$ There are $2j$ initial states as in the previous case. For the final state, we know that there must at least one q_i or $\bar{q}_i$ so there are $(n-1)+q_i$ or $(n-1)+\bar{q}_i$ partons.
- $\boldsymbol{q_iq_i}$, $\boldsymbol{\bar{q}_i\bar{q}_i}$ For the scattering of identical quarks (anti-quarks), there are j initial states and since the same partons must appear in the final state we can have $n-2$ partons plus the initial quarks or anti-quarks.
- $\boldsymbol{q_iq_k}$, $\boldsymbol{\bar{q}_i\bar{q}_k}$, $\boldsymbol{i \neq k}$ For the scattering of different quarks (anti-quarks) we have $j(j-1)$ possibilities for the initial state, and again $n-2$ partons plus the initial quarks (anti-quarks), for the final state.
- $\boldsymbol{q_i\bar{q}_k}$, $\boldsymbol{i \neq k}$ For this final case we have $2j(j-1)$ initial states and $n-2$ partons plus the quark and the anti-quark in the final state.

All of the above can be summarized in the following table.

Initial States	# possibilities	Final States
gg	1	n
$q_i\bar{q}_i$	$2j$	n
gq_i	$2j$	$(n-1)+q_i$
$g\bar{q}_i$	$2j$	$(n-1)+\bar{q}_i$
q_iq_i	j	$(n-2)+q_i+q_i$
$q_iq_j, i \neq j$	$j(j-1)$	$(n-2)+q_i+q_j$
$\bar{q}_i\bar{q}_i$	j	$(n-2)+\bar{q}_i+\bar{q}_i$
$\bar{q}_i\bar{q}_j, i \neq j$	$j(j-1)$	$(n-2)+\bar{q}_i+\bar{q}_j$
$q_i\bar{q}_j, i \neq j$	$2j(j-1)$	$(n-2)+q_i+\bar{q}_j$

where $i,k = 1,\ldots,j$. From the second column we can read off the total number of initial-state momentum configurations:

$$1+3(2j)+j+j(j-1)+j+j(j-1)+2j(j-1) = (1+2j)^2 \tag{3.68}$$

From this table we can arrange four different groups of initial states, which differ in the flavour structure of their final states. They are shown in the following table:

Group	Initial state	# of final states
A	$gg,\ q_i\bar{q}_i$	$A(n)$
B	$gq_i,\ g\bar{q}_i$	$B(n)$
C	$q_iq_i,\ \bar{q}_i\bar{q}_i$	$C(n)$
D	$q_iq_k,\ \bar{q}_i\bar{q}_k,\ q_i\bar{q}_k, i \neq k$	$D(n)$

3.3.2 Counting of the final states

Group A The distinct possibilities for flavourless final states are:

$$n = n_0 * (g) + n_1 * (q_1\bar{q}_1) + n_2 * (q_2\bar{q}_2) + \cdots + n_f * (q_f\bar{q}_f) \tag{3.69}$$

where n_0 is the number of gluons g and $n_1, n_2, \ldots, n_f$ are the numbers of q_f and $\bar{q}_f$ quarks with different flavour f. The number of different processes $A(n)$ is the number of the various dinstinct ways to distribute n different final momenta among n partons:

$$A(n) = \sum_{n_0,n_1,\ldots,n_f \geq 0} \frac{(n)!}{(n_0)!(n_1)!^2(n_2)!^2\cdots(n_f)!^2}\Theta(n_0+2n_1+2n_2+\cdots+2n_f = n) \tag{3.70}$$

where $\Theta(a = b) = \delta_{a,b}$. We can evaluate this number by forming the generating function:

$$\begin{aligned}\mathcal{A}(x) = \sum_{k\geq 0}\frac{x^n}{n!}A(n) &= \sum_{n_0,n_1,\ldots,n_f\geq 0}\frac{x^{n_0}}{n_0!}\frac{x^{2n_1}}{(n_1)!^2}\frac{x^{2n_2}}{(n_2)!^2}\cdots\frac{x^{2n_f}}{(n_f)!^2} \\ &= \left(\sum_{n\geq 0}\frac{x^n}{n!}\right)\left(\sum_{n\geq 0}\frac{x^{2n}}{(n)!^2}\right)^f = e^x\cdot I_0(2x)^f \end{aligned} \tag{3.71}$$

where $I_0(x)$ is the modified Bessel function of the first kind and zeroth order [Abramowitz and Stegun,].

Group B All the possible final states for this case have a single net flavour, and can be written as follows

$$n = n_0 * (g) + n_1 * (q_1\bar{q}_1) + n_2 * (q_2\bar{q}_2) + \cdots + n_f * (q_f\bar{q}_f) + q_i \tag{3.72}$$

The number of different processes $B(n)$ is:

$$B(n) = \sum_{n_0,n_1,\ldots,n_f\geq 0}\frac{(n_0+2n_1+2n_2+\cdots+2n_f+1)!}{n_0!(n_1+1)!(n_1)!(n_2)!^2\cdots(n_f)!^2}\Theta(n_0+2n_1+2n_2+\cdots+2n_f+1 = n)$$

(3.73)

This gives the generating function

$$\begin{aligned}\mathcal{B}(x) &= \left(\sum_{n\geq 0}\frac{x^n}{n!}\right)\left(\sum_{n\geq 0}\frac{x^{2n}}{(n)!^2}\right)^{f-1}\left(\sum_{n\geq 0}\frac{x^{2n+1}}{(n)!(n+1)!}\right)\\ &= e^x\cdot I_0(2x)^{f-1}\cdot I_0'(2x)\end{aligned} \tag{3.74}$$

where the prime denotes the derivative of the Bessel function with respect to the argument $2x$.

Group C For this case the final state is

$$n = 2n_0 * (g) + n_1 * (q_1\bar{q}_1) + n_2 * (q_2\bar{q}_2) + \cdots + n_f * (q_f\bar{q}_f) + 2 * (q_i) \tag{3.75}$$

and the number of possibilities is

$$C(n) = \sum_{n_0,n_1,\ldots,n_f\geq 0}\frac{(n_0+2n_1+2n_2+\cdots+2n_f+2)!}{n_0!(n_1+2)!(n_1)!(n_2)!^2\cdots(n_f)!^2}\Theta(n_0+2n_1+2n_2+\cdots+2n_f+2=n) \tag{3.76}$$

The generating function is

$$\mathcal{C}(x) = \sum_{n\geq 0}\frac{x^n}{n!}C(n) = e^x I_0(2x)^{f-1}\cdot\{2I_0''(2x) - I_0(2x) \tag{3.77}$$

Group D The derivation goes through as in the previous cases and the result is

$$\mathcal{D}(x) = \sum_{n\geq 0}\frac{x^n}{n!}D(n) = e^x I_0(2x)^{f-2}\cdot(I_0'(2x))^2 \tag{3.78}$$

The total number of possibilities for the final state can now be determined:

$$G(n) = (1+2j)A(n) + 4jB(n) + 2jC(n) + 4j(j-1)D(n) \tag{3.79}$$

with the generating function

$$\begin{aligned}\mathcal{G}(x) = \sum_{n\geq 0}\frac{x^n}{n!}G(n) = e^x \quad \{ \quad & (1+2j)\ I_0(2x)^f + 4j\ I_0(2x)^{f-1}\ I_0'(2x)\\ & + \quad 2j\ I_0(2x)^{f-1}\,(2I_0''(2x) - I_0(2x))\\ & + \quad 4j(j-1)\ I_0(2x)^{f-2}\ (I_0'(2x))^2\ \}\end{aligned} \tag{3.80}$$

We can put this in a more compact form:

$$\mathcal{G}(x) = e^x I_0(2x)^{f-j} \left(1 + \frac{d}{dx}\right)^2 I_0(2x)^j \tag{3.81}$$

To get the number of processes we expand the generating function $\mathcal{G}(x)$ and pick out the relevant coefficients. For example, for $f = 3, 4, 5$ flavours we have:

Total number of amplitudes					
	$f=3$		$f=4$		
n	$j=2$	$j=3$	$j=2$	$j=3$	$j=4$
2	71	127	81	141	217
3	299	511	377	625	921
4	1,763	3,301	2,645	4,867	7,761
5	8,955	16,297	15,325	27,087	41,889
6	54,353	103,279	113,733	213,879	345,465
7	304,701	570,367	745,421	1,364,811	2,162,617
8	1,879,723	3,595,177	5,704,061	10,836,831	17,605,249

Total number of amplitudes				
	$f=5$			
n	$j=2$	$j=3$	$j=4$	$j=5$
2	91	155	235	331
3	455	739	1,071	1,451
4	3,647	6,601	10,419	15,101
5	23,255	40,157	61,059	85,961
6	200,473	372,719	598,005	876,331
7	1,470,061	2,636,375	4,118,865	5,917,531
8	13,229,719	24,937,645	40,333,059	59,415,961

3.3.3 Gluonic contributions

An interesting question that arises is the issue of contribution of gluonic processes, compared to the total number of processes, since often the purely gluonic process is assumed to be typical or 'dominant'. In particular we would like to examine to what degree purely gluonic amplitudes dominate over other kinds of processes, since gluons have a different color charge than quarks [2]. To this end we assign to each external

[2]Note that we do not address the question of the singularity structure of gluonic versus other amplitudes.

gluon an additional factor k, resulting in a modification of the generating function (3.81):

$$\mathcal{G}_k(x) = e^{kx} I_0(2x)^{f-j} \left(k + \frac{d}{dx}\right)^2 I_0(2x)^j \tag{3.82}$$

The corresponding generating function for purely gluonic processes would be:

$$\mathcal{G}_k^0(x) = k^2 e^{kx} \tag{3.83}$$

We may compare the coefficients of the expansion of the two generating functions. This can be seen in the graph that follows, where we have plotted the ratio $\mathcal{G}_{k,n}^0/\mathcal{G}_{k,n}$ of the coefficients, for number of jets ranging from $n = 2$ up to $n = 8$, against k, and for the particular case of $f = 3, j = 3$. Notice that the ratio approaches one as the factor k grows larger, but decreases with n.

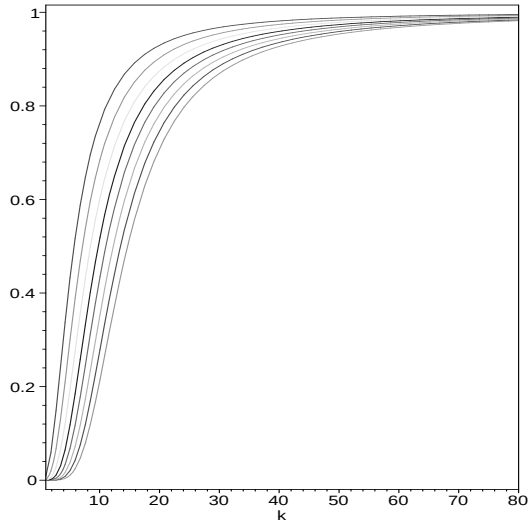

In order to estimate how large k has to make the gluonic amplitude the dominant one, we look for values of k that give $\mathcal{G}_{k,n}^0/\mathcal{G}_{k,n} = 1/2$. These can be seen in the table that follows, for the case $f = 3, j = 3$ again and for various numbers of jets.

n	2	3	4	5	6	7	8	9
k	5.72	7.13	8.47	9.78	11.04	12.27	13.48	14.67

Another extension would be to account for the fact that the gluonic structure function is typically larger than that for a quark. Then the generating function becomes:

$$\mathcal{G}_S(x) = e^{x} I_0(2x)^{f-j} \left(S + \frac{d}{dx}\right)^2 I_0(2x)^j \tag{3.84}$$

where S denotes the gluon structure function enhancement factor. We see that this is a monotonically increasing, quadratic function of S. For large S the generating function can be approximated by

$$\mathcal{G}_S(x) = S^2 e^x I_0(2x)^f \tag{3.85}$$

The coefficients of $\mathcal{G}_S(x)$ may be written $\mathcal{G}_n = C_n S^2$ where the C_n depend on n. We can estimate the 'strength' of the 'S-extended' gluonic amplitudes compared to purely gluonic processes, $\mathcal{G}_n^0 = S^2$, by computing the ratio $r = \lim_{s\to\infty} \mathcal{G}_n^0/\mathcal{G}_n$. These ratios are tabulated below:

The ratio $\mathcal{G}_n^0/\mathcal{G}_n$			
n	$f=3$	$f=4$	$f=5$
2	0.1428	0.1111	0.0909
3	0.0526	0.40	0.0322
4	0.0078	0.0046	0.0030
5	0.0019	0.00108	0.00068
6	0.0003	0.00012	0.000066
7	0.000061	0.000023	0.000011
8	0.96810^{-5}	0.28910^{-5}	0.11410^{-5}

We conclude that for sizeable n the purely gluonic amplitude gives only a very small contribution.

3.3.4 Asymptotic results

It may be interesting to estimate the number of amplitudes for large number of jets. To this end, we would like to obtain the asymptotic form of the generating function for large n. The asymptotic expansion for $I_0(2z)$ is

$$I_0(2z) \sim \frac{e^{2z}}{\sqrt{4\pi z}} \sum_{n\geq 0} \frac{\tau_n}{z^n} \quad , \quad \tau_n = \frac{(2n)!^2}{64^n\ n!^3} \quad , \quad z \to \infty. \tag{3.86}$$

This expansion holds for $\mathrm{Re}(z) > 0$, but we also have $I_0(-z) = I_0(z)$. For the function

$$f(x) = I_0(2x)^p \tag{3.87}$$

the asymptotic expansion is

$$f(x) = N e^{2px} x^{-\frac{p}{2}} \sum_{n\geq 0} \frac{\alpha_n}{x^n} \quad , \quad \alpha_n = \sum_{n_1,\ldots,n_p} \tau_{n_1}\tau_{n_2}\cdots\tau_{n_p}\Theta(n_1+\cdots+n_p = n) \tag{3.88}$$

where $N = (4\pi)^{-\frac{p}{2}}$. So the derivatives in the generating function $\mathcal{G}(x)$, read:

$$\left(1+\frac{d}{dx}\right)^2 f(x) = f(x) + 2f'(x) + f''(x) = Ne^{2px}x^{-\frac{p}{2}}\sum_{n\geq 0}\frac{\beta_n}{x^n} \tag{3.89}$$

where

$$\beta_n = (1+2p)^2\alpha_n - 2(1+2p)(n+\frac{p}{2}-1)\alpha_{n-1} + (n+\frac{p}{2}-1)(n+\frac{p}{2}-2)\alpha_{n-2}, \tag{3.90}$$

and for the generating function we get

$$\mathcal{G}(x) = \frac{1}{(4\pi)^{f/2}}\, e^{x(1+2f)}\, \frac{1}{x^{f/2}}\, \sum_{n\geq 0}\frac{\gamma_n}{x^n} \tag{3.91}$$

where

$$\gamma_n = \sum_{n_1,n_2\geq 0} \Theta(n_1+n_2=n)\; \alpha_{n_1}(f-j)\; \beta_{n_2}(j) \tag{3.92}$$

The first few γ's for various numbers of initial and final flavours, are shown in the next table.

Number of flavours		γ_0	γ_1	γ_2	γ_3
$f=3$	$j=2$	25	$-85/16$	$249/512$	$1873/8192$
	$j=3$	49	$-189/16$	$177/512$	$1337/8192$
$f=4$	$j=2$	25	$-15/4$	$19/32$	$101/256$
	$j=3$	49	$-35/4$	$15/32$	$109/256$
	$j=4$	81	$-63/4$	$3/32$	$93/256$
$f=5$	$j=2$	25	$-35/16$	$409/512$	$4871/8192$
	$j=3$	49	$-91/16$	$401/512$	$6143/8192$
	$j=4$	81	$-171/16$	$273/512$	$6831/8192$
	$j=5$	121	$-275/16$	$25/512$	$6935/8192$

The most important term in the series is of course the first

$$\gamma_0 = \alpha_0(f-j)\;\beta_0(j) = \alpha_0(f-j)\;(1+2j)^2\;\alpha_0(j) = (1+2j)^2 \tag{3.93}$$

Keeping only this term in the generating function we have

$$\mathcal{G}(x) \sim \frac{1}{(4\pi)^{f/2}}\, e^{x(1+2f)}\, \frac{1}{x^{f/2}}\, (1+2j)^2 \quad , \quad x\to\infty \tag{3.94}$$

Let us, now, assume that we want to include the first K terms in the asymptotic expansion of $\mathcal{G}(x)$, that is, we set γ_j to zero for $j > K$. The Borel transform

$$\mathcal{F}(x) = \int_0^\infty dy\ y^{K+f/2} e^{-y} \mathcal{G}(xy) \tag{3.95}$$

has the expansion

$$\mathcal{F}(x) = \sum_{n\geq 0} \Gamma(n + K + f/2 + 1) \mathcal{G}_n\ x^n \ , \tag{3.96}$$

where $\mathcal{G}(x) = \sum_{n\geq 0} \mathcal{G}_n x^n$; our approach consists in finding the coefficients of $\mathcal{F}(x)$ by studying its singularity structure. The integral for $\mathcal{F}(x)$ can be written as

$$\begin{aligned} \mathcal{F}(x) &= \frac{1}{(4\pi)^{f/2}} \int_0^\infty dy\ \exp[(-y + xy(2f+1))] \sum_{k=0}^{K} \gamma_k \frac{y^{K-k}}{x^{k+f/2}} \\ &= \frac{1}{(4\pi)^{f/2}} \sum_{k=0}^{K} \frac{\gamma_k (K-k)!}{x^{k+f/2}(1 - x(2f+1))^{K-k+1}} \ . \end{aligned} \tag{3.97}$$

This expression is has a pole at $x_0 = 1/(2f+1)$. Note that, due to our use of the factor $y^{K+f/2}$, the integral (3.95) is indeed dominated by large values of xy when x approaches x_0, thus justifying the use of the asymptotic expression (3.91). Furthermore, there is of course a similar singularity which appears when we use negative x values: however, since that is located at $-1/(2f-1)$ and hence further away from the origin than x_0, this pole will give exponentially suppressed contributions which will not show up in our result for $\mathcal{G}_n$. The k^{th} term in the series for $\mathcal{F}(x)$ is seen to contain poles at $x = x_0$ of order up to and including $K - k + 1$:

$$\begin{aligned} &x^{-k-f/2}(1 - \frac{x}{x_0})^{-K+k-1} = \\ &\qquad \frac{1}{x_0^{k+f/2}} \sum_{r=0}^{K-k} \frac{(k + f/2 + r)!}{r!(k + f/2 - 1)!} (1 - \frac{x}{x_0})^{-K+k+r-1} \ + \ \text{regular terms} \ . \end{aligned} \tag{3.98}$$

The dominant behaviour of the coefficient of x^n in the series expansion of this term is, therefore,

$$\begin{aligned} &\frac{1}{x_0^{n+k+f/2}} \sum_{r=0}^{K-k} \frac{(k + f/2 + r)!}{r!(k + f/2 - 1)!} \frac{(n + K - k - r)!}{n!(K - k - r)!} = \\ &\qquad \frac{1}{x_0^{n+k+f/2}} \frac{(n + K + f/2)!}{(K-k)!(n + k + f/2)!} \ . \end{aligned} \tag{3.99}$$

Inserting this in the expression for $\mathcal{F}(x)$ and dividing by the factor $\Gamma(n+K+f/2+1)$ to get the coefficient $\mathcal{G}_n$, we see that K drops out from the expression, so that we may take it as large as we please. The resultant form for $\mathcal{G}_n$ is, therefore

$$\mathcal{G}_n \sim \mathcal{G}_n^{asy} = \frac{(2f+1)^{n+f/2}}{(4\pi)^{f/2}} \sum_{k\geq 0} \frac{\gamma_k (2f+1)^k}{\Gamma(n+k+f/2+1)} \quad , \quad n \to \infty. \tag{3.100}$$

In order to estimate how accurate this asymptotic expansion is, we have calculated the ratio between the exact and the "asymptotic" number of processes. The results are shown in the next table, where we have recorded the way these numbers improve as we add more terms in the asymptotic expansion of the generating function. Thus n_0 is such that $\mathcal{G}_n/\mathcal{G}_n^{asy}$ is between 0.95 and 1.05 for all $n \geq n_0$, when we include only the first term in the expansion, i.e. the term that contains γ_0. Similarily, n_1 is the number of jets when we include γ_0 and γ_1, n_2 when we include γ_0, γ_1 and γ_2, etc.

Number of flavours		n_0	n_1	n_2	n_3
$f=3$	$j=2$	26	6	6	6
	$j=3$	31	5	4	5
$f=4$	$j=2$	21	8	8	6
	$j=3$	28	8	6	6
	$j=4$	31	7	7	7
$f=5$	$j=2$	11	12	10	8
	$j=3$	21	12	10	10
	$j=4$	25	12	10	10
	$j=5$	29	12	11	10

Note that on some occasions, like for example $f=5,\ j=2$, the number increases as we add more terms in the expansion. But this is due to a small increase of the ratio which is improved immediately when we add the next term.

3.3.5 Distinct amplitudes

In the above we have shown how *all* amplitudes contributing to a certain cross section can be enumerated. This would also, then, be the computational complexity in an approach where each amplitude is calculated from scratch. However, there is of course a simplification owing to the fact that amplitudes that differ only by a relabelling of the (massless!) quark flavours are equal apart from a trivial difference in the structure function. It therefore behooves us to take this simplification into account.

Now it must be kept in mind that, when a quark flavour occurs in the initial state, we should not relabel it since that is also taken care of by the factors $2j$, $j(j-1)$ etcetera in table 1. Only those quark flavours that do not occur in the initial state may be relabelled. At this point it should be mentioned that in keeping the treatment essentially the same as in the previous sections, we count final states that differ by a relabelling of the momenta as different. This results for example, in treating the final states $u\bar{u}d\bar{d}$ and $d\bar{d}u\bar{u}$ as distinct. From a practical point of view this state should be counted once. We give a derivation of the number of distinct processes *without* momenta relabelling in Appendix B.

Let us perform the relabelling of flavours in such a way that the relabelled flavours occur in order of increasing multiplicity. As an example, in the process $gg \to X$ this means that instead of

$$A(x) = \sum_{n_{0,1,\ldots,f}\geq 0} \frac{n! x^{n_0+2(n_1+\cdots+n_f)}}{n_0!(n_1!)^2\cdots(n_f!)^2} \quad , \tag{3.101}$$

we have to determine, rather,

$$\tilde{A}_f(x) = \sum_{n_0\geq 0} \sum_{0\leq n_1\leq n_2\leq\cdots\leq n_f} \frac{n! x^{n_0+2(n_1+\cdots+n_f)}}{n_0!(n_1!)^2\cdots(n_f!)^2} \quad ; \tag{3.102}$$

likewise, for the process $gq \to X$ we have to compute

$$\tilde{B}_f(x) = \sum_{n_{0,1}\geq 0} \sum_{0\leq n_2\leq n_3\leq\cdots\leq n_f} \frac{n! x^{n_0+1+2(n_1+\cdots+n_f)}}{n_0! n_1!(n_1+1)!(n_2!)^2\cdots(n_f!)^2} \quad . \tag{3.103}$$

It is important to note that those quark flavours that can be relabelled occur symmetrically in these sums.

The straightforward implementation of such inequalities appears to lead to horrendous complications. An exception is the following generating function:

$$Z_f(x) = \sum_{0\leq n_1\leq n_2\leq\cdots\leq n_f} x^{n_1+n_2+\cdots+n_f} = \frac{1}{(1-x)(1-x^2)(1-x^3)\cdots(1-x^f)} \quad , \tag{3.104}$$

familiar from the theory of partitions [Hardy and Wright, 1988].

In fact, we may employ the symmetry in the relabelled indices. To see how this works, let us symmetrize the case $f = 2$:

$$\theta(n_1 \leq n_2) \to \frac{1}{2}(\theta(n_1 \leq n_2) + \theta(n_2 \leq n_1)) = \frac{1}{2}(1 + \theta(n_1 = n_2)) \ . \tag{3.105}$$

This can be obviously extended to larger f: the inequalities lead to a combination of terms with no restriction, terms where two labels are equated, terms where three labels are equated, terms where four labels are grouped in two pairs of equal ones, and so on. Using the function $Z(x)$, we can convieniently determine the various coefficients by working out how $Z_f(x)$ can be split up in the corresponding way. Again for the case $f = 2$, this means writing

$$Z_2(x) = \frac{\alpha}{(1-x)^2} + \frac{\beta}{(1-x^2)} \ , \tag{3.106}$$

and solving this for general x gives, indeed, $\alpha = \beta = 1/2$. As usual in the theory of partitions, a result for general f is prohibitively complicated, and therefore we give only the first few values of f:

$$\begin{aligned}
Z_2(x) &= \frac{1}{2}\frac{1}{(1-x)^2} + \frac{1}{2}\frac{1}{(1-x^2)} \ , \\
Z_3(x) &= \frac{1}{6}\frac{1}{(1-x)^3} + \frac{1}{2}\frac{1}{(1-x)(1-x^2)} + \frac{1}{3}\frac{1}{(1-x^3)} \ , \\
Z_4(x) &= \frac{1}{24}\frac{1}{(1-x)^4} + \frac{1}{4}\frac{1}{(1-x)^2(1-x^2)} + \frac{1}{3}\frac{1}{(1-x)(1-x^3)} \\
&\quad + \frac{1}{8}\frac{1}{(1-x^2)^2} + \frac{1}{4}\frac{1}{(1-x^4)} \ , \\
Z_5(x) &= \frac{1}{120}\frac{1}{(1-x)^5} + \frac{1}{12}\frac{1}{(1-x)^3(1-x^2)} + \frac{1}{6}\frac{1}{(1-x)^2(1-x^3)} \\
&\quad + \frac{1}{4}\frac{1}{(1-x)(1-x^4)} + \frac{1}{8}\frac{1}{(1-x)(1-x^2)^2} + \frac{1}{6}\frac{1}{(1-x^2)(1-x^3)} \\
&\quad + \frac{1}{5}\frac{1}{(1-x^5)} \ .
\end{aligned} \tag{3.107}$$

The result for $\tilde{A}(x)$ in these cases is therefore:

$$\begin{aligned}
\tilde{A}_1(x) &= e^x H_2(x) \ , \\
\tilde{A}_2(x) &= \frac{e^x}{2}\left(H_2(x)^2 + H_4(x)\right) \ , \\
\tilde{A}_3(x) &= \frac{e^x}{6}\left(H_2(x)^3 + 3H_2(x)H_4(x) + 2H_6(x)\right) \ , \\
\tilde{A}_4(x) &= \frac{e^x}{24}\left(H_2(x)^4 + 6H_2(x)^2 H_4(x) + 8H_2(x)H_6(x)\right. \\
&\qquad \left. +3H_4(x)^2 + 6H_8(x)\right) \ , \\
\tilde{A}_5(x) &= \frac{e^x}{120}\left(H_2(x)^5 + 10H_2(x)^3 H_4(x) + 20H_2(x)^2 H_6(x) + 30H_2(x)H_8(x)\right. \\
&\qquad \left. +15H_2(x)H_4(x)^2 + 20H_4(x)H_6(x) + 24H_{10}(x)\right) \ . \qquad (3.108)
\end{aligned}$$

These identities can easily be checked explicitly to modest order in x. Here, we have introduced the class of generalized hypergeometric functions

$$H_m(x) = \sum_{n\geq 0}\left(\frac{x^n}{n!}\right)^m \ . \qquad (3.109)$$

Obviously, $H_1(x) = e^x$, while $H_2(x) = I_0(2x)$. The rest of the cases are treated in a similar fashion. The number of dinstinct amplitudes that need to be calculated contains:

$$\begin{aligned}
\tilde{\mathcal{B}}(x) &= I_0'(2x)\tilde{A}_{f-1}(x) \qquad (3.110) \\
\tilde{\mathcal{C}}(x) &= \tilde{A}_{f-1}(x)\cdot\{2I_0''(2x) - I_0(2x)\} \qquad (3.111) \\
\tilde{\mathcal{D}}(x) &= \tilde{A}_{f-2}(x)\left(I_0'(2x)\right)^2 \qquad (3.112)
\end{aligned}$$

The generating function $\tilde{\mathcal{G}}$ for the dinstict amplitudes can be written as in (3.80):

$$\tilde{\mathcal{G}}(x) = \tilde{\mathcal{A}}_f(x) + 2I_0(2x)\tilde{\mathcal{A}}_{f-1}(x) + 4\tilde{\mathcal{B}}(x) + 2\tilde{\mathcal{C}}(x) + 6\tilde{\mathcal{D}}(x) \qquad (3.113)$$

Note the occurence of coefficients 4 and 6, which are dictated by a careful examination of the differing initial states that contribute. Some numbers for the case of $f = 3, 4, 5$ flavours, are shown in the following table

Total number of dinstinct amplitudes			
n	$f=3$	$f=4$	$f=5$
2	35	35	35
3	123	123	123
4	777	777	777
5	3,853	3,853	3,853
6	25,327	31,087	31,087
7	139,975	200,455	200,455
8	870,485	1,676,885	1,999,445

Note that for small n the numbers coincide: this is due to the fact that, $n = 4$, say, allows no room for 4 different quark flavours to occur in one diagram, and the difference between $f = 3$ and $f = 4$ can therefore only appear for $n \geq 6$. This is reflected in the fact that $\tilde{\mathcal{A}}_f(x)$ coincides with $\tilde{\mathcal{A}}_{f-1}(x)$ up to the x^{2f} term.

In order to estimate the large x expansion of the generating function, as in section 2, we note that $H_f(x)$ is

$$H_f(x) \sim \frac{e^{2xf}}{(4\pi)^{1/2}x^{1/2}}\left(1+\mathcal{O}(\frac{1}{x})\right) \quad , \quad x \to \infty \tag{3.114}$$

In the Appendix we show how the asymptotic expansion can be computed systematically and using this, we can approximate $\tilde{\mathcal{A}}_f(x)$ by

$$\tilde{\mathcal{A}}_f(x) = \frac{1}{f!}H_2^f(x) + \frac{1}{2(f-2)!}H_2^{f-2}(x)H_4(x) \tag{3.115}$$

taking into account equations (3.108) and keeping only the largest powers of x. The second term in the previous equation, gives $\frac{1}{\sqrt{x}}$ corrections to the leading result. Using this and the derivatives of the Bessel function

$$I_0'(2x) \quad , \quad I_0''(2x) \sim H_2(x)\left(1+\mathcal{O}(\frac{1}{x})\right) \quad , \quad x \to \infty \tag{3.116}$$

we can estimate the large x expansion of the functions in (3.110-3.112):

$$\tilde{\mathcal{B}}(x) \sim \tilde{\mathcal{A}}_{f-1}(x)H_2(x) = \frac{1}{(f-1)!}H_2^f(x) + \frac{1}{2(f-3)!}H_2^{f-2}(x)H_4(x) \tag{3.117}$$

$$\tilde{\mathcal{C}}(x) \sim \tilde{\mathcal{A}}_{f-1}(x)\left(I_0''(2x) - I_0(2x)\right) = \tilde{\mathcal{A}}_{f-1}(x)H_2(x) = \tilde{\mathcal{B}}(x) \tag{3.118}$$

$$\tilde{\mathcal{D}}(x) \sim \tilde{\mathcal{A}}_{f-2}(x)(I_0')^2 = \frac{1}{(f-2)!}H_2^f(x) + \frac{1}{2(f-4)!}H_2^{f-2}(x)H_4(x) \tag{3.119}$$

and the generating function:

$$\tilde{\mathcal{G}}(x) \sim \frac{1+2f+6f^2}{f!} H_2^f(x) + \frac{6f^2-22f+2}{2(f-2)!} H_2^{f-2}(x) H_4(x) \tag{3.120}$$

We can also compute the coefficients of the asymptotic expansion of $\tilde{\mathcal{G}}(x)$. To this end we calculate the coefficient in the expansion of the functions $H_2(x), H_4(x)$ using the Borel transform. In particular for $H_2(x)$ we define

$$P(x) = e^x H_2^f(x) = \sum_n K_n x^n \tag{3.121}$$

To estimate the coefficients K_n we perform a transform on $P(x)$:

$$\int_0^\infty dy e^{-y} y^{f/2} P(xy) = \sum_n K_n \Gamma(n + \frac{f}{2} + 1) x^n \tag{3.122}$$

and we get

$$K_n \sim \frac{1}{(4\pi)^{f/2}} \frac{(1+2f)^{n+f/2}}{\Gamma(n+\frac{f}{2}+1)} \tag{3.123}$$

Similarily, for $H_4(x)$, approximated by

$$H_4(x) \sim \frac{e^{4x}}{(32\pi^3)^{1/2} x^{3/2}} \quad , \quad x \to \infty \tag{3.124}$$

we use $Q(x) = e^x H_2^{f-2}(x) H_4(x) = \sum_n L_n x^n$. Performing a Borel transform we get

$$\int_0^\infty dy e^{-y} y^{\frac{f}{2}+\frac{1}{2}} Q(xy) = \sum_n L_n \Gamma(n + \frac{f}{2} + \frac{3}{2}) x^n \tag{3.125}$$

and for the coefficients

$$L_n \sim \frac{1}{(4\pi)^{f/2}} \frac{(1+2f)^{n+f/2+1/2}}{\sqrt{2\pi}\Gamma(n+\frac{f}{2}+\frac{3}{2})} = K_n \left(\frac{1+2f}{2\pi}\right)^{1/2} \frac{\Gamma(n+\frac{f}{2}+1)}{\Gamma(n+\frac{f}{2}+\frac{3}{2})} \tag{3.126}$$

Using these coefficients we can estimate the coefficients for the generating function in (3.120).

3.4 Appendix A: Asymptotic form of $H_m(x)$

Here we study the asymptotic form of the function $H_m(x)$, which was defined as

$$H_m(x) = \sum_{n\geq 0} \frac{x^{mn}}{(n!)^m} \tag{3.127}$$

One can easily see that the following relation holds

$$\begin{aligned} H_m(x) &= \frac{1}{2\pi i}\oint \frac{dz}{z} H_{m-1}(xz) H_1(\frac{x}{z}) \\ &= \frac{1}{(2\pi i)^{m-1}} \oint \cdots \oint \frac{dz_1}{z_1}\cdots\frac{dz_{m-1}}{z_{m-1}} H_1(xz_1)H_1(xz_2)\cdots H_1(\frac{x}{z_1 z_2\cdots z_{m-1}}) \end{aligned} \tag{3.128}$$

If we put $z_i = e^{i\phi_i}$ the integral becomes

$$H_m(x) = \frac{1}{(2\pi)^{m-1}} \int_0^{2\pi}\cdots\int_0^{2\pi} d\phi_1\cdots d\phi_{m-1} e^{xW} \tag{3.129}$$

where

$$W = e^{i\phi_1} + \cdots e^{i\phi_{m-1}} + e^{-i(\phi_1+\cdots\phi_{m-1})} \tag{3.130}$$

We can estimate this integral by using the saddle point approximation. The first few derivatives of W are

$$\begin{aligned} \frac{\partial W}{\partial\phi_k} &= i\left(e^{i\phi_k} - e^{-i(\phi_1+\cdots\phi_{m-1})}\right) , \\ \frac{\partial^2 W}{\partial\phi_k\partial\phi_\ell} &= -\left(e^{i\phi_k}\delta_{k\ell} + e^{-i(\phi_1+\cdots\phi_{m-1})}\right) , \\ \frac{\partial^3 W}{\partial\phi_k\partial\phi_\ell\partial\phi_p} &= -i\left(e^{i\phi_k}\delta_{k\ell p} - e^{-i(\phi_1+\cdots\phi_{m-1})}\right) , \\ \frac{\partial^4 W}{\partial\phi_k\partial\phi_\ell\partial\phi_p\partial\phi_q} &= \left(e^{i\phi_k}\delta_{k\ell pq} + e^{-i(\phi_1+\cdots\phi_{m-1})}\right) \quad ,\ldots \end{aligned} \tag{3.131}$$

The saddle point can be found from the first derivative, and it is the solution of the equation

$$e^{i\phi} + e^{-i(m-1)\phi} = 0 \to e^{im\phi} = 1 \to \phi = \frac{2\pi}{m}k, \quad k = 0, 1, \ldots m-1 \tag{3.132}$$

The value of xW at the saddle point is $x((m-1)e^{i\phi}+e^{i\phi}) = mxe^{i\phi}$. The saddle point that gives the largest real part of $mxe^{i\phi}$ is the one that dominates. We see that the function has an m-fold symmetry: if we restrict ourselves to $|arg(x)| < \frac{\pi}{m}$ the saddle point that dominates is $\phi = 0$. The derivatives now take the values:

$$\begin{aligned} \frac{\partial^2 W}{\partial\phi_k\partial\phi_\ell} &= -\left(\delta_{k\ell}+1\right) \ , \\ \frac{\partial^3 W}{\partial\phi_k\partial\phi_\ell\partial\phi_p} &= -i\left(\delta_{k\ell p}-1\right) \ , \\ \frac{\partial^4 W}{\partial\phi_k\partial\phi_\ell\partial\phi_p\partial\phi_q} &= \left(\delta_{k\ell pq}+1\right) \ , \ldots \end{aligned} \tag{3.133}$$

and the exponent is

$$xW = mx - \frac{x}{2}\sum_{k\ell}\left(\delta_{k\ell}+1\right)\phi_k\phi_\ell - \frac{ix}{6}\sum_{k\ell p}\left(\delta_{k\ell p}-1\right)\phi_k\phi_\ell\phi_p + \frac{x}{24}\sum_{k\ell pq}\left(\delta_{k\ell pq}+1\right)\phi_k\phi_\ell\phi_p\phi_q + \cdots \tag{3.134}$$

This is reminiscent of a zero-dimensional scalar field theory with vertices of arbitrary multiplicity, with the Feynman rules

$\frac{1}{x}\left(\delta_{\mu\nu}-\frac{1}{m}\right)$ 

,

$-ix\left(\delta_{\mu\nu\alpha}-1\right)$ 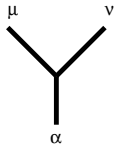

,

$x\left(\delta_{\mu\nu\alpha\beta}+1\right)$ 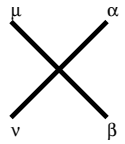

,

$ix\left(\delta_{\mu\nu\alpha\beta\rho}-1\right)$ 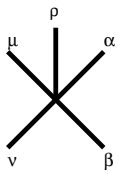

,

$-x\left(\delta_{\mu\nu\alpha\beta\rho\sigma}+1\right)$ 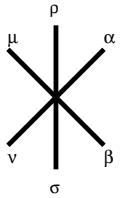

, ...

where $\delta_{\mu\nu\alpha} = \delta_{\mu\nu}\delta_{\mu\alpha}$, $\delta_{\mu\nu\alpha\beta} = \delta_{\mu\nu}\delta_{\mu\alpha}\delta_{\mu\beta}$, and so on. We can use the familiar tools of field theory to evaluate the integral. The first subleading term is computed by taking into account the two-loop diagrams that contribute. The result is

$$\frac{1}{8}\;\text{ 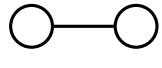 }+\frac{1}{8}\;\text{ 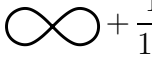 }+\frac{1}{12}\;\text{  }=0+\frac{(m-1)^2}{8mx}-\frac{(m-1)(m-2)}{12mx}=\frac{m^2-1}{24mx} \tag{3.135}$$

where the factors in front of the diagrams are symmetry factors. The next subleading term can be computed by including three-loop graphs. Due to the fact that  $= 0$, there are 8 non-zero connected three-loop diagrams, and in addition to these we must also include the disconnected diagrams that are shown below. The contributing three-loop diagrams and their values, are:

 $\dfrac{(m-1)^3}{m^2}$

 $\dfrac{(m-1)^2(m-2)}{m^2}$

 $\dfrac{(m-1)((m-1)^3+1)}{m^3}$

 $\dfrac{(m-1)^3}{m^2}$

 $\dfrac{(m-1)(m-2)(m-3)}{m^2}$

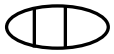 $\dfrac{(m-1)(m-2)^2}{m^2}$

 $\dfrac{(m-1)(m-2)^2}{m^2}$

 $\dfrac{(m-1)^2(m-2)}{m^2}$

Putting it all together we get the next term in the expansion of $H_m(x)$ (including the symmetry factors shown below) is:

$$+ \quad \frac{1}{48}$$  $$+ \frac{1}{12}$$  $$+ \frac{1}{48}$$  $$+ \frac{1}{16}$$  $$+ \frac{1}{24}$$  $$+ \frac{1}{16}$$ 

$$+ \quad \frac{1}{8}$$  $$+ \frac{1}{8}$$  $$+ \frac{1}{2}\Big($$ $$\Big)^2$$

$$= \quad \frac{1}{1152m^2x^2}(m-1)(m^3+289m^2-1129m+1175) \tag{3.136}$$

The result for the asymptotic expansion of $H_m(x)$ to this order is:

$$H_m(x) \sim \frac{e^{mx}}{\sqrt{m(2\pi x)^{m-1}}}\{1+\frac{m^2-1}{24mx}+\frac{1}{1152m^2x^2}(m-1)(m^3+289m^2-1129m+1175)+\mathcal{O}(\frac{1}{x^3})\} \tag{3.137}$$

and higher terms can be obtained in a similar way.

3.5 Appendix B: Distinct processes revisited

In Section 3.3.5 we calculated all the distinct processes that contribute to a particular point in phase space. However when integration over phase space is what we are interested in, then the relabelling of the momenta is 'redundant'. In this appendix we discuss how to count (and identify) distinct processes without any 'redundancy' due to relabelling of momenta in the final state. We start by tabulating the five types of initial states (not counting trivial charge conjugation), with the corresponding number of distinct processes, and the functions needed to compute their multiplicity factors, in a slightly different way than in Section 3.3.1. We denote by n the number of final state partons:

initial-state type		distinct processes	multiplicity factor
A	(gg)	$C_1(n)$	$\chi(n_0, n_1, \ldots, n_f; f)$
B	$(q\bar{q})$	$C_2(n)$	$\chi(n_0, n_2, \ldots, n_f; f-1)$
C	$(gq$ and $qg)$	$C_2(n-1)$	$\chi(n_0, n_2, \ldots, n_f; f-1)$
D	(qq)	$C_2(n-2)$	$\chi(n_0, n_2, \ldots, n_f; f-1)$
E	$(qq'$ and $q\bar{q}')$	$C_3(n-2)$	$\chi(n_0, n_3, \ldots, n_f; f-2)$

In order to clarify what we mean we consider the example of the type A initial state. Each distinct process is defined by an array $(n_0, n_1, \ldots, n_f)$. For instance, in the case of four-jet production we have

$$
\begin{array}{ll}
(4,0,0,0,0,0) & gg \to gggg \\
(2,1,0,0,0,0) & gg \to ggq\bar{q} \\
(0,2,0,0,0,0) & gg \to q\bar{q}q\bar{q} \\
(0,1,1,0,0,0) & gg \to q\bar{q}r\bar{r}
\end{array}
$$

Therefore, in order to count the distinct processes we need the following three functions:

$$C_1(n) = \sum_{n_0+2n_1+\ldots+2n_f=n} \Theta(n_1 \geq n_2 \geq \ldots \geq n_f)$$

$$C_2(n) = \sum_{n_0+2n_1+\ldots+2n_f=n} \Theta(n_2 \geq n_3 \geq \ldots \geq n_f)$$

and

$$C_3(n) = \sum_{n_0+2n_1+\ldots+2n_f=n} \Theta(n_3 \geq n_4 \geq \ldots \geq n_f)$$

Of course each distinct process, given by the array $(n_0, n_1, \ldots, n_f)$ has a multiplicity factor that is easily computed:

$$\chi(n_0, n_1, \ldots, n_f; f) = n_f(n_f - 1)...(n_f - j + 1)/j!$$

where j is defined as

$$
\begin{array}{lll}
j = f & \text{if} & \prod_{i=1}^{f} n_i \neq 0 \\
j = f-1 & \text{if} & \prod_{i=1}^{f-1} n_i \neq 0 \\
\ldots & & \\
j = 1 & \text{if} & n_1 \neq 0 \\
j = 0 & \text{otherwise} &
\end{array}
$$

Results for $f = 5$ final state flavours, and $f = 4$ initial state flavours, are shown in the table of section 2, in the discussion of flavour treatment, just to compare with ref. [Kuijf, 1991].

Moreover it is very easy to produce the list of the distinct processes to be computed for each case as well as the multiplicity factors χ. A code doing this is available.

To study high-n behaviour we may use the generating function technique. Then we get

$$\begin{aligned} F_1(x) &= \sum_{n=0}^{\infty} C_1(n)x^n = \frac{1}{(1-x)} \prod_{j=1}^{f} \frac{1}{(1-x^{2j})} \\ F_2(x) &= \sum_{n=0}^{\infty} C_2(n)x^n = \frac{1}{(1-x)(1-x^2)} \prod_{j=1}^{f-1} \frac{1}{(1-x^{2j})} \\ F_3(x) &= \sum_{n=0}^{\infty} C_3(n)x^n = \frac{1}{(1-x)(1-x^2)^2} \prod_{j=1}^{f-2} \frac{1}{(1-x^{2j})} \end{aligned}$$

As one can easily see, that the order of the pole at $x = 1$ is always given by $f + 1$.

Our results may be compared directly to those obtained in ref. [Kuijf, 1991]. In fact, using our method, we were able to detect several errors in Table 9.3 page 125, among which the fact that a processes is missing for the cases $m = 6$ and $m = 7$, namely $qr \to qrr\bar{r}(g)$. Correcting for this error we get full agreement.

Chapter 4

Colour connections and antennas

4.1 Introduction

The amplitude of any process in QCD can be factorised in a part that contains only the colour information and a part with the momenta. For example for a process with n gluons the amplitude can be written as

$$M(1,2,\ldots,n) \equiv \sum_{P(1,\ldots,n-1)} Tr(t^{a_1}t^{a_2}\cdots t^{a_n})\, C(1,2,\ldots,n) \tag{4.1}$$

where t^{a_i} are the colour matrices in the fundamental representation and $C(1,2,\ldots,n)$ are the so called dual amplitudes, which depend on the momenta and the helicities of the gluons but *not* the colour. $P(1,\ldots,n-1)$ denotes all the permutations among the $n-1$ gluon labels. When the process involves quarks as well, we can write down a similar result for the amplitude

$$M(q_\alpha,\bar{q}_\beta,1,\ldots,n) \equiv \sum_{P(1,\ldots,n)} (t^{a_1}t^{a_2}\cdots t^{a_n})_{\alpha\beta}\, C(q,\bar{q},1,2,\ldots,n) \tag{4.2}$$

The dual amplitudes are gauge invariant, cyclically-symmetric functions of the momenta and the helicities. They obey some additional properties which makes a reduced number of them truly independent [Giele, 1989]. However, even in that factorised form, it is still quite difficult to perform analytic calculations even when the number of partons is small (> 5). For instance, it is no easy matter to square (4.1) analytically to obtain a cross-section. Several methods have been developed in the past to tackle the problem analytically and numerically [Giele, 1989, Kuijf, 1991, Caravaglios et al., 1999, Draggiotis et al., 1998]. In this chapter we concern ourselves

with the colour part of the amplitude only. We introduce a new way to describe colour, based on a projection to a continuum complex space. We derive the relevant representations of the colour for gluons and quarks and use them to deal with the problem of generation of the colour part of the amplitude.

4.2 Colour generation

We assign to a fermion a complex vector z_i, where the index runs from 1 to 3, representing its colour content. These vectors parametrize the 5-dimensional representation of $SU(3)$ on the sphere and are subjected to the constraint:

$$z \cdot \bar{z} = z_i \, \bar{z}^i = 1 \tag{4.3}$$

In this space, integration is defined through the proper definition for the invariant group measure, $[dz]$:

$$[dz] \equiv d^N z \; d^N \bar{z} \; \delta \left(z_i \cdot \bar{z}_i - 1 \right) \frac{\Gamma(N)}{(2\pi)^N} \tag{4.4}$$

such that

$$\int [dz] = 1 \tag{4.5}$$

It is easy to see that

$$\begin{aligned} \int d[z] z^i \bar{z}_j &= \frac{1}{N} \delta^i{}_j \;\; , \\ \int d[z] z^i z^k \bar{z}_j \bar{z}_l &= \frac{1}{N(N+1)} \left(\delta^i{}_j \delta^k{}_l + \delta^i{}_l \delta^k{}_j \right) \;\; . \end{aligned} \tag{4.6}$$

The first of these identities is easily seen to be true by contracting both sides with $\delta^j{}_i$. For the second we denote the right hand side as

$$\int d[z] z^i z^k \bar{z}_j \bar{z}_l = K \delta^i{}_j \delta^k{}_l + M \delta^i{}_l \delta^k{}_j \tag{4.7}$$

Contracting both sides with $\delta^j{}_i \delta^l{}_k$ and $\delta^j{}_k \delta^l{}_i$, gives two conditions for the constants:

$$\begin{aligned} KN^2 + MN &= 1 \\ KN + MN^2 &= 1 \end{aligned}$$

using (4.3). Solving these we get the desired result. Tensors with unequal numbers of colours and anti-colours average to zero.

We construct gluonic colours η^a for a theory with N quark colours: $a = 1, 2, \ldots, N^2 - 1$, and

$$\left\langle \eta^a \bar{\eta}^b \right\rangle = \delta^{ab} \quad , \quad \langle \bar{\eta} \cdot \eta \rangle = N^2 - 1 \ . \tag{4.8}$$

so that we actually are discussing sums over gluon colours rather than averages. To do so, we assume two N-dimensional complex vectors y and z, distributed under the normalized measure proportional to

$$\delta(\bar{z} \cdot z - 1)\delta(\bar{y} \cdot y - 1)\delta(\bar{y} \cdot z) \ . \tag{4.9}$$

First, we consider

$$\xi^i{}_j = \int d[y] \; y^i \bar{y}_j \ = A\delta^i{}_j - B z^i \bar{z}_j \ . \tag{4.10}$$

We have

$$\int d[y] y^i \bar{y}_j \ = \ \frac{1}{N-1}(\delta^i{}_j - z^i \bar{z}_j) \ , \tag{4.11}$$

Also, we use the representation-independent identity for the traceless hermitian colour matrices t^a:

$$\sum_a (t^a)^i{}_j (t^a)^k{}_l = \frac{1}{2}\left(\delta^i{}_l \delta^k{}_j - \frac{1}{N}\delta^i{}_j \delta^k{}_l\right) \ , \tag{4.12}$$

which gives

$$\sum_a \mathrm{Tr}\,(t^a t^a) = \frac{1}{2}(N^2 - 1) \tag{4.13}$$

as a check. The gluon colour vector is defined as

$$\eta^a = C \bar{y}_i (t^a)^i{}_j z^j \quad \Rightarrow \quad \bar{\eta}^b = C \bar{z}_i (t^b)^i{}_j y^j \ , \tag{4.14}$$

with C a real number to be determined. We write

$$\begin{aligned}\left\langle \eta^a \bar{\eta}^b \right\rangle &= \int d[z]\, d[y] C^2 \bar{y}_i (t^a)^i{}_j z^j \bar{z}_k (t^b)^k{}_l y^l \\ &= \frac{C^2}{N-1} \int d[z] \left((t^a)^i{}_j z^j \bar{z}_k (t^b)^k{}_i - \bar{z}_i (t^a)^i{}_j z^j \bar{z}_k (t^b)^k{}_l z^l \right) \\ &= \frac{C^2}{N-1} \left(\frac{1}{N} \mathrm{Tr}\left(t^a t^b\right) - \frac{1}{N(N+1)} \left(\mathrm{Tr}\left(t^a\right) \mathrm{Tr}\left(t^b\right) + \mathrm{Tr}\left(t^a t^b\right) \right) \right) \\ &= \frac{C^2}{2(N^2-1)} \delta^{ab} \quad , \end{aligned} \tag{4.15}$$

which leads to

$$C^2 = 2(N^2-1) \ . \tag{4.16}$$

We are interested in colour antennas of the form

$$R_n = \mathrm{Tr}\left(t^{a_1} t^{a_2} \cdots t^{a_n}\right) \eta^{a_1} \eta^{a_2} \cdots \eta^{a_n} \ . \tag{4.17}$$

Since

$$(t^a)^i{}_j \eta^a = C (t^a)^i{}_j (t^a)^k{}_l \bar{y}_k z^l = \frac{C}{2} \left(z^i \bar{y}_j - \frac{1}{N} (\bar{y} z) \delta^i{}_j \right) = \frac{C}{2} z^i \bar{y}_j \ , \tag{4.18}$$

we have

$$R_n = \left(\frac{C}{2} \right)^n (z_1 \cdot \bar{y}_2)(z_2 \cdot \bar{y}_3)(z_3 \cdot \bar{y}_4) \cdots (z_{n-1} \cdot \bar{y}_n)(z_n \cdot \bar{y}_1) \ . \tag{4.19}$$

Let us compute

$$Q_n = \left\langle |R_n|^2 \right\rangle = \mathrm{Tr}\left(t^{a_1} t^{a_2} \cdots t^{a_{n-1}} t^{a_n}\right) \mathrm{Tr}\left(t^{a_n} t^{a_{n-1}} \cdots t^{a_2} t^{a_1}\right) \ . \tag{4.20}$$

First, we integrate over the y's, which results in

$$\begin{aligned} &\int d[y_1 y_2 \cdots y_n]\, |R_n|^2 = \left(\frac{N+1}{2} \right)^n S_n(1,-1) \ , \\ &S_n(a_n, \lambda_n) \equiv \left(1 - |z_1 \bar{z}_2|^2\right) \left(1 - |z_2 \bar{z}_3|^2\right) \left(1 - |z_3 \bar{z}_4|^2\right) \cdots \\ &\qquad \cdots \left(1 - |z_{n-1} \bar{z}_n|^2\right) \left(a_n + \lambda_n |z_n \bar{z}_1|^2\right) \ . \end{aligned} \tag{4.21}$$

Integrating over z_n, we establish that

$$\begin{aligned}
&\int d[z_n] S_n(a_n, \lambda_n) = S_{n-1}(a_{n-1}, \lambda_{n-1}) \ , \\
&a_{n-1} = a_n \frac{N-1}{N} + \lambda_n \frac{1}{N+1} \ , \\
&\lambda_{n-1} = -\lambda_n \frac{1}{N(N+1)} \ .
\end{aligned} \tag{4.22}$$

This is a recursive relation. Let us define

$$\begin{aligned}
\beta_p &= \theta(p=0) + \theta(p>0) \left(\beta_{p-1} \frac{N-1}{N} + \mu_{p-1} \frac{1}{N+1} \right) \ , \\
\mu_p &= -\mu_{p-1} \frac{1}{N(N+1)} \ .
\end{aligned} \tag{4.23}$$

Then,

$$\int d[z_n, z_{n-1}, \ldots, z_{n-p+1}] \ S_n(1,-1) = S_{n-p}(\beta_p, \mu_p) \ . \tag{4.24}$$

The recursion relation has the explicit solution

$$\beta_p = \left(\frac{N-1}{N} \right)^{p+1} + \frac{1}{N} \left(\frac{-1}{N(N+1)} \right)^p \quad , \quad \mu_p = -\left(\frac{-1}{N(N+1)} \right)^p \ . \tag{4.25}$$

Putting $p = n-2$ we have

$$\int d[z_n, z_{n-1}, \ldots, z_3] \ S_n(1,-1) = \left(1 - |\bar{z}_1 z_2|^2\right) \left(\beta_{n-2} + \mu_{n-2} |\bar{z}_2 z_1|^2\right) \ , \tag{4.26}$$

and the final two integrations over z_2 and z_1 (of which the last is trivial) give

$$\left\langle |R_n|^2 \right\rangle = \left(\frac{N+1}{2} \right)^n (\beta_{n-1} + \mu_{n-1}) = \frac{(N^2-1)^n + (-)^n (N^2-1)}{(2N)^n} \ . \tag{4.27}$$

Another way to derive this result, which serves as a check, can be found in the appendix at the end of this chapter.

A last item is the efficiency of the z generation. The z's are, of course generated in the reverse order in which they were integrated, and the distribution of z_{n-p} is proportional to

$$F(z_{n-p}) = \left(1 - |\bar{z}_{n-p+1} z_{n-p}|^2\right) \left(\beta_p + \mu_p |\bar{z}_{n-p} z_1|^2\right) \ . \tag{4.28}$$

Now,

$$\int d[z_{n-p}]F(z_{n-p}) = \beta_{p+1} + \mu_{p+1}|\bar{z}_{n-p+1}z_1|^2 \geq \beta_{p+1} + \min(0,\mu_{p+1}) \ , \tag{4.29}$$

and

$$F(z_{n-p}) \leq \beta_p + \max(0,\mu_p) \ . \tag{4.30}$$

The efficiency is therefore bounded from below by

$$\text{Eff} \geq E_p = \frac{\beta_{p+1} + \min(0,\mu_{p+1})}{\beta_p + \max(0,\mu_p)} \ . \tag{4.31}$$

The result is given below for $1 \leq p \leq 10$.

p	1	2	3	4	5	6	7	8	9	10
E_p	.4731	.5743	.6125	.6381	.6517	.6590	.6628	.6647	.6657	.6662

The efficiency approaches 2/3 for large p, reflecting the fact that the correlation between z_{n-p} and z_1 becomes small if there are many z's in between them.

4.3 Appendix: Colour Traces

Let Ω_k denote a string of k t-matrices, $\Omega_k = t^{a_1}t^{a_2}\cdots t^{a_k}$ and Ω_k^R the same string, in the reversed order (summation over repeated indices implied), $\Omega_k^R = t^{a_k}\cdots t^{a_2}t^{a_1}$. Let O_1 and O_2 denote general $N \times N$ matrices. We then have the following two identities:

$$\begin{aligned} \text{Tr}\,(t^a O_1)\,\text{Tr}\,(t^a O_2) &= \frac{1}{2}\text{Tr}\,(O_1O_2) - \frac{1}{2N}\text{Tr}\,(O_1)\,\text{Tr}\,(O_2) \ , \\ \text{Tr}\,(t^a O_1 t^a O_2) &= \frac{1}{2}\text{Tr}\,(O_1)\,\text{Tr}\,(O_2) - \frac{1}{2N}\text{Tr}\,(O_1O_2) \ . \end{aligned} \tag{4.32}$$

We want to compute traces like

$$L_k \equiv \text{Tr}\left(\Omega_k\Omega_k^R\right) \ , \quad K_k \equiv \text{Tr}\,(\Omega_k)\,\text{Tr}\left(\Omega_k^R\right) \tag{4.33}$$

We have for L_k

$$\begin{aligned} L_k &\equiv \text{Tr}\left(\Omega_k\Omega_k^R\right) = (\Omega_k)_{ij}(\Omega_k^R)_{ji} = t^a_{im}(\Omega_{k-1})_{mj}(\Omega_{k-1}^R)_{jl}\ t^a_{li} \\ &= t^a_{im}\ t^a_{li}(\Omega_{k-1})_{mj}(\Omega_{k-1}^R)_{jl} = \frac{1}{2}\left(\delta_{ii}\delta_{ml} - \frac{1}{N}\delta_{im}\delta_{li}\right)(\Omega_{k-1})_{mj}(\Omega_{k-1}^R)_{jl} \\ &= \frac{1}{2}\{N\ \text{Tr}\left(\Omega_{k-1}\Omega_{k-1}^R\right) - \frac{1}{N}\text{Tr}\left(\Omega_{k-1}\Omega_{k-1}^R\right)\} = \frac{N^2-1}{2N}L_{k-1} \end{aligned} \tag{4.34}$$

and for K_k

$$\begin{aligned} K_k &\equiv \mathrm{Tr}\left(\Omega_k\right)\mathrm{Tr}\left(\Omega_k^R\right) = \mathrm{Tr}\left(t^a\ \Omega_{k-1}\right)\mathrm{Tr}\left(t^a\ \Omega_{k-1}^R\right) \\ &\overset{(4.32)}{=} \frac{1}{2}\underbrace{\mathrm{Tr}\left(\Omega_{k-1}\Omega_{k-1}^R\right)}_{L_{k-1}} - \frac{1}{2N}\underbrace{\mathrm{Tr}\left(\Omega_{k-1}\right)\mathrm{Tr}\left(\Omega_{k-1}^R\right)}_{K_{k-1}} \\ &= \frac{1}{2}L_{k-1} - \frac{1}{2N}K_{k-1} \end{aligned} \tag{4.35}$$

(4.34)(4.35) is a system of recurrence equations. With the initial values $L_1 = \mathrm{Tr}\left(t^a t^a\right) = \frac{N^2-1}{2}$ and $K_1 = \mathrm{Tr}\left(t^a\right)\mathrm{Tr}\left(t^a\right) = 0$ we have the solutions

$$\mathrm{Tr}\left(\Omega_k\Omega_k^R\right) = N\left(\frac{N^2-1}{2N}\right)^k \tag{4.36}$$

$$\mathrm{Tr}\left(\Omega_k\right)\mathrm{Tr}\left(\Omega_k^R\right) = \frac{(N^2-1)^k + (-)^k(N^2-1)}{(2N)^k} \tag{4.37}$$

Following similar steps we can also prove the following identities

$$\mathrm{Tr}\left(\Omega_k\Omega_k\right) = \frac{N(N^2-1)}{2(2N)^k}\{(N-1)^{k-1} - (-1)^k(N+1)^{k-1}\} \tag{4.38}$$

$$\mathrm{Tr}\left(\Omega_k\right)\mathrm{Tr}\left(\Omega_k\right) = \frac{N(N^2-1)}{2(2N)^k}\{(N-1)^{k-1} + (-1)^k(N+1)^{k-1}\} \tag{4.39}$$

Chapter 5

The battle for phase space integration: SARGE versus RAMBO

5.1 Introduction

All QCD-amplitudes, no matter what kind of partons are involved, share a common characteristic. It is well known [Kuijf, 1991] that the leading kinematic singularity structure of the squared matrix elements is given by the so-called *antenna pole structure* (APS). In particular, for n gluons it is given by all permutations in the momenta of

$$\frac{1}{(p_1p_2)(p_2p_3)(p_3p_4)\cdots(p_{n-1}p_n)(p_np_1)} \ , \tag{5.1}$$

where (p_ip_j) denotes the Lorentz invariant scalar product of the gluon momenta p_i and p_j. Actually, it is this kinematical structure that is implemented in algorithms based on the so called SPHEL approximation to calculate the amplitudes [Kuijf, 1991]. But it is expected, and observed, that the same structure occurs in the exact matrix elements [Draggiotis et al., 1998, Caravaglios et al., 1999].

For the integration of the differential cross-sections of the processes under consideration, the Monte Carlo method is the only option, and a phase space generator is needed. RAMBO [Stirling et al., 1986] is a robust and efficient algorithm to generate any number of random massless momenta in their center-of-mass frame (CMF) with a given energy. However, RAMBO generates the momenta distributed uniformly in phase space, so that a large number of events is needed to integrate integrands with the APS to acceptable precision. Especially when the evaluation of the integrand

is time-consuming, which is the case for the exact matrix elements, this is highly inconvenient.

In this chapter, we introduce SARGE[1], an algorithm to generate any number of random massless momenta in their CMF with a given energy, distributed with a density that contains the APS. We compare it with RAMBO and show that it takes account for a substantial reduction in computing time in the calculation of cross-sections of multi-parton processes.

5.2 The adversaries

5.2.1 At first there was ...RAMBO

The aim is to generate the following phase space distribution, for massless particles, as uniformly as possible:

$$dV_n(\{p\}) \;:=\; \delta(\sqrt{s} - P^0)\delta^3(\vec{P}\,) \prod_{i=1}^{n} d^4p_i\, \delta(p_i^2)\, \theta(p_i^0) \quad , \tag{5.2}$$

where $P := \sum_{i=1}^{n} p_i$ and $\sqrt{s}$ is the overall energy. The RAMBO algorithm consists of the following steps:

1. generate massless vectors q_j^μ without constraints but under some normalized density $f(q_j)$;
2. compute the sum Q^μ of the momenta q_j^μ;
3. determine the Lorentz boost and scaling transform that brings Q^μ to P^μ;
4. perform these transforms on the q_j^μ, and call the result p_j^μ.

The algorithm generates momenta that satisfy the various δ-constaints, but to actually prove it one needs to employ the so called *unitary algorithm* formalism [van Hameren and Kleiss, 2000b]. Basically it consists of using certain integrals that represent unity, to prove that the previous steps generate the density:

$$d\Phi_n(\{p\}) = dV_n(\{p\}) \left(\frac{2}{\pi}\right)^{n-1} \frac{\Gamma(n)\Gamma(n-1)}{s^{n-2}} \tag{5.3}$$

[1] Any resemblance with actual or fictitious characters is almost accidental

As a byproduct of this calculation we get the volume of the phase space for n massless particles:

$$\int dV_n(\{p\}) = \left(\frac{\pi}{2}\right)^{n-1} \frac{s^{n-2}}{\Gamma(n)\Gamma(n-1)} \tag{5.4}$$

5.2.2 SARGE...the Challenger

The name SARGE stands for Staggered Antenna Radiation GEnerator, and is inspired by the structure of the algorithm. It consists of the repeated use of the *basic antenna* density for the generation of a momentum k, given two momenta p_1 and p_2:

$$dA(p_1, p_2; k) \;:=\; d^4k\,\delta(k^2)\,\theta(k^0)\,\frac{1}{\pi}\,\frac{(p_1p_2)}{(p_1k)(kp_2)}\,g\left(\frac{(p_1k)}{(p_1p_2)}\right)g\left(\frac{(kp_2)}{(p_1p_2)}\right) \quad . \tag{5.5}$$

Here, g is a function that serves to regularize the infrared and collinear singularities, as well as to ensure normalization over the whole space for k: therefore, $g(\xi)$ has to vanish sufficiently fast for both $\xi \to 0$ and $\xi \to \infty$. A possible choice for $g(\xi)/\xi$ could for instance be a generalized inverse Gaussian density:

$$g(\xi) = \frac{1}{2K_0(\sqrt{4\alpha\beta})} \exp\left(-\frac{\alpha}{\xi} - \beta\xi\right)\theta(\xi), \quad \alpha, \beta > 0 \tag{5.6}$$

where K_0 is a modified Bessel function of the second kind. Other options might be a gamma density:

$$g(\xi) = \frac{\beta^\alpha}{\Gamma(\alpha)}\xi^\alpha \exp\left(-\beta\xi\right)\theta(\xi), \quad \alpha, \beta > 0 \tag{5.7}$$

or a simple truncated exponential:

$$g(\xi) = \frac{1}{E_1(\alpha\beta)} \exp\left(-\beta\xi\right)\theta(\xi - \alpha), \quad \alpha, \beta > 0 \tag{5.8}$$

where E_1 is the exponential integral. At this point, we take the simplest possible function we can think of, that has a sufficiently regularizing behavior. We introduce a positive non-zero number ξ_{m} and take

$$g(\xi) \;:=\; \frac{1}{2\log\xi_{\mathrm{m}}}\,\theta(\xi - \xi_{\mathrm{m}}^{-1})\theta(\xi_{\mathrm{m}} - \xi) \quad , \tag{5.9}$$

which forces the value of ξ to be between $\xi_{\rm m}^{-1}$ and $\xi_{\rm m}$, and is normalized such that $\int dA = 1$. Let us immediately adopt the notation

$$\xi_1 := \frac{(p_1 k)}{(p_1 p_2)} \qquad \text{and} \qquad \xi_2 := \frac{(k p_2)}{(p_1 p_2)} \ . \tag{5.10}$$

The main motivation to make the regularizing function depend on ξ_1 and ξ_2 is that it makes dA completely invariant under Lorentz-and scale transformations of the momenta. Consequently, the number $\xi_{\rm m}$ gives a cut-off for the quotients ξ_1 and ξ_2 of the scalar products of the momenta, and not for the scalar products themselves. It is, however, possible to relate $\xi_{\rm m}$ to the total energy $\sqrt{s}$ in the CMF and a cut-off s_0 on the invariant masses, i.e., the requirement that

$$(p_i + p_j)^2 \geq s_0 \tag{5.11}$$

for all pairs of momenta $p_i \neq p_j$. This can be done by choosing

$$\xi_{\rm m} \ := \ \frac{s}{s_0} - \frac{(n+1)(n-2)}{2} \ , \tag{5.12}$$

where n is the total number of momenta. With this choice, the invariant masses $(p_1+k)^2$ and $(k+p_2)^2$ are regularized, but can still be smaller than s_0 so that the whole of the demanded phase space is covered. The s_0 can be derived from physical cuts p_T on the transverse momenta and θ_0 on the angles between the outgoing momenta:

$$s_0 \ = \ 2p_T^2 \cdot \min\left(1 - \cos\theta_0 \, , \, \left(1 + \sqrt{1 - p_T^2/s}\right)^{-1}\right) \ . \tag{5.13}$$

We now give the algorithm to generate k under the basic antenna density. Let k^0, ϕ and θ denote the absolute value, the polar angel and the azimuthal angle of $\vec{k}$ in the frame for which $\vec{p}_1 = -\vec{p}_2$ with $\vec{p}_1$ along the positive z-axis. To generate k, one should

Algorithm 5.2.1 (BASIC ANTENNA)

1. determine the direction of $\vec{p}_1$ in the CMF of p_1 and p_2;
2. generate two numbers ξ_1, ξ_2 independently, each from the density $g(\xi)/\xi$;
3. compute from these the values k^0 and $\cos\theta$;
4. generate ϕ uniformly in $[0, 2\pi)$;

5. construct the momentum k in the CMF of p_1 and p_2;

6. boost the result to the actual frame in which p_1 and p_2 were given.

Let us denote

$$dA^i_{j,k} := dA(q_j, q_k; q_i) \ , \qquad \text{and} \qquad \xi^{i,j}_{k,l} := \frac{(p_i p_j)}{(p_k p_l)} \ . \tag{5.14}$$

To include the APS in the density, one should

Algorithm 5.2.2 (`QCD ANTENNA`)

1. generate massless momenta q_1 and q_n in CMF;

2. generate $n-2$ momenta q_j by the basic antennas $dA^2_{1,n} dA^3_{2,n} dA^4_{3,n} \cdots dA^{n-1}_{n-2,n}$;

3. compute $Q = \sum_{j=1}^n q_j$, and the boost and scaling transforms that bring Q^0 to $\sqrt{s}$
   and $\vec{Q}$ to $(0,0,0)$;

4. for $j = 1, \ldots, n$, boost and scale the q_j accordingly, into the p_j.

This way, the momenta p_j are generated with differential density $dV_n(\{p\}) A_n^{QCD}(\{p\})$, where

$$A_n^{QCD}(\{p\}) \ = \ \frac{s^2}{2\pi^{n-1}} \cdot \frac{g(\xi^{1,2}_{1,n}) g(\xi^{2,n}_{1,n}) g(\xi^{2,3}_{2,n}) g(\xi^{3,n}_{2,n}) \cdots g(\xi^{n-2,n-1}_{n-2,n}) g(\xi^{n-1,n}_{n-2,n})}{(p_1 p_2)(p_2 p_3)(p_3 p_4) \cdots (p_{n-1} p_n)(p_n p_1)} \ . \tag{5.15}$$

We point out that, whereas the product $dA^2_{1,n} \cdots dA^{n-1}_{n-2,n}$ contains a factor $(p_1 p_n)$ in the numerator, the scaling transformation carries a Jacobian that is precisely $s^2/(p_1 p_n)^2$, thus leading to a perfectly symmetric APS.

Usually, the event generator is used to generate cut phase space. If a generated event does not satisfy the physical cuts, it is rejected. In the calculation of the weight coming with an event, the only contribution coming from the functions g is, therefore, their normalization. In total, this gives a factor $1/(2 \log \xi_{\rm m})^{2n-4}$ in the density.

The density, as was derived by the previous algorithm, is not exactly what we want. First of all we have to include the incoming momenta, so that the density is propotional to $[(p_0 p_1)(p_1 p_2) \cdots (p_{n-1} p_n)(p_n \tilde{p}_0)]^{-1}$ instead of $[(p_1 p_2) \cdots (p_{n-1} p_n)]^{-1}$, where $p_0 = (p^0, \vec{p})$ and $\tilde{p}_0 = (p^0, -\vec{p})$ are the incoming momenta. In addition we have to sum over all permutations of the momenta, including the incoming ones. The idea

is to replace a factor $(p_i p_{i+1})$ in the denominator by $(p_0 p_i)(p_{i+1}\tilde{p}_0)$. We can get rid of this factor by choosing it at random with weight

$$\frac{(p_i p_{i+1})}{(p_1 p_2) + (p_2 p_3) + \cdots + (p_{n-1} p_n) + (p_n p_1)} \tag{5.16}$$

where the denominator is the sum of all scalar products in the antenna. We can see that this weight is properly defined since all scalar products are positive. the total density will then get this factor that cancels $(p_i p_{i+1})$. The chosen factor $(p_i p_{i+1})$ is used to generate massless momenta p_0 and $\tilde{p}_0$. Proof of this and further details about incoming momenta and summing over permutations can be found in [van Hameren and Kleiss, 2000b].

When doing calculations with this algorithm on a phase space cut such that $(p_i + p_j)^2 > s_0$ for all $i \neq j$ and some reasonable $s_0 > 0$, we notice that a very high percentage of the generated events does not pass the cuts. An important reason why this happens is that the cuts, generated by the choices of g (Eq.(5.9)) and ξ_{m} (Eq.(5.12)), are implemented only on the variables $\xi^{i,j}_{k,l}$ that appear explicitly in the generation of the QCD-antenna. An improvement on this is obtained by generating $\xi^{i,j}_{k,l}$ inside a convex polytope $\mathbf{P}_m$. A polytope is defined as the subspace of $[-1,1]^m$ for which $|x_i - x_j| \leq 1$ for all $i, j = 1, \ldots, m$. Details on this can be found in [van Hameren and Kleiss, 2000b], [van Hameren and Kleiss, 2000a].

5.3 The Confrontation

We compare SARGE with RAMBO in the calculation of the cross-section of the processes

$$e^+e^- \longrightarrow \gamma^* \longrightarrow q\bar{q}g,\ q\bar{q}q\bar{q},\ q\bar{q}q'\bar{q}',\ q\bar{q}gg,\ q\bar{q}q\bar{q}g,\ q\bar{q}q'\bar{q}'g,\ q\bar{q}ggg\ . \tag{5.17}$$

The squared matrix element was calculated with the algorithm presented in [Draggiotis et al., 1998], suitably adapted for these processes. We used massless electrons and quarks, and took the sum over final-state helicities and the average over initial-state helicities. We also summed over the color configurations of the final states. The center-of-mass energy $\sqrt{s}$ was fixed to 500 GeV for the processes with 5 outgoing momenta, and to 100 GeV for the other processes. The cuts on the phase space where fixed with choices of a parameter τ, which is related to the cut-off s_0 on the squares of the outgoing momenta (Eq.(5.11)) by

$$s_0 = \frac{2s\tau}{n(n-1)}\ , \tag{5.18}$$

where n is the number of outgoing momenta. If $\tau = 1$, then s_0 is larger than the maximal value that is kinematically allowed. The couplings and charges in various processes were all set to the value 1, since they only contribute a factor to the cross-section, which is irrelevant for this analysis. The results of the computer runs are given in the tables below. Presented are the final result for the cross-section σ in units of GeV^{-2}, the number of generated events N_{ge}, the number of accepted events N_{ac}, and the cpu-time consumed t_{cpu} in seconds. All Monte Carlo runs were performed on a single 440-MHz UltraSPARC-IIi processor, and were stopped when an expected error of 3% was reached.

The final results for the cross-sections are irrelevant in our discussion, and are just printed to show that the results with `SARGE` and `RAMBO` are compatible within the 3% error estimate. The most important conclusion that can be drawn from the results is that `SARGE` needs less accepted events than `RAMBO` for the given error estimate, especially for small values of τ, *i.e.*, for phase space that comes close to the singularities of the QCD-amplitudes. (Remember that the ratio of the volumes of cut phase space and whole phase space is given by $N_{\mathrm{ac}}/N_{\mathrm{ge}}$ for `RAMBO`.) As a result, less evaluations of the matrix elements have to be done which accounts for a large gain in computer time. It is true that `SARGE` is "ineffective" in the sense that many of the generated events have to be rejected because they do not satisfy the cuts imposed, but this is fully compensated by the fact that generating random numbers is much cheaper than evaluating matrix elements nowadays. For the last four processes, no results with `RAMBO` and $\tau = 0.01$ are presented, but we observe that $t_{\mathrm{cpu}} > 130,000$ seconds. The fraction of phase space covered with five massless momenta and $\tau = 0.01$ is 0.893 ± 0.001.

$e^+e^- \to q\bar{q}g$								
τ	0.5		0.1		0.05		0.01	
alg.	`SARGE`	`RAMBO`	`SARGE`	`RAMBO`	`SARGE`	`RAMBO`	`SARGE`	`RAMBO`
σ	1.85e-5	1.85e-5	1.53e-4	1.58e-4	2.61e-4	2.66e-4	6.26e-4	6.41e-4
N_{ge}	7,691	25,782	10,777	24,801	10,806	37,121	11,437	366,614
N_{ac}	5,503	6,536	9,436	20,112	9,852	33,577	10,860	359,447
t_{cpu}	251	293	429	899	451	1,503	497	16,124

$e^+e^- \to q\bar{q}q\bar{q}$								
τ	0.5		0.1		0.05		0.01	
alg.	SARGE	RAMBO	SARGE	RAMBO	SARGE	RAMBO	SARGE	RAMBO
σ	9.79e-9	10.4e-9	7.72e-7	7.86e-7	1.90e-6	1.83e-6	7.39e-6	7.00e-6
N_{ge}	64,384	158,678	32,492	27,091	34,701	29,642	41,744	113,368
N_{ac}	4,428	4,551	9,894	15,328	13,081	22,297	20,150	107,021
t_{cpu}	775	786	1,718	2,606	2,256	3,778	3,578	18,038

$e^+e^- \to q\bar{q}q'\bar{q}'$								
τ	0.5		0.1		0.05		0.01	
alg.	SARGE	RAMBO	SARGE	RAMBO	SARGE	RAMBO	SARGE	RAMBO
σ	5.38e-9	5.30e-9	4.07e-7	4.24e-7	1.00e-6	1.02e-6	3.95e-6	3.89e-6
N_{ge}	98,840	245,138	50,052	45,963	63,398	50,873	71,254	366,166
N_{ac}	6,696	7,022	15,392	25,883	23,989	38,145	34,584	345,323
t_{cpu}	1,165	1,198	2,664	4,346	4,133	6,434	5,843	58,708

$e^+e^- \to q\bar{q}gg$							
τ	0.5		0.1		0.05		0.01
alg.	SARGE	RAMBO	SARGE	RAMBO	SARGE	RAMBO	SARGE
σ	1.76e-7	1.70e-7	1.86e-5	1.95e-5	5.19e-5	5.27e-5	5.40e-4
N_{ge}	96,942	268,407	42,321	86,608	50,552	298,073	50,414
N_{ac}	6,579	7,677	12,945	48,902	19,091	223,530	26,551
t_{cpu}	1,363	1,597	3,619	6,398	3,802	43,913	5,287

$e^+e^- \to q\bar{q}q\bar{q}g$							
τ	0.5		0.1		0.05		0.01
alg.	SARGE	RAMBO	SARGE	RAMBO	SARGE	RAMBO	SARGE
σ	2.04e-11	1.91e-11	4.05e-8	4.08e-8	1.68e-7	1.61e-7	1.48e-6
N_{ge}	4,028,648	4,017,888	238,220	97,035	203,237	210,325	176,710
N_{ac}	5,616	5,094	14,216	33,239	19,522	121,734	29,492
t_{cpu}	4,530	3,941	10,333	23,875	14,159	87,756	21,407

$e^+e^- \to q\bar{q}q'\bar{q}'g$							
τ	0.5		0.1		0.05		0.01
alg.	SARGE	RAMBO	SARGE	RAMBO	SARGE	RAMBO	SARGE
σ	1.05e-11	1.05e-11	2.19e-8	2.23e-8	9.07e-8	8.86e-8	7.85e-7
N_{ge}	5,596,725	6,929,475	436,225	188,693	377,384	522,602	305,426
N_{ac}	7,730	8,844	26,154	64,558	36,042	302,724	51,044
t_{cpu}	5,882	6,494	17,595	43,104	24,764	201,801	34,700

$e^+e^- \to q\bar{q}ggg$							
τ	0.5		0.1		0.05		0.01
alg.	SARGE	RAMBO	SARGE	RAMBO	SARGE	RAMBO	SARGE
σ	1.31e-11	1.30e-11	3.63e-7	3.54e-7	1.63e-6	1.54e-6	1.85e-5
N_{ge}	5,926,016	6,650,538	366,538	131,617	303,003	186,257	335,307
N_{ac}	8,194	8,475	21,918	45,157	29,018	107,897	56,008
t_{cpu}	7,407	7,398	18,120	36,958	24,036	88,318	46,673

As an extra illustration, we also present the convergence to zero of the expected error during the Monte Carlo-run for a few cases. In Fig.5.2, we plot the relative error as function of the number of generated events using a double-log scale. We first of all observe that the curves for SARGE are less spiky, which shows that SARGE takes care for a substantial part of the singular behavior of the integrand. Every time a RAMBO-event hits a singularity, a term much larger than the average so far is added to the Monte Carlo sum, resulting in an increase of the expected error. Furthermore, we observe that the SARGE-error converges quicker than the RAMBO-error, except in the case of $e^+e^- \to q\bar{q}ggg$ with $\tau = 0.05$. However, this is a plot of the error as function of the number of generated events, and we know that many SARGE-events have to be rejected. A more realistic view is given by a plot of the error as function of cpu-time (Fig.5.1), which clearly shows that SARGE outperforms RAMBO.

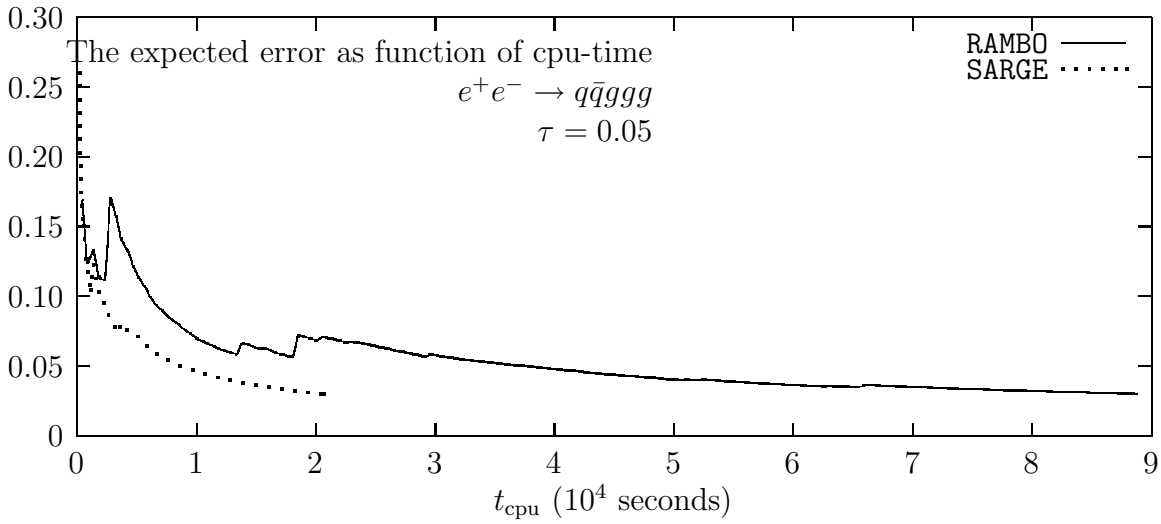

Figure 5.1: The expected relative error as function of cpu-time.

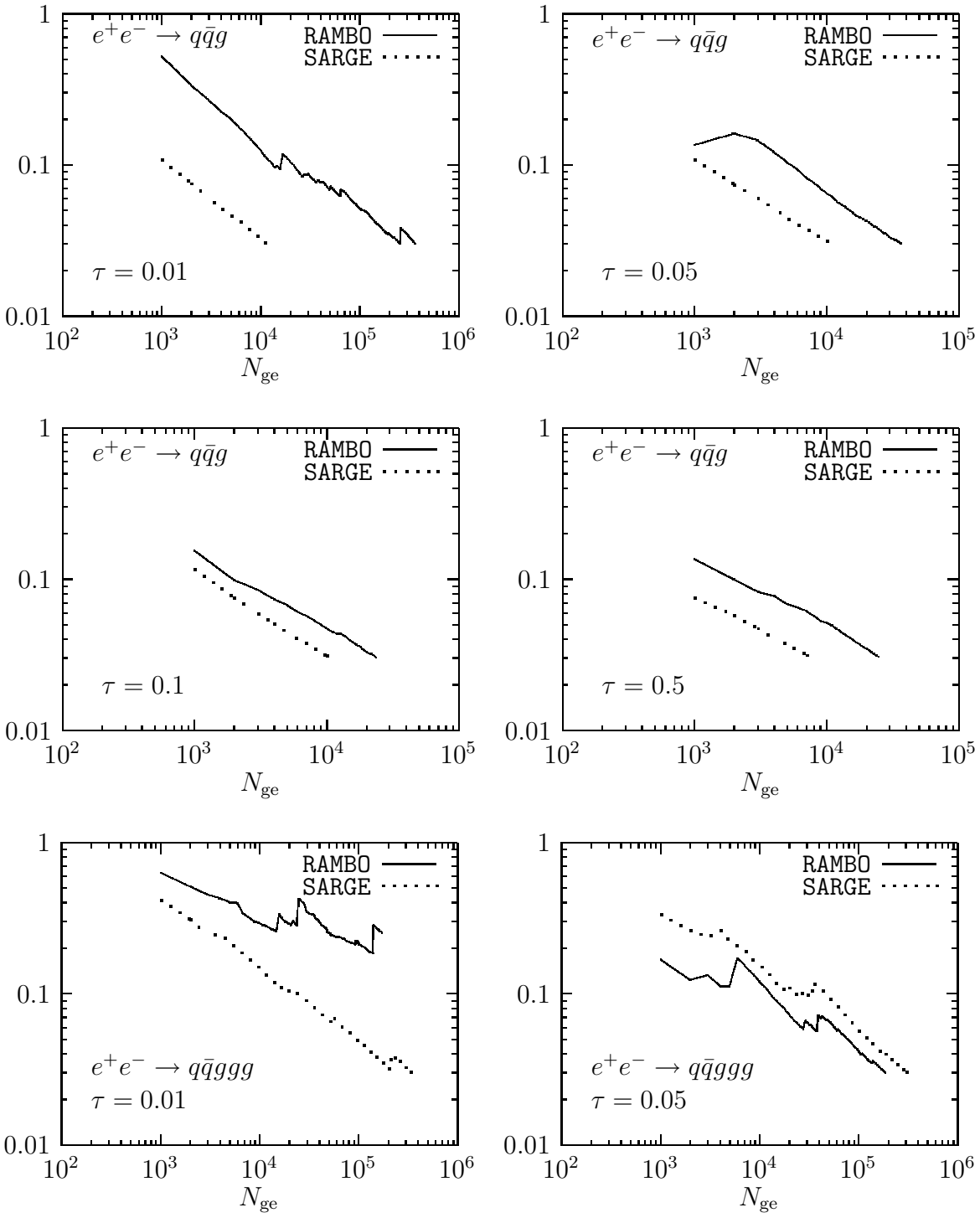

Figure 5.2: The expected relative error as function of the number of generated events.

Chapter 6

The Recursive Equations for QCD

6.1 Introduction

With the recommissioning of the Tevatron, and the forseeable commencement of physics at the LHC, the need for fast and accurate QCD calculations is now larger than ever. In this chapter, we describe our efforts to arrive at such calculations. To set the stage: we have in mind the computation of QCD cross sections with many observed jets that, as usual, are modelled by assuming that each jet comes from a single fragmenting parton. With the large amount of energy available, the number n of jets can easily be as large as 8, thus requiring the computation of amplitudes with 10 or even more external legs.

Although in principle straightforward enough, the usual techniques of evaluating Feynman diagrams and integrating the resulting cross section by Monte Carlo are in practice hampered by the computational complexity of the problem. The following obstacles can be recognized:

1. The flavours of the initial partons are never detected, and in most cases (barring, say, b tagging) neither are the flavours of the final-state partons. In what follows we take all quarks (u, d, s, c, and b) to be essentially massless, although a version of the code with massive fermions exists. In the case of flavour integration, to be discussed later on, we always treat quarks as massless. This means that to any given jet configurations there are usually very many contributing processes. Even enumerating these is a nontrivial task, and calculating each individual process cross section is even more so.

2. In addition to flavour, neither the colour nor the spin of any parton is observed. For an amplitude with p quark partons and q gluons this implies that in principle

$(6)^p(16)^q$ contributions have to be added. It is true that, in particular, many colour configurations lead to zero amplitudes, but figuring out precisely which these are is very hard.

3. Each individual amplitude, with specified flavours, colours and spins, contains very many Feynman diagrams. In Chapter 3 we gave a recipe for determining the precise number of graphs, at the tree level. Typical results are that the process $gg \to 8g$ is described by 10,525,900 diagrams, and the process $gg \to 2g3u3\bar{u}$ by 946,050 diagrams. Inclusion of loop corrections worsens this dramatically, of course.

4. Each amplitude peaks in complicated ways inside the momentum phase space. Straightforward integration is therefore impractical, and one has to search for efficient mappings to do importance sampling in a multi-particle phase space.

All these difficulties are adressed in this chapter, and here we describe our solutions, in reverse order.

4. The peaking structure of the amplitude is dealt with by our phase-space generating algorithm `SARGE` [van Hameren et al., 2000] [van Hameren and Kleiss, 2000b]. This algorithm is tailored to the generation of so-called antenna structures. Let $p_1, \ldots, p_n$ be the momenta of the n produced partons, and $p_0, \tilde{p}_0$ those of the incoming partons. The peaking behaviour of the cross section for the purely gluonic process involving n gluons, $gg \to (n-2)g$ is then dominated by the following antenna structure:

$$\Big[(p_1p_2)(p_2p_3)(p_3p_4)\cdots(p_{n-1}p_n)(p_np_1)\Big]^{-1}$$

and any permutation of labels. Since processes involving quarks do not show other dominant peaking behaviour than the above ones, we can cover the n-particle momentum phase space with good efficiency. More details about `SARGE` can be found in [van Hameren, 2001]

3. Over the last years new algorithms, along with their implementations, for computing the tree-order scattering amplitude have been emerged [Caravaglios and Moretti, 1995, Draggiotis et al., 1998, Kanaki and Papadopoulos, 2000]. These do not involve calculation of individual diagrams, but rather reorganize, in a systematic way, the various off-shell subamplitudes in such a way that as little of the computation as possible is repeated. The improvement in computational

efficiency of these algorithms is nevertheless dramatic, down from about $n!$ to something like 3^n. In the algorithm suggested originally in reference [Caravaglios and Moretti, 1995] the scattering amplitude was computed through a set of recursive equations derived from the effective action as a function of the classical fields. These classical equations represent nothing but the tree-order Schwinger-Dyson equations, a fact that was already emphasized in subsequent approaches [Kanaki and Papadopoulos, 2000] and it will be illustrated below for the special case of QCD. In fact, recursive techniques have already been used in the past to compute multi-gluon amplitudes [Giele, 1989].

2. The usual spin and colour summation is replaced by a Monte Carlo integration. In the purely gluonic case [Draggiotis et al., 1998] this has been shown to work *rather* well. It must be realized that since we replace the more usual sum over discrete colour and spin states by a continuous (Monte Carlo) integration, the variance of the cross section can indeed be expected to be smaller.

1. In the same spirit, we tackle the flavour combinatorics in the same way: we assign to each quark and antiquark a flavour quantum number, that is, we extend the definition of the external legs by a direct product with a flavour vector in the space of the 5 available flavours. By taking these vectors randomly we can perform a sum over flavours by Monte Carlo as well, and the only computational difference between the case of one single flavour and that of f flavours is simply a factor f, whereas the discrete-flavour-sum combinatorics would lead to a much bigger loss in speed. The possiblity of coherent superpositions of different flavours might seem awkward but is in fact quite natural since all quarks are treated as massless and therefore the distinction between flavours is to a large extent arbitrary. The only place where flavours are *not* treated on an equal footing is in the structure functions that describe the difference in probability of picking out different flavours: by a judicious weighting of the flavour vectors for incoming quarks and antiquarks we can handle this as well.

Considering the Monte Carlo treatment of spin, colour and flavour, the essential point is to realize that we are entitled to use *any* representation for the corresponding information, as long as we end up with the correct sums *on the average*.

Before finishing this introduction we want to mention that, so far, we can calculate partonic cross sections. These are typically good for global quantities like total cross sections, p_T distributions and the like. A fuller treatment involves coupling the generated events to fragmentation programs like `HERWIG` [Corcella and et al., 2001]. These programs typically require additional information on the 'spanning of

the colour string'. In [Caravaglios et al., 1999] a way to do this for processes with zero or one quark lines is described.

6.2 Building the amplitude

6.2.1 Iteration of the SD equation

The traditional way of computing the amplitude of a process, has been writing down the Feynman graphs, calculating every one of them and then summing them together to obtain the result. This is a rather tedious task especially when one is confronted with processes with a high multiplicity of particles since the number of graphs becomes forbiding for analytical evaluation. Moreover this by itself contains a high degree of redundancy. That is because the majority of graphs contain pieces in them, subamplitudes, that are common to a large number of graphs. This means that these particular pieces are computed again and again. In Chapter 3 we computed the number of graphs for several theories. There we saw in particular, that in the case of QCD, this number behaves asymptotically as:

$$a(\varphi \to k\varphi, n\chi\bar{\chi}) \sim (n-1)!^2 k! C_1^n C_2^{k+1} D \tag{6.1}$$

where k is the number of gluons and n the number of quark-antiquark pairs and C_1, C_2 and D are defined in (3.34). We see that the number of graphs grows very quickly. In this section we start the setting up of a different approach to compute the amplitude numerically, bypassing the need to write down Feynman graphs.

Our starting point are the Dyson-Schwinger (DS) equations, (2.36), which give recursively the n-point Green's functions in terms of the $1-, 2-, \ldots, (n-1)-$ point functions. The action for the case of QCD is $S = \int d^4x \mathcal{L}$ where $\mathcal{L}$ is:

$$\mathcal{L} = -\frac{1}{4} F^a_{\mu\nu} F^{a\mu\nu} - \frac{1}{2\xi} \left(\partial^\mu A^a_\mu\right)^2 + \bar{\psi}^i \left(i\gamma^\mu D^{ij}_\mu\right) \psi^j \tag{6.2}$$

Note that since we are dealing only with tree diagrams we discard ghost fields. Also we consider all quarks massless. The couplings between fields, derived from this Langrangian are shown in section 2.1. By using the Euler-Lagrange equations we can derive the equations for the gluon and quark fields

$$D^\mu_{ab} F^b_{\mu\nu} = g\bar{\psi}_i \gamma_\nu t^a_{ij} \psi_j \tag{6.3}$$

$$\not{\partial}\psi_i = igt^a_{ij} \not{A}^a \psi_j \tag{6.4}$$

$$\not{\partial}\bar{\psi}_i = ig\bar{\psi}_j t^a_{ij} \not{A}^a \tag{6.5}$$

where $D^{\mu}_{ab} = \delta_{ab}\partial_{\mu} - g f_{abc} A_{\mu\, a}$ is the covariant derivative acting on the gluon field. The recursive content of the DS equation, for the gluon field for example, can be understood pictorially as follows:

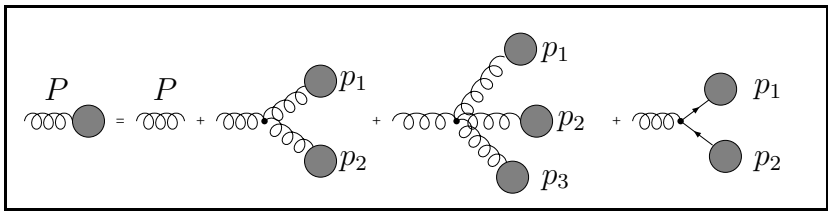

Recursion equation for gluons

The figure shows that a subamplitude with an off-shell gluon of momentum P, has contributions from three- and four-vertices plus a fermion-antifermion vertex. The shaded blobs denote subamplitudes with the same structure. So, in effect, this is a recursion equation which we can write down immediately in momentum space (suppressing the colour), using the Feynman rules:

$$\begin{aligned} A^{\mu}(P) &= \sum_{i=1}^{n} \delta_{P=p_i} A^{\mu}(p_i) + (ig_s) \sum_{P=p_1+p_2} \Pi^{\mu}_{\nu} \bar{\psi}(p_1)\gamma^{\nu}\psi(p_2)\sigma(p_1,p_2) \\ &+ \frac{(ig_s)}{2} \sum_{P=p_1+p_2} \Pi^{\mu}_{\rho}\, V^{\rho\nu\lambda}(P,p_1,p_2) A_{\nu}(p_1) A_{\lambda}(p_2)\sigma(p_1,p_2) \\ &- \frac{(g_s^2)}{6} \sum_{P=p_1+p_2+p_3} \Pi^{\mu}_{\sigma}\, G^{\sigma\nu\lambda\rho} A_{\nu}(p_1) A_{\lambda}(p_2) A_{\rho}(p_3)\sigma(p_1,p_2) \end{aligned} \tag{6.6}$$

where $V^{\mu\nu\lambda}(P,p_1,p_2)$ and $G^{\mu\nu\lambda\rho}$ are the 3 and 4-point vertices (see Eq.(2.24)) and

$$\Pi^{\mu}_{\nu} = \frac{-ig^{\mu}_{\nu}}{P^2} \tag{6.7}$$

is the gluon propagator (in the Feynman gauge, $\xi = 1$). The symbol $\sigma(p_1,p_2)$ -we will call it the sign function-takes into account the Fermi sign and has the values ± 1. More on the sign function will be presented later on. The sum $\sum_{P=p_1+p_2}$ is over all combinations of p_1, p_2 that sum up to P. Similarly for $\sum_{P=p_1+p_2+p_3}$. For a quark of momentum P (supressing the colour again)

$$\psi(P) = \sum_{i=1}^{n} \delta_{P=p_i} \psi(p_i) + (ig_s) \sum_{P=p_1+p_2} S\not{A}(p_1)\psi(p_2)\sigma(p_1,p_2) \tag{6.8}$$

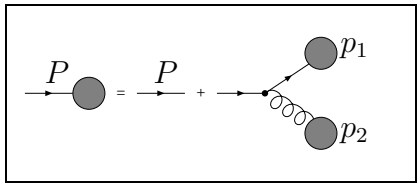

Recursion equation for quarks

where S is the propagator

$$S = \frac{i\not{P}}{P^2} \tag{6.9}$$

and for an antiquark

$$\bar{\psi}(P) = \sum_{i=1}^{n} \delta_{P=p_i} \bar{\psi}(p_i) + (ig_s) \sum_{P=p_1+p_2} \bar{\psi}(p_2) \not{A}(p_1) \tilde{S} \sigma(p_1, p_2) \tag{6.10}$$

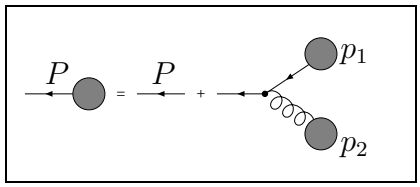

Recursion equation for antiquarks

where

$$\tilde{S} = \frac{-i\not{P}}{P^2} \tag{6.11}$$

In order to reduce computational complexity, as we will discuss later on, we replace the four gluon vertex with a three-vertex by introducing an auxiliary field $H_{\mu\nu}$. We rewrite the part of the QCD Lagrangian that describes the four-vertex in terms of the auxiliary field as follows:

$$\mathcal{L}_H = -g f^{abc} A^a_\mu A^b_\nu H^{\mu\nu\, c} - H^a_{\mu\nu} H^{\mu\nu\, a} \tag{6.12}$$

The recursion for the gluons changes slightly, namely only the part with the four-vertex. Additionally, we also have an equation for the auxiliary field:

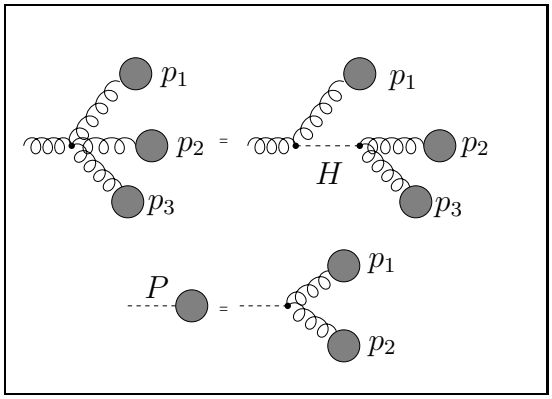

Ellimination of the four-vertex and the new H-gluon-gluon vertex.

$$\begin{aligned} A^\mu(P) &= \sum_{i=1}^{n} \delta_{P=p_i} A^\mu(p_i) + (ig_s) \sum_{P=p_1+p_2} \Pi^\mu_\nu \bar{\psi}(p_1)\gamma^\nu \psi(p_2)\sigma(p_1,p_2) \\ &+ \frac{(ig_s)}{2} \sum_{P=p_1+p_2} \Pi^\mu_\rho \, V^{\rho\nu\lambda}(P,p_1,p_2) A_\nu(p_1) A_\lambda(p_2)\sigma(p_1,p_2) \\ &- (g_s) \sum_{P=p_1+p_2} \Pi^\mu_\sigma \, X^{\sigma\nu\lambda\rho} A_\nu(p_1) H_{\lambda\rho}(p_2)\sigma(p_1,p_2) \end{aligned} \tag{6.13}$$

$$H_{\mu\nu}(P) = -\frac{(g_s)}{4} \sum_{P=p_1+p_2} X^{\mu\nu\lambda\rho} A_\lambda(p_1) A_\rho(p_2)\sigma(p_1,p_2) \tag{6.14}$$

where $X^{\mu\nu\lambda\rho}$ is the new H-gluon-gluon vertex:

$$X^{\mu\nu\lambda\rho} = g^{\mu\lambda}g^{\nu\rho} - g^{\nu\lambda}g^{\mu\rho} \tag{6.15}$$

These four equations, namely (6.13),(6.14),(6.8),(6.10), represent off-shell fields that are the building blocks of any process. They are used iteratively, combining two (or three) momenta, at each step, to build a subamplitude. The iteration begins with the initial conditions for the external particles. In particular for a gluon we have:

$$A^\mu_a(p_i) = \epsilon^\mu_\lambda(p_i)\, \delta_{aa_i} \ , \quad i = 1,..n \tag{6.16}$$

where a is the colour, $a = 1,\ldots,8$, $\epsilon^\mu_\lambda(p)$ denotes the polarization vector and i denotes one the external gluons. The polarization vector is defined as

$$\epsilon^\mu_\lambda(p) = \frac{\bar{u}_\lambda(p)\gamma^\mu u_\lambda(k)}{2\sqrt{(p\cdot k)}} \tag{6.17}$$

where k is any lightlike vector not colinear to p, and $\lambda = \pm 1$. This choice satisfies the usual conditions for the polarization vector

$$\begin{aligned} \epsilon_\lambda \cdot p = 0 \quad &, \quad \epsilon_\lambda \cdot \epsilon_\lambda = 0 \\ \epsilon^\mu_{-\lambda} = (\epsilon^\mu_\lambda)^* \quad &, \quad \epsilon_\lambda \cdot \epsilon_{-\lambda} = -1 \end{aligned}$$

For the quarks and antiquarks the iteration starts with

$$\psi_k(p_i) = \begin{cases} u(p_i)\delta_{kk_i} & \text{if } i \text{ incoming} \\ \bar{u}(p_i)\delta_{kk_i} & \text{if } i \text{ outgoing} \end{cases} \tag{6.18}$$

$$\bar{\psi}_k(p_i) = \begin{cases} \bar{u}(p_i)\delta_{kk_i} & \text{if } i \text{ incoming} \\ u(p_i)\delta_{kk_i} & \text{if } i \text{ outgoing} \end{cases} \tag{6.19}$$

where k is the colour, $k = 1, 2, 3$. For a massless particle, the spinors that we use are:

$$\begin{aligned} u_R(p) = \begin{pmatrix} \sqrt{p_0 + p_z} \\ \frac{p_x + ip_y}{\sqrt{p_0 + p_z}} \\ 0 \\ 0 \end{pmatrix} \quad &, \quad \bar{u}_R(p) = \begin{pmatrix} 0 \\ 0 \\ -\sqrt{p_0 + p_z} \\ -\frac{p_x - ip_y}{\sqrt{p_0 + p_z}} \end{pmatrix} \\ u_L(p) = \begin{pmatrix} 0 \\ 0 \\ -\frac{p_x - ip_y}{\sqrt{p_0 + p_z}} \\ \sqrt{p_0 + p_z} \end{pmatrix} \quad &, \quad \bar{u}_L(p) = \begin{pmatrix} \frac{p_x + ip_y}{\sqrt{p_0 + p_z}} \\ -\sqrt{p_0 + p_z} \\ 0 \\ 0 \end{pmatrix} \end{aligned} \tag{6.20}$$

The next step is combining two of the external momenta, in all possible ways, according to the Feynman rules, to compute the next subamplitude. The iteration goes through in the same manner, using the equations (6.13), (6.14),(6.8),(6.10) repeatedely, each time combining the new momenta obtained with the remaining of the external ones, in all possible ways. After $n - 1$ steps there is only one momentum left to be combined, so the last step gives us the amplitude $\mathcal{A}(p_1, p_2, \ldots, p_n)$. This combination with the remaining momentum is done as follows:

$$\mathcal{A}(p_1, p_2, \ldots, p_n) = \begin{cases} \hat{A}^{\mu\, a}(P_i)\; A^a_\mu(p_i) & \text{if } i \text{ corresponds to a gluon,} \\ \hat{\bar{\psi}}(P_i)\psi(p_i) & \text{if } i \text{ corresponds to an incoming quark line,} \\ \bar{\psi}(p_i)\hat{\psi}(P_i) & \text{if } i \text{ corresponds to an outgoing quark line} \end{cases} \tag{6.21}$$

where $P_i = \sum_{j \neq i} p_j$, so that $P_i + p_i = 0$. The $\hat{}$ means that the field, which is computed from the previous iterations, is amputated, that is the propagator term is dropped in the calculation. This is consistent with the LSZ formalism.

For a given subamplitude, the total momentum flowing in, is the sum of all momenta contributing to this particular subamplitude. In order to keep track of the relevant momenta combinations, we have developed a systematic way of labeling these momenta using the binary system. **From now on we consider all momenta incoming**, for convenience. The idea is as follows: for a process involving n external particles with momenta $p_i^\mu,\ i = 1, \ldots, n$ we assign to the momentum P^μ defined as

$$P^\mu = \sum_{i \in I} p_i^\mu \tag{6.22}$$

where $I \subset \{1, \ldots, n\}$, a binary vector $\vec{m} = (m_1, \ldots, m_n)$, with components that take the values 0 or 1, in such a way that

$$P^\mu = \sum_{i=1}^{n} m_i p_i^\mu \tag{6.23}$$

The external momenta, $p_i^\mu,\ i = 1, \ldots, n$, are represented by $m = 2^{i-1},\ i = 1, \ldots, n$. This representation allows us to establish a natural ordering of the momenta based on the notion of the *level* l:

$$l = \sum_{i=1}^{n} m_i \tag{6.24}$$

Thus, all external momenta are of level 1, whereas the amplitude is of level n. Using the notion of the level we understand the natural path of the iteration of the equations: starting from level 1 subamplitudes (the external momenta used in the initial conditions), then level 2 subamplitudes, etc., until we reach level n and we have the amplitude.

To give an example of the binary representation let us assume a process with 6 particles. The momenta involved in the various levels of the calculation are:

$$\begin{cases} \textit{Level } 1: & P_1 = (000001) = p_1\ , \ldots, P_{32} = (100000) = p_6 \\ \textit{Level } 2: & P_3 = (000011) = p_1 + p_2\ , \ldots, P_{48} = (110000) = p_5 + p_6 \\ \quad \ldots & \quad \ldots \quad \ldots \quad \ldots \quad \ldots \quad \ldots \\ \textit{Level } 5: & P_{31} = (011111) = p_1 + p_2 + p_3 + p_4 + p_5\ , \ldots \\ \textit{Level } 6: & P_{63} = (111111) = p_1 + p_2 + p_3 + p_4 + p_5 + p_6 = 0 \end{cases} \tag{6.25}$$

It is clear that at each level k there are $\left(\begin{array}{c} n \\ k \end{array} \right)$ momenta that represent currents, and the total amount of currents is

$$\sum_{k=1}^{n-1} \left(\begin{array}{c} n \\ k \end{array} \right) = 2^n - 2 \tag{6.26}$$

As an illustration of the iteration of the SD equation, consider the process $\bar{u}(1)u(2) \to \bar{d}(4)d(8)\bar{s}(16)s(32)$. The level 1 of the iteration is the initialization of the spinors with the momenta shown in parentheses. The level 2 subamplitude consists of

$$\begin{aligned} A^\mu(12) &= -(ig_s)\, \Pi^\mu_{12\ \nu} \bar{\psi}(8)\gamma^\nu \psi(4) \\ A^\mu(48) &= -(ig_s)\, \Pi^\mu_{48\ \nu} \bar{\psi}(16)\gamma^\nu \psi(32), \end{aligned}$$

where $P_{12} = P_{(001100)} = P_8 + P_4 = p_4 + p_3$, $P_{48} = P_{(110000)} = P_{32} + P_{16} = p_6 + p_5$, etc. Π_{12} is the gluon propagator evaluated at momentum P_{12},etc. All other combinations of momenta are ruled out because of the absence of flavour changing vertices. Then it is the level 3 subamplitudes

$$\begin{aligned} \psi(14) &= (ig_s)\, S_{14} \not{A}(12)\psi(2) \\ \psi(28) &= (ig_s)\, S_{28} \not{A}(12)\psi(16) \\ \psi(50) &= (ig_s)\, S_{50} \not{A}(48)\psi(2) \\ \psi(52) &= (ig_s)\, S_{52} \not{A}(48)\psi(4) \\ \bar{\psi}(44) &= (ig_s)\, \bar{\psi}(32) \not{A}(12) \tilde{S}_{44} \\ \bar{\psi}(56) &= (ig_s)\, \bar{\psi}(8) \not{A}(48) \tilde{S}_{56}, \end{aligned}$$

the level 4 subamplitudes, combining 4 of the external momenta

$$\begin{aligned} A^\mu(60) &= (ig_s)\, \Pi^\mu_{60\ \rho} \{ \frac{1}{2} V^{\rho\nu\lambda}(60, 48, 12) A_\nu(48) A_\lambda(12) \\ &- \bar{\psi}(56)\gamma^\rho \psi(4) - \bar{\psi}(8)\gamma^\rho \psi(52) - \bar{\psi}(44)\gamma^\rho \psi(16) - \bar{\psi}(32)\gamma^\rho \psi(28) \}, \end{aligned}$$

and finally the 5^{th} level

$$\psi(62) = (ig_s)\, \{ \not{A}(60)\psi(2) + \not{A}(12)\psi(50) + \not{A}(48)\psi(14) \}$$

The amplitude is then given by combining this last spinor with the antispinor that carries the momentum p_1, that is the remaining particle:

$$\mathcal{A} = \bar{\psi}(1)\psi(62)$$

Some of the fields calculated here are shown in Fig.6.1 on top of the Feynman diagrams that contribute to this process.

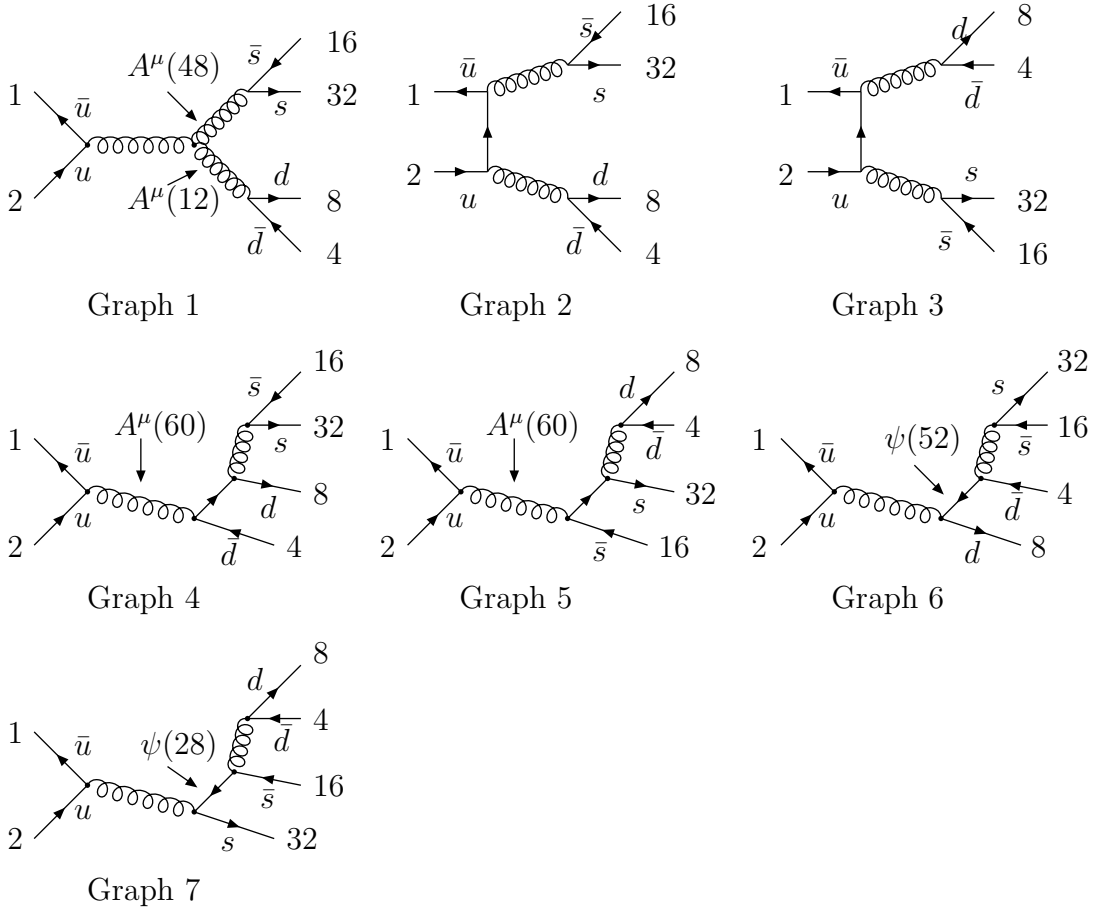

Figure 6.1: Feynman graphs for the process $\bar{u}u \to \bar{d}d\bar{s}s$. The building blocks of the amplitude are shown by indicating some of the off-shell fields

6.2.2 Computational complexity

In the previous section we stated that we prefered equations that contained only 3-vertices because it is more cost effective. Here we will make this a bit more concrete. For simplicity let us consider a scalar theory with a $\phi^3 + \phi^4$ interaction. In analogy with the QCD case, the recursion for a scalar field ϕ will look like

$$\phi(m,k)P_m^2 = \frac{1}{2!}\sum \phi(m_1,k_1)\phi(m_2,k_2) + \frac{1}{3!}\sum \phi(m_1,k_1)\phi(m_2,k_2)\phi(m_3,k_3) \quad (6.27)$$

where in $\phi(m,k)$ the first argument denotes the momentum label and the second the level. We need to determine the cost function, that is how many operations one needs to compute the n-point amplitude. The basic steps one has to take are:

- $\#\phi(m,k)$ to be computed at each level k
- # of ways to split a number of level k to two (three) numbers of levels k_1 and k_2 (k_1,k_2 and k_3).
- then sum over all levels

According to these steps, the number of operations $O(n)$ would be

$$O(n) = \sum_{k=1}^{n-1} \left(\begin{array}{c} n \\ k \end{array} \right) \sum_{l=1}^{k-1} \left(\begin{array}{c} k \\ l \end{array} \right) = \sum_{k=1}^{n-1} \left(\begin{array}{c} n \\ k \end{array} \right) \{2^k - 2\} = 3^n - 3 \cdot 2^n + 3 \qquad (6.28)$$

We see that asymptotically ($n \to \infty$), the number of operations grows like 3^n instead of the $\sim n!$ growth using Feynman graphs. Alternatively the increase in computational cost each time one adds one more external leg is

$$\frac{O(n+1)}{O(n)} = \frac{3^{n+1} - 6 \cdot 2^n - 3}{3^n - 3 \cdot 2^n - 3} \qquad (6.29)$$

which goes to 3 as $n \to \infty$. For the four-point vertex we have

$$\sum_{k=0}^{n} \left(\begin{array}{c} n \\ k \end{array} \right) \sum_{l_1+l_2+l_3=k} \frac{k!}{l_1!\, l_2!\, l_3!} = 4^n - 4 \cdot 3^n + 6 \cdot 2^n - 4 \qquad (6.30)$$

This clearly shows the advantage of using three-vertices only. The reduction in cost using the recursion approach is due mainly to the fact that once a subamplitude is known it is not computed again, as opposed to using graphs.

6.2.3 Colour treatment

In order to have an estimate of the production probability, one has to sum over all colour and helicity configurations. Summation over colours is a delicate subject. If one performs the summation in a straightforward way then one has to consider something like $8^{n_g} \times 3^{n_q} \times 3^{n_{\bar{q}}}$ configurations for the n-parton scattering, where $n_g, n_q, n_{\bar{q}}$ is the number of gluons, quarks and antiquarks respectively. What's more, a large

number of these configurations are zero. In this section we show how this summation can be replaced by integration, which is then suitable for Monte Carlo computation.

A first step is to convert the discrete colour space of the partons to a continuous one. We do that by projecting the colour vectors to a complex continuous space, as was discussed in Chapter 4. We take a complex vector $z_i,\ i = 1, \ldots, N$, where N denotes the number of colours, normalized to unity, to denote the colour vector of a fermion. This complex space, together with a definition for the measure for this space:

$$[dz] \equiv d^N z\ d^N \bar{z}\ \delta\left(z_i \cdot \bar{z}_i - 1\right) \frac{\Gamma(N)}{(2\pi)^N} \tag{6.31}$$

provide all the information for the colour. The measure of course is defined so that

$$\int [dz] = 1 \tag{6.32}$$

For the case of QCD ($N = 3$) we can parametrize this space using polar coordinates to represent the complex vectors z_i:

$$z_1 = e^{i\phi_1} \cos\theta \tag{6.33}$$

$$z_2 = e^{i\phi_2} \sin\theta \cos\xi \tag{6.34}$$

$$z_3 = e^{i\phi_3} \sin\theta \sin\xi \tag{6.35}$$

$$0 \leq \phi_i \leq 2\pi \ \ ; \ \ 0 \leq \theta \leq \tfrac{\pi}{2} \ \ ; \ \ 0 \leq \xi \leq \tfrac{\pi}{2}$$

and in terms of these variables, the invariant measure becomes:

$$\frac{1}{\pi^3} \left(\prod_{i=1}^{3} \int_0^{2\pi} d\phi_i \right) \int_0^{\frac{\pi}{2}} d\theta \int_0^{\frac{\pi}{2}} d\xi \cos\theta \sin^3\theta \cos\xi \sin\xi \tag{6.36}$$

To describe the colour carried by a gluon we need a vector $\eta^a(z),\ a = 1, \ldots, N^2 - 1$. One way of constructing such a vector is to take it to be real and normalized as follows:

$$\int [dz] \eta^a(z) \eta^b(z) = \delta^{ab} \tag{6.37}$$

A choice that satisfies these conditions is (for the particular case of $N = 3$):

$$\eta^a(z) = \sqrt{24} \sum_{i,j=1}^{3} z_i^* (t^a)_{ij} z_j \qquad a = 1, \ldots, 8 \tag{6.38}$$

where t^a are the Gell-Mann matrices. This vector is real, because $(\eta^a)^* = \eta^a$ due to the hermiticity of the Gell-Mann matrices. Another choice, discussed in Section 4.2, would be a complex vector $\eta^a(z)$:

$$\eta^a(z) = 4 \sum_{i,j=1}^{3} \bar{y}_i (t^a)^i{}_j z^j \tag{6.39}$$

with the normalization

$$\int [dz] \eta^a(z) \bar{\eta}^b(z) = \delta^{ab} \tag{6.40}$$

A further simplification can be introduced, particularly for the gluon fields, by introducing the following object:

$$G_{AB} \equiv \sum_{a=1}^{8} t^a_{AB} G^a, \quad A, B = 1, 2, 3 \tag{6.41}$$

where G^a is the gluon field and all other indices have been temporarily supressed. The new objects are of course traceless, 3×3 matrices in colour space. The interesting property of this colour representation is that it leads to a "diagonalization" of the colour structure of the three-gluon vertex. More specifically the colour part of the three-gluon vertex is now given by

$$f^{abc} t^a_{AB} t^b_{CD} t^c_{EF} = -\frac{i}{4} (\delta_{AD}\, \delta_{CF}\, \delta_{EB} - \delta_{AF}\, \delta_{CB}\, \delta_{ED}) \tag{6.42}$$

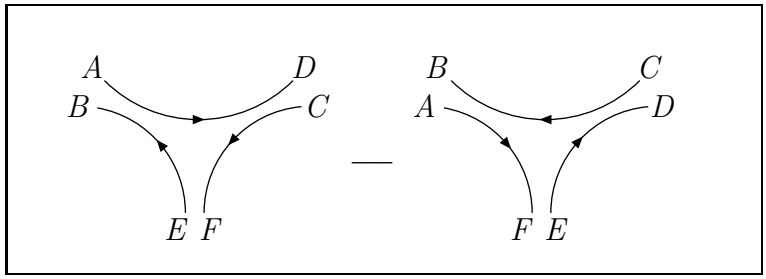

Colour flow in the gluon 3-vertex, as represented in Eq.(6.42).

This colour structure shows the colour flow in the real physical process, where gluons can be represented by quark-antiquark states in colour space and their self-interaction, as given by Eq.(6.42), reflects the fact that colour remains unchanged on an uninterrupted colour line. The recursion equations that include the gluon, like Eq.(6.13),

now are modified according to Eq.(6.41), to reflect the new colour structure. The full content of the recursion equations, including the colour structure as we just described it, is listed in the Appendix.

As far as our recursive equations are concerned their structure remains unaffected and the only thing to be changed are the initial conditions. For the real choice for the gluon colour vector we have :

$$\begin{aligned} G^{\mu}_{AB}(P_i) &= \sum_{a=1}^{8} G^a(P_i)\eta^a(z) = \sqrt{6}\left(z_{iA}z^*_{iB} - \frac{1}{3}\delta_{AB}\right)\epsilon^{\mu}_{\lambda}(P_i) \\ \psi_A(P_i) &= \sqrt{3}\; u(P_i)\; z_{iA} \\ \bar{\psi}_A(P_i) &= \sqrt{3}\; \bar{u}(P_i)\; z^*_{iA} \end{aligned} \tag{6.43}$$

where as usual $i = 1, \ldots, n$, λ is the helicity and $\vec{z}_i$ are the new continuous colour coordinates of the i-th parton. For the complex choice the initial conditions become a bit simpler:

$$\begin{aligned} G^{\mu}_{AB}(P_i) &= \sum_{a=1}^{8} G^a(P_i)\eta^a(z) = 2\; z_{iA}\; \bar{y}_{iB}\; \epsilon^{\mu}_{\lambda}(P_i) \\ \psi_A(P_i) &= \sqrt{3}\; u(P_i)\; z_{iA} \\ \bar{\psi}_A(P_i) &= \sqrt{3}\; \bar{u}(P_i)\; \bar{y}_{iA} \end{aligned} \tag{6.44}$$

6.2.4 Helicity treatment

In the same spirit summation over helicity configurations of the external partons can be replaced by an integration over a phase variable. For example, for a gluon this is achieved by introducing the polarization vector

$$\epsilon^{\mu}_{\phi}(p) = e^{i\phi}\epsilon^{\mu}(p,+) + e^{-i\phi}\epsilon^{\mu}(p,-) \tag{6.45}$$

where ϕ is a random number. Then by integrating over ϕ we obtain the sum over helicities,

$$\frac{1}{\pi}\int_0^{\pi} d\phi\, \epsilon^{\mu}_{\phi}(p)(\epsilon^{\nu}_{\phi}(p))^* = \sum_{\lambda=\pm} \epsilon^{\mu}(p,\lambda)(\epsilon^{\nu}(p,\lambda))^* \tag{6.46}$$

The same thing can be used for the helicity of quark or an anti-quark. For example, for the quark we have

$$u_{\phi}(p) = e^{i\phi}u_{+}(p) + e^{-i\phi}u_{-}(p) \tag{6.47}$$

and when integrated over ϕ it gives the sum over polarizations

$$\sum_{\lambda=\pm} u_\lambda(p)\bar{u}_\lambda(p) = \not{p} \tag{6.48}$$

and the same for an antiquark.

6.2.5 The Fermi sign function

Since we are dealing with fermions, we must find a way to incorporate Grassman variables in the code. This means that we must include a sign change when we interchange two identical fermions in a process. To this end we use the binary representation of the momentum labels of the external particles (e.g. $P_1 \to (0001), P_2 \to (0010), P_3 = P_1 + P_2 \to (0011)$, etc.) So the sign relative to the permutation of two momenta, $\sigma(P_m, P_l)$ is computed as an operation on the two binary strings representing those momenta, $\sigma(m,l)$. The function that performs that operation is defined as:

$$\sigma(m,l) = (-1)^{\chi(m,l)} \tag{6.49}$$

with

$$\chi\,(m,l) = \sum_{i=n}^{2} \hat{m}_i \left(\sum_{j=1}^{i-1} \hat{l}_j \right) \tag{6.50}$$

A hat over the binary string means that this particular bit is set to 0 if the corresponding external particle is a boson. As an illustration let us consider the process $u(P_1)u(P_2) \to u(P_4)u(P_8)$. At level 2 we write formally the subamplitudes

$$\begin{aligned} A^\mu(P_6) &\sim \bar{u}(P_4)\gamma^\mu u(P_2)\sigma_{4,2} \\ A^\mu(P_{10}) &\sim \bar{u}(P_8)\gamma^\mu u(P_2)\sigma_{8,2} \end{aligned}$$

We can calculate the signs using (6.50):

$$\begin{aligned} \chi(4,2) &= 0 \to \sigma_{4,2} = 1 \\ \chi(8,2) &= 0 \to \sigma_{8,2} = 1 \end{aligned}$$

At the next level we have:

$$\bar{\psi}(P_{14}) \sim \bar{u}(P_4)\not{A}_{10}\sigma_{4,10} + \bar{u}(P_8)\not{A}_6\sigma_{8,6}$$

For the sign we have:

$$\begin{aligned}\chi(4,10) &= (0100)\otimes(1010)=1\rightarrow\sigma_{4,10}=-1\\ \chi(8,6) &= (1000)\otimes(0110)=0\rightarrow\sigma_{8,6}=1\end{aligned}$$

where the $\otimes$ symbol denotes the operation of χ on the two binary strings. We see at this stage that we have a relative minus sign between the two subamplitudes, due to interchange of identical fermions, as it should be.

The χ function has some interesting properties. First of all it can be written in the convenient form (for the rest of the section we leave out the hat over the strings):

$$\chi\left(m,l\right)=\sum_{i,j=1}^{n}\Theta(j<i)m_{i}l_{j} \tag{6.51}$$

We can form the polynomials $\mu(x)=\sum_{i}^{n}m_{i}x^{i}$ and $\lambda(x)=\sum_{i}^{n}l_{i}x^{i}$ and use them to prove the following relation:

$$\left(\sum_{i}m_{i}\right)\left(\sum_{j}l_{j}\right)=\sum_{i}\left(m_{i}l_{i}\right)+\chi\left(m,l\right)+\chi\left(l,m\right) \tag{6.52}$$

Using (6.24), we see that the left hand is the product of the levels M,L of the binary strings m,l respectively:

$$\sum_{i}\left(m_{i}l_{i}\right)+\chi\left(m,l\right)+\chi\left(l,m\right)=ML \tag{6.53}$$

From this equation we can get a special property for two identical strings

$$\begin{aligned}&\sum_{i}\left(m_{i}m_{i}\right)+2\,\chi\left(m,m\right)=M^{2}\rightarrow M+2\,\chi\left(m,m\right)=M^{2}\\ &\rightarrow\chi\left(m,m\right)=\frac{M(M-1)}{2}=\left(\begin{array}{c}M\\2\end{array}\right)\end{aligned} \tag{6.54}$$

However the combination of the same two momenta in a sign function is an unphysical situation. For a binary string and its complementary we see that $\sum_{i}\left(m_{i}l_{i}\right)=0$ so that

$$\chi\left(m,\bar{m}\right)+\chi\left(\bar{m},m\right)=M(n-M) \tag{6.55}$$

6.3 Appendix: The complete recursion relations

Below we give the full recursion equations including the colour.

- Gluon field $A^\mu(p)$

$$\begin{aligned} A^\mu_{AB}(P) &= \frac{g_s}{2P^2}\sum_{P=p_1+p_2}\{\bar\psi_B(p_1)\gamma^\mu\psi_A(p_2)-\frac{1}{3}\left(\sum_C\bar\psi_C(p_1)\gamma^\mu\psi_C(p_2)\right)\delta_{AB}\} \\ &\quad\times\sigma(p_1,p_2) \\ &+ \frac{g_s}{2P^2}\sum_{P=p_1+p_2}V^{\mu\nu}_\lambda(P,p_1,p_2)\{A^\nu_{AC}(p_1)A^\lambda_{CB}(p_2)-A^\lambda_{AC}(p_2)A^\nu_{CB}(p_1)\} \\ &\quad\times\sigma(p_1,p_2) \\ &+ \frac{ig_s}{2P^2}\sum_{P=p_1+p_2}X^{\mu\nu}_{\lambda\rho}\{A^\nu_{AC}(p_1)H^{\lambda\rho}_{CB}(p_2)-H^{\lambda\rho}_{AC}(p_2)A^\nu_{CB}(p_1)\}\,\sigma(p_1,p_2) \end{aligned} \tag{6.56}$$

- Auxiliary field $H_{\mu\nu}(p)$

$$H^{\mu\nu}_{AB}(P)=\frac{(ig_s)}{4}\sum_{P=p_1+p_2}X^{\mu\nu}_{\lambda\rho}\{A^\lambda_{AC}(p_1)A^\rho_{CB}(p_2)-A^\rho_{AC}(P_2)A^\lambda_{CB}(p_1)\}\,\sigma(p_1,p_2) \tag{6.57}$$

- Fermion field $\psi_A(p)$

$$\psi_A(P)=\frac{g_s}{P^2}\sum_{P=p_1+p_2}\not{P}\not{A}_{AB}(p_1)\;\psi_B(p_2)\;\sigma(p_1,p_2) \tag{6.58}$$

- Anti-fermion field $\bar\psi_A(p)$

$$\bar\psi_A(P)=\frac{g_s}{P^2}\sum_{P=p_1+p_2}\bar\psi_B(p_2)\not{A}_{BA}(p_1)\not{P}\;\sigma(p_1,p_2) \tag{6.59}$$

Sum over repeated indices is implied.

Chapter 7

Jets

7.1 Introduction

Jets have by now become a major component of high energy particle physics. It is widely accepted that jets are implied by perturbative QCD and that they are the simplest and perhaps the best evidence supporting it. This means that jets can be to found in all large p_T phenomena irrespective of whether they are initiated by hadronic or leptonic processes. Large p_T events proceed via hard scattering involving the collision of one constituent from each initial hadron. The partons involved scatter through large p_T and later 'materialize' as a set of fairly well collimated hadrons called a jet. This is the natural outcome of the parton model.

7.2 Jet kinematics

As described before, the scattering of two hadrons produces two beams of incoming partons. The parton distribution functions provide a spectrum of longitudinal momenta. At the level of scattering between partons, usually one boosts the CoM frame with respect to that of the incoming hadrons. therefore it is useful to use variables for the characterization of jets that transform simply under longitudinal boosts. One such variable is the transverse momentum. For a *massless* particle the four-momentum can be written in terms of p_T:

$$p^\mu = (p_T \cosh y, p_T \sin\phi, p_T \cos\phi, p_T \sinh y) \tag{7.1}$$

where $p_T = \sqrt{p_x^2 + p_y^2}$ is the transverse momentum, y is the rapidity

$$y = \frac{1}{2} \ln \left(\frac{E + p_z}{E - p_z} \right) \tag{7.2}$$

and ϕ is the azimuthal angle. Rapidity deifferences are boost invariant. For massless particles the rapidity coincides with the pseudorapidity variable η

$$\eta = -\ln \tan (\theta/2) \tag{7.3}$$

where θ is the angle from the beam.

Many methods can be used to define what is meant by a jet of hadrons. One of the most commonly used is the cone algorithm: a jet is a concentration of transverse energy E_T in a 'cone' of radius ΔR, where

$$\Delta R = \sqrt{\Delta\Phi^2 + \Delta\eta^2} \tag{7.4}$$

and $\Delta\Phi_{ij} = \arccos \left(\frac{p_{xi}\, p_{xj} + p_{yi}\, p_{yj}}{p_{Ti}\, p_{Tj}} \right)$ is the azimuthal angle. By defining ΔR in terms of η we obtain a jet measure invariant under longitudinal boosts.

7.3 Hadron scattering

Let us now consider the scattering of two hadrons. As was already mentioned the content of a hadron is characterized by the parton structure function $f(x, Q^2)$ where x is the fraction of the momentum P of the hadron, carried by the parton, $p = xP$, and Q^2 is the QCD scale. The scale is considered to be large enough, so partons within the same hadron do not interact with each other. The cross section for the scattering of two hadrons is given by the sum of all subprocesses between the parton constituents of the hadrons, weighted with the corresponding structure functions of the incoming partons:

$$\sigma(s) = \sum_{ij} \int_0^1 dx_1 dx_2 \int d\Phi\; F_i(x_1)\; F_j(x_2) \int d\hat{s}\; \delta(\hat{s} - x_1 x_2 s)\; \Theta(s_0 < \hat{s} < s) \left(\frac{d\hat{\sigma}(\hat{s})}{d\Phi} \right)_{ij} \tag{7.5}$$

where s is the centre of mass(CoM) energy squared at the hadron level and $\hat{s}$ is the available energy squared at the parton level. We have also introduced a low energy cut-off to $\hat{s}$, denoted s_0. The functions $F_m(x)$ are defined as $F_m(x) = f_m(x)/x$, where

$f_m(x)$ are the various parton structure functions. The $\left(\frac{d\hat{\sigma}(\hat{s})}{d\Phi}\right)_{ij}$ is the matrix element squared, summed over helicity and colour degrees of freedom, and $d\Phi$ is the element of the phase space. The sum is over all partonic processes. We make a change of variables from (x_1, x_2) to (τ, ξ) where $\tau = \hat{s}/s$, as follows:

$$\begin{aligned} x_1 &= \tau^{\xi} \\ x_2 &= \tau^{1-\xi} \end{aligned} \tag{7.6}$$

The Jacobian of the transformation is $J(x_1, x_2; \tau, \xi) = \ln(\frac{1}{\tau})$ and Eq.(7.5) now becomes:

$$\sum_{ij} \int_0^1 d\tau \int_0^1 d\xi \frac{f_i(\tau^{\xi})\ f_j(\tau^{1-\xi})}{\tau} \ln(\frac{1}{\tau}) \int d\hat{s}\ \delta(\hat{s} - \tau s)\ \Theta(s_0 < \hat{s} < s)\ [\ \frac{d\hat{\sigma}(\hat{s})}{d\Phi}]_{ij} \tag{7.7}$$

Integrating over $\hat{s}$ and writting $\mathcal{H}_{ij}(\tau, \xi) = f_i(\tau^{\xi})\ f_j(\tau^{1-\xi})$ we get:

$$\begin{aligned} \sigma(s) &= \sum_{ij} \int_0^1 d\tau \int_0^1 d\xi\ \frac{\mathcal{H}_{ij}(\tau, \xi)}{\tau}\ \ln(\frac{1}{\tau})\ \Theta(\tau_0 < \tau < 1)\ [\ \frac{d\hat{\sigma}(\tau s)}{d\Phi}]_{ij} \\ &= \sum_{ij} \int_{\tau_0}^1 d\tau \frac{\ln(\frac{1}{\tau})}{\tau} \int_0^1 d\xi\ \mathcal{H}_{ij}(\tau, \xi)\ [\ \frac{d\hat{\sigma}(\tau s)}{d\Phi}]_{ij} \end{aligned} \tag{7.8}$$

We use Eq.(7.8) to estimate jet production rates.

Putting the procedure described so far to work, we present in this section some results. We have computed cross sections for single flavour partonic processes. For comparison we have used a well established code for QCD calculations `NJETS` [Kuijf, 1991], [Berends et al., 1990], [F.A.Berends and H.Kuijf, 1991]. We denote quarks with the generic letters q, r, s. Each of these, can be any flavour since we consider all quarks massless. To avoid collinear or infrared singularities we have inposed the following cuts:

$$p_{T\,i} > 60\ GeV, \qquad \theta_{ij} > 30^o \qquad \eta < 3 \tag{7.9}$$

The CoM energy used is $\sqrt{s} = 14$ TeV. The running of the strong coupling constant is given by (2.25):

$$\alpha_s(Q^2) = \frac{12\pi}{23 \log(Q^2/\Lambda^2)}. \tag{7.10}$$

Process	OUR CODE (nb)	NJETS (nb)
$gg \to gggg$	6.973	7.019
$q\bar{q} \to gggg$	$5.454\ 10^{-3}$	$5.820\ 10^{-3}$
$qg \to qggg$	2.925	3.270
$gg \to q\bar{q}gg$	0.2836	0.2930
$q\bar{q} \to q\bar{q}gg$	0.1538	0.1586
$q\bar{q} \to r\bar{r}gg$	$1.454\ 10^{-3}$	$1.525\ 10^{-3}$
$qq \to qqgg$	0.2746	0.2543
$q\bar{r} \to q\bar{r}gg$	0.4026	0.4309
$qr \to qrgg$	0.4890	0.522
$qg \to q\bar{q}qg$	0.0839	0.0880
$qg \to r\bar{r}qg$	0.0860	0.0847
$gg \to q\bar{q}q\bar{q}$	$1.548\ 10^{-3}$	$1.588\ 10^{-3}$
$gg \to q\bar{q}r\bar{r}$	$3.034\ 10^{-3}$	$2.525\ 10^{-3}$
$q\bar{q} \to q\bar{q}q\bar{q}$	$1.986\ 10^{-3}$	$1.968\ 10^{-3}$
$q\bar{q} \to q\bar{q}r\bar{r}$	$2.001\ 10^{-3}$	$1.889\ 10^{-3}$
$q\bar{q} \to r\bar{r}r\bar{r}$	$2.188\ 10^{-5}$	$2.244\ 10^{-5}$
$q\bar{q} \to r\bar{r}s\bar{s}$	$4.160\ 10^{-5}$	$4.218\ 10^{-5}$
$qq \to qqq\bar{q}$	$3.481\ 10^{-3}$	$4.260\ 10^{-3}$
$qq \to qqr\bar{r}$	$3.583\ 10^{-3}$	$3.015\ 10^{-3}$
$qr \to qrq\bar{q}$	$6.473\ 10^{-3}$	$6.538\ 10^{-3}$
$qr \to qrr\bar{r}$	$6.291\ 10^{-3}$	–
$qr \to qrs\bar{s}$	$6.523\ 10^{-3}$	$6.116\ 10^{-3}$
$q\bar{r} \to q\bar{r}q\bar{q}$	$5.430\ 10^{-3}$	$5.439\ 10^{-3}$
$q\bar{r} \to q\bar{r}r\bar{r}$	$5.423\ 10^{-3}$	$5.250\ 10^{-3}$
$q\bar{r} \to q\bar{r}s\bar{s}$	$5.286\ 10^{-3}$	$5.096\ 10^{-3}$

Table 7.1: Cross sections for 4 parton production in (nb) and comparison with NJETS . The CoM energy is $\sqrt{s} = 14$ TeV. All results have an estimated error of 2%.

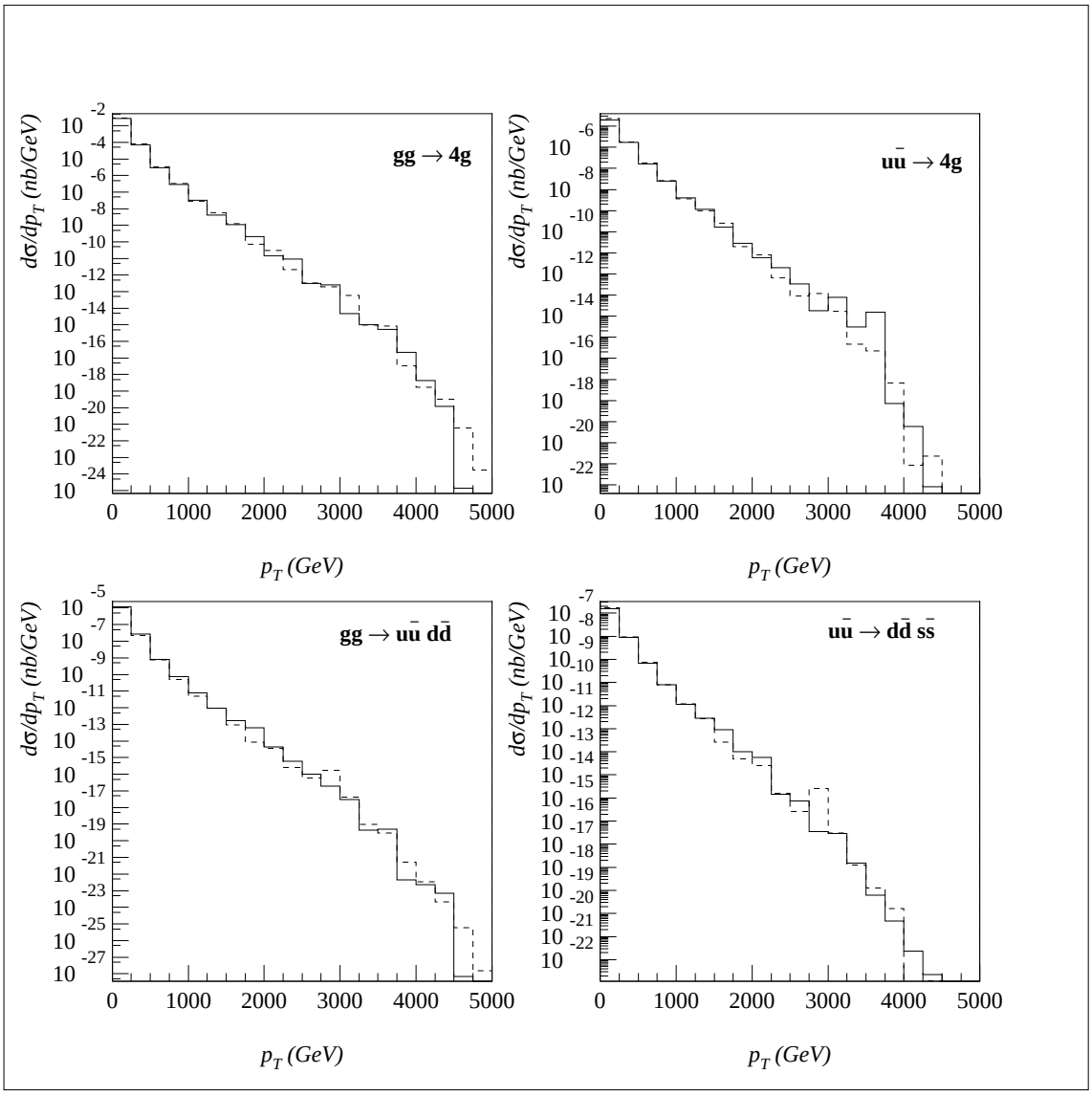

Figure 7.1: Tranverse momenta distributions for $0, 1, 2, 3$ fermion pairs. The solid line is the exact result and the dashed line is the `NJETS` result.

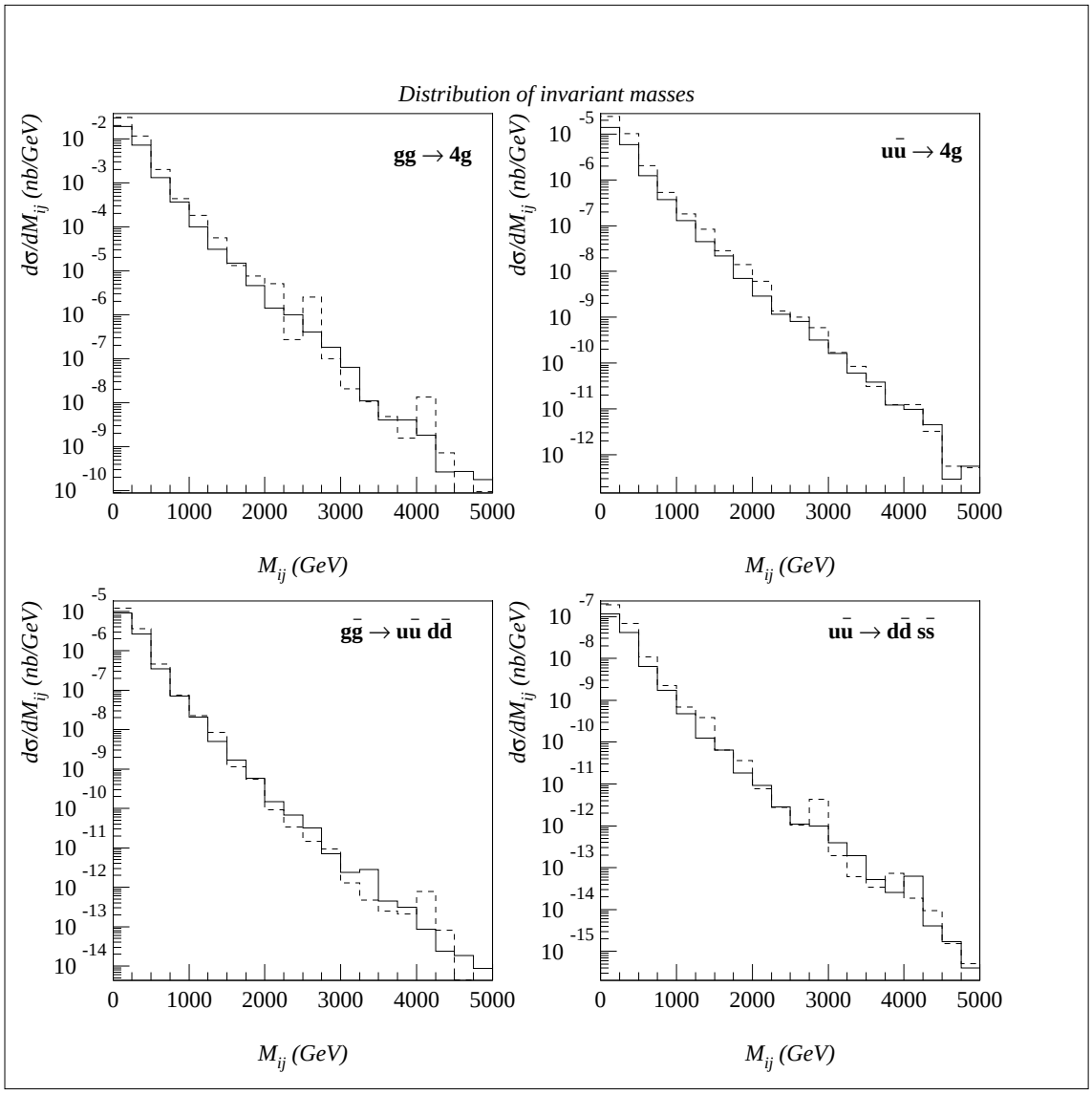

Figure 7.2: Invariant mass distributions for $0, 1, 2, 3$ fermion pairs. The solid line is the exact result and the dashed line is the `NJETS` result.

Process	OUR CODE (pb)	NJETS (pb)
$gg \to ggggg$	436.1	433.5
$q\bar{q} \to ggggg$	0.367	0.357
$qg \to qgggg$	213.2	208.1
$gg \to q\bar{q}ggg$	2.62	2.52
$q\bar{q} \to q\bar{q}ggg$	10.5	9.908
$q\bar{q} \to r\bar{r}ggg$	0.0934	0.0939
$qq \to qqggg$	25.0	22.89
$q\bar{r} \to q\bar{r}ggg$	10.5	12.07
$qr \to qrggg$	38.01	35.1
$qg \to q\bar{q}qgg$	9.251	8.956
$qg \to r\bar{r}qgg$	9.616	8.917
$gg \to q\bar{q}q\bar{q}g$	0.304	0.300
$gg \to q\bar{q}r\bar{r}g$	0.611	0.595
$q\bar{q} \to q\bar{q}q\bar{q}g$	0.307	0.292
$q\bar{q} \to q\bar{q}r\bar{r}g$	0.313	0.269
$q\bar{q} \to r\bar{r}r\bar{r}g$	$2.755\ 10^{-3}$	$2.742\ 10^{-3}$
$q\bar{q} \to r\bar{r}s\bar{s}g$	$5.398\ 10^{-3}$	$5.373\ 10^{-3}$
$qq \to qqq\bar{q}g$	0.737	0.709
$qq \to qqr\bar{r}g$	0.728	0.683
$qr \to qrq\bar{q}g$	1.466	1.404
$qr \to qrr\bar{r}g$	1.127	–
$qr \to qrs\bar{s}g$	1.108	0.925
$q\bar{r} \to q\bar{r}q\bar{q}g$	0.832	0.760
$q\bar{r} \to q\bar{r}r\bar{r}g$	0.790	0.774
$q\bar{r} \to q\bar{r}s\bar{s}g$	0.828	0.706
$qg \to q\bar{q}q\bar{q}q$	0.0437	0.0459
$qg \to q\bar{q}r\bar{r}q$	0.0873	0.0867
$qg \to r\bar{r}r\bar{r}q$	0.0444	0.0404
$qg \to r\bar{r}s\bar{s}q$	0.0914	0.0881

Table 7.2: Cross sections for 5 parton production in (nb) and comparison with NJETS . The CoM energy is $\sqrt{s} = 14$ TeV. All results have an estimated error of 2%.

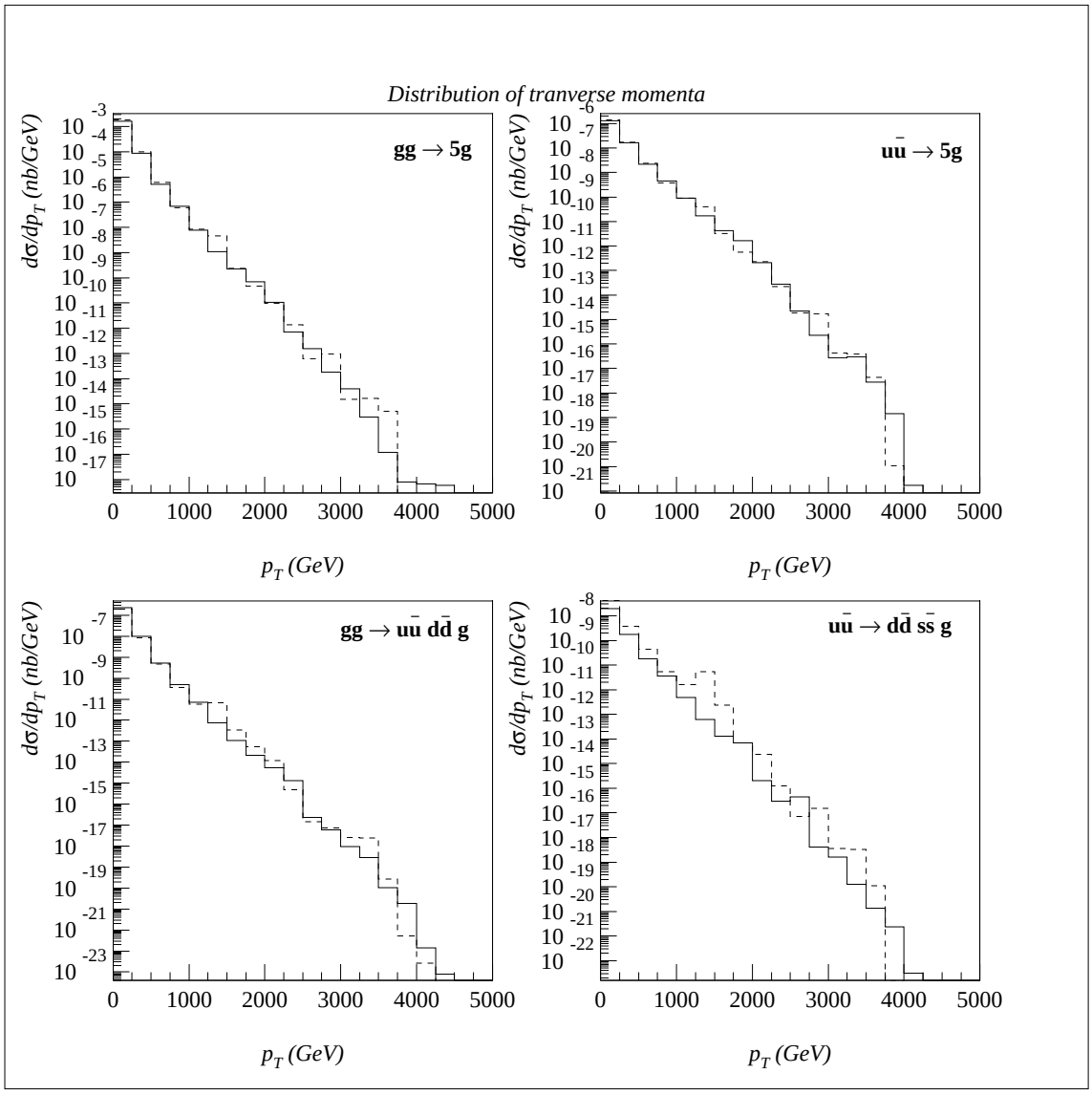

Figure 7.3: Tranverse momenta distributions for $0, 1, 2, 3$ fermion pairs. The solid line is the exact result and the dashed line is the `NJETS` result.

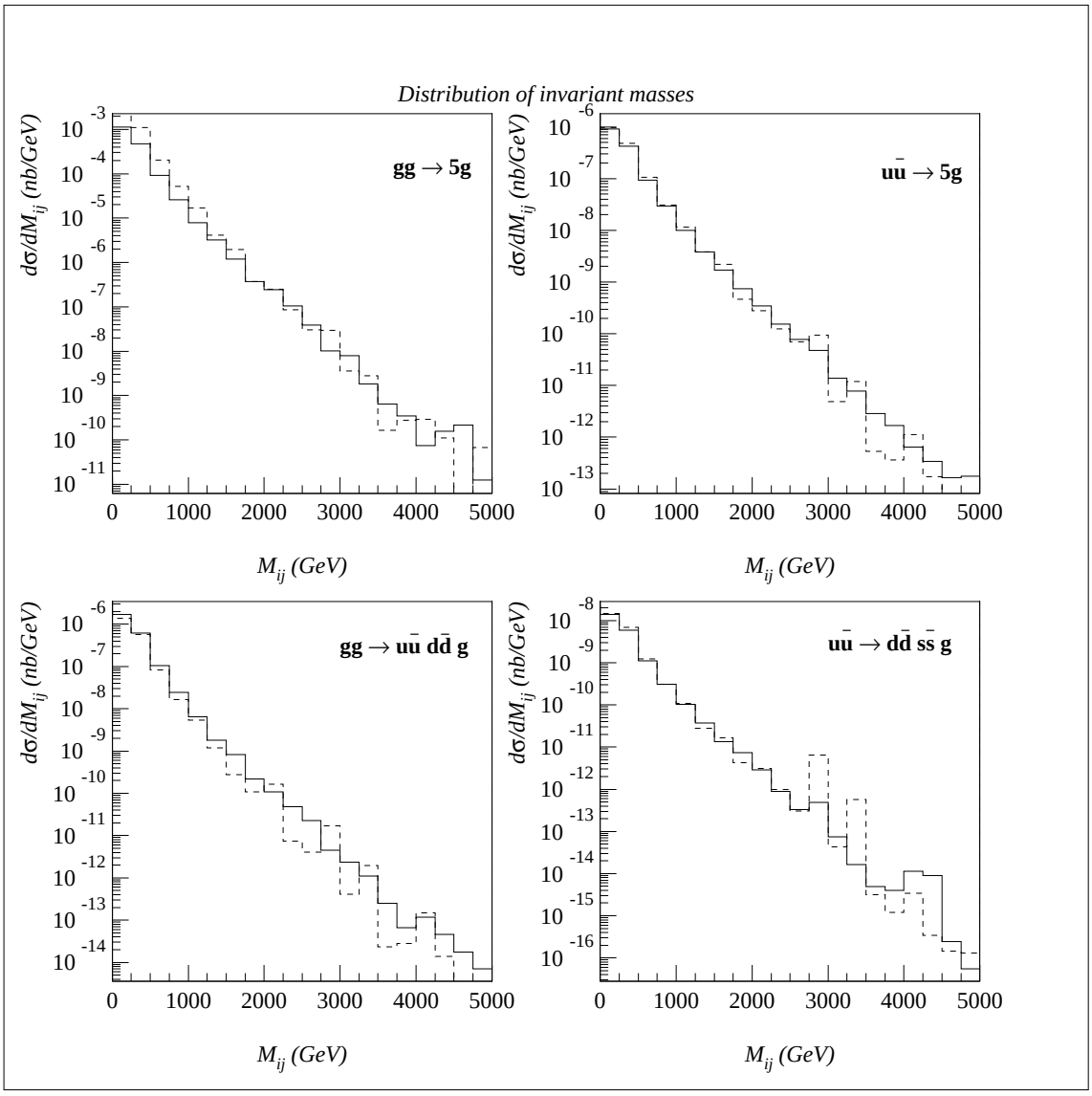

Figure 7.4: Invariant mass distributions for $0, 1, 2, 3$ fermion pairs. The solid line is the exact result and the dashed line is the `NJETS` result.

In this formula we have included 5 quark flavours and we fix the QCD scale Λ, the boundary between perturbative and non-perturbative regions, to be at $\Lambda = 0.230$ MeV. The energy Q^2 is the energy available at the partonic level, that is τs. As far as the distribution functions are concerned, there are several parametrizations in the literature. The one we use is the MRST parametrization [Martin et al., 2000]. In Table 7.1 we present cross sections for the production of 4 partons and the corresponding `NJETS` results. In Fig. 7.1, 7.2 we have plotted p_T and invariant mass distributions for processes with four final partons and $0, 1, 2$ and 3 fermion pairs with the corresponding `NJETS` curves. We also present results on five parton production in Table 7.2, with the same CoM energy and the same cuts. Some plots of distributions are shown in Figs. 7.3, 7.4.

7.4 Flavor treatment

The classification of processes contributing to the production of n jets is simplified when certain symmetries are taken into account. For instance processes like $gg \to u\bar{u}u\bar{u}$ and $gg \to d\bar{d}d\bar{d}$ can be grouped together in the general class with representative $gg \to q\bar{q}q\bar{q}$; obviously an extra factor f, representing the number of light flavours, has to be taken into account. We may call the representative 'a distinct processes' and attempt a complete classification of such processes. Is clear that the number of distinct processes for a given number n of jets will be a small fraction of the total number of processes; this has a major implication on the computational complexity of the problem, since we may have the total contribution by just computing the contribution of a relatively small number of distinct processes. In the following table we give the number of distinct processes, as defined in Appendix B, Chapter 3, for $f = 5$ final state flavours, and $f = 4$ initial state flavours, where we used these numbers in order to be able to compare with ref. [Kuijf, 1991].

# of jets	2	3	4	5	6	7	8	9	10
# of dist.processes	10	14	28	36	64	78	130	154	241
total # of processes	126	206	621	861	1862	2326	4342	5142	8641

Another way to tackle all these different processes is to introduce quarks (antiquarks) that are a mixture of different flavours. Thus, keeping with the spirit of colour and helicity treatment, we integrate over flavours instead of summing over them. This is done by attaching a vector $\vec{f}$ to each spinor describing a fermion, the components of which are random numbers between 0 and 1:

$$\psi_p = u(p) \times \vec{f}$$

with

$$\vec{f} = \begin{pmatrix} f_1 \\ f_2 \\ f_3 \\ \vdots \\ f_{N_f} \end{pmatrix}$$

where $f_1, f_2, \ldots, f_{N_f}$ are random numbers and N_f is the number of flavours. We choose the vectors $\vec{f}$ in such a way so that they are normalized as follows:

$$\langle f_i f_j \rangle = \delta_{ij}$$

where $i, j = 1, \ldots, N_f$. As far as the final state is concerned, all flavours are equally treated (massless quarks). In the initial state however, due to different structure functions, special care should be taken of different flavours by a suitable weighting of the initial conditions with the structure function appropriate for each flavour.

In Table 7.3 we have collected some results and we compare flavour integration with flavour summation. We list cross sections for various process with a four parton final state. We have also quoted the `NJETS` result. We denote a unidentified quark flavour with the letter $q, \bar{q}$ (it can be anything from $u, d, s, \ldots, \bar{u}, \bar{d}, \ldots$, etc.). A generic process like $q\bar{q} \to q\bar{q}gg$ includes all permutations of quark flavours that give a non-zero cross section (these include $u\bar{u} \to u\bar{u}gg$, $u\bar{u} \to d\bar{d}gg$, $u\bar{d} \to u\bar{d}gg$, $d\bar{d} \to s\bar{s}gg$, etc.) We have included 5 flavours in the calculations.

Process	`F.I.` (nb)	`F.S.` (nb)	`NJETS` (nb)
$q\bar{q} \to q\bar{q}gg$	0.284	0.281	0.297
$q\bar{q} \to q\bar{q}q\bar{q}$	0.0189	0.0185	0.0179
$qq \to qqgg$	0.752	0.763	0.776
$gg \to q\bar{q}q\bar{q}$	0.0391	0.0380	0.0396
$qg \to q\bar{q}qg$	0.435	0.428	0.427

Table 7.3: Cross sections in nbarn for 4 parton production with flavour integration. `F.I.` is the flavour integration result, using the technique described in the previous chapter and `F.S.` is the summation of flavours result. The CoM energy is $\sqrt{s} = 14$ TeV and the estimated error is at 2%

In Table 7.4 we have listed cross sections for a five parton final state.

Process	F.I. (pb)	F.S. (pb)	NJETS (pb)
$q\bar{q} \to q\bar{q}ggg$	25.36	21.37	22.35
$qq \to qqggg$	64.82	63.01	57.99
$gg \to q\bar{q}q\bar{q}g$	7.43	7.63	7.45
$qg \to q\bar{q}qgg$	46.99	47.71	44.62
$qg \to q\bar{q}q\bar{q}q$	1.124	1.119	1.083

Table 7.4: Same as in Table 7.3 for 5 parton production. Cross sections in pbarn

7.5 Jet production rates

The features discussed in the previous sections have been implemented in a FORTRAN code with which we are able to perform pertubative calculations in QCD. We can divide the structure of the calculation leading to jet production rates in four parts: event generation, phase-space generation, squared amplitude computation and sum over processes calculation. In somewhat more detail these parts consist of:

Amplitude computation The basic structure of the algorithm for the amplitude was discussed in section 6.2. In order to obtain squared amplitudes we use projection to a continuous colour space and colour MC integration and integration over helicity states.

Phase space generation In the current status of the code we have implemented two ways of phase-space generation. First of all we have RAMBO [Stirling et al., 1986], a flat phase space generator which has been around for many years and has proved reliable for the relevant calculations. Recently though, a new generator has been developed, SARGE [van Hameren and Kleiss, 2000b], which take into account the so called antenna structure of QCD amplitudes. So far it has been proved very efficient for the generation of this type of phase-space [van Hameren et al., 2000] and it is also part of this code.

Sum over processes In treating flavour as described so far a new 'definition' of the concept of distinct process emerges. Any process is now composed by three primary objects, namely g, q and $\bar{q}$, where $q(\bar{q})$ represents a coherent superposition of all flavour states. The possible initial states are nine, namely $gg, gq, g\bar{q}, qg, \bar{q}g, q\bar{q}, \bar{q}q, qq, \bar{q}\bar{q}$ and a final state will be determined by fixing the number m of $q\bar{q}$ pairs. Obviously

m should satisfy, $2m \leq n - c_i$, with c_i counts the net quark (antiquark) content of the initial state, namely

$$c_{gg} = c_{q\bar{q}} = c_{\bar{q}q} = 0 \quad c_{gq} = c_{qg} = c_{\bar{q}g} = c_{g\bar{q}} = 1 \quad c_{qq} = c_{\bar{q}\bar{q}} = 2$$

So the number of 'distinct processes' is now given by

$$9k + 3 \text{ if } n = 2k \quad \text{and} \quad 9k + 7 \text{ if } n = 2k + 1 \tag{7.11}$$

which represents a further reduction compared with the number of distinct processes indicated in a previous table. Finally, once given the number of jets, we are able to compute all the relevant subprocesses that contribute at one go. This is done by randomly choosing a subprocess and then using Monte-Carlo to obtain the total cross section from all contributions. The random choice of a subprocess is based on the choice of a pair of integers (i, m), i selecting one out of the nine possible initial states, and m being the number of $q\bar{q}$ pairs in the final state, see Eq.(7.11).

There is also the option to use an optimization based on the fact that some processes overwhelm the total cross section over others (for example the purely gluonic process, $gg \to ng$ has the largest cross section by an order of magnitude, compared to processes with different initial or final states).

Using all these that we just described we are able to compute the total cross sections for any number of produced jets. In this case we have used a slightly different set of cuts. Those used for the tables and plots that follow are:

$$p_{T\,i} > 60\ GeV, \qquad \Delta R_{ij} > 0.5 \qquad \eta < 3 \tag{7.12}$$

The CoM energy and all other parameters remain as before. In Table 7.5 we show the cross sections for the production of up to 8 jets. Also shown in the table is the contribution of the purely gluonic process to the total cross section. We see that this contribution decreases with the number of jets. This is mainly because the number of processes -save the gluonic- becomes very large so the sum of all of them, eventually, overwhelms the cross section. We have also plotted distributions for the different number of jets. Specifically shown are:

- Transverse momenta p_T of the products and minimum/maximium p_T distributions
- Invariant masses M_{ij} and minimum/maximium M_{ij}.
- Cone of radius ΔR distributions with minimum and maximum ΔR plots.

# of jets	3	4	5
$\sigma(nb)$	296.79 ± 2.97	31.45 ± 0.61	3.41 ± 0.06
% Gluonic	45.9	39.0	32.9

# of jets	6	7	8
$\sigma(nb)$	0.373 ± 0.011	0.045 ± 0.002	$(4.61 \pm 0.56) \times 10^{-3}$
% Gluonic	30.4	27.2	21.3

Table 7.5: Total cross sections for the production of up to 8 jets. The last row shows the percentage contribution of the purely gluonic process ($gg \to ng$).

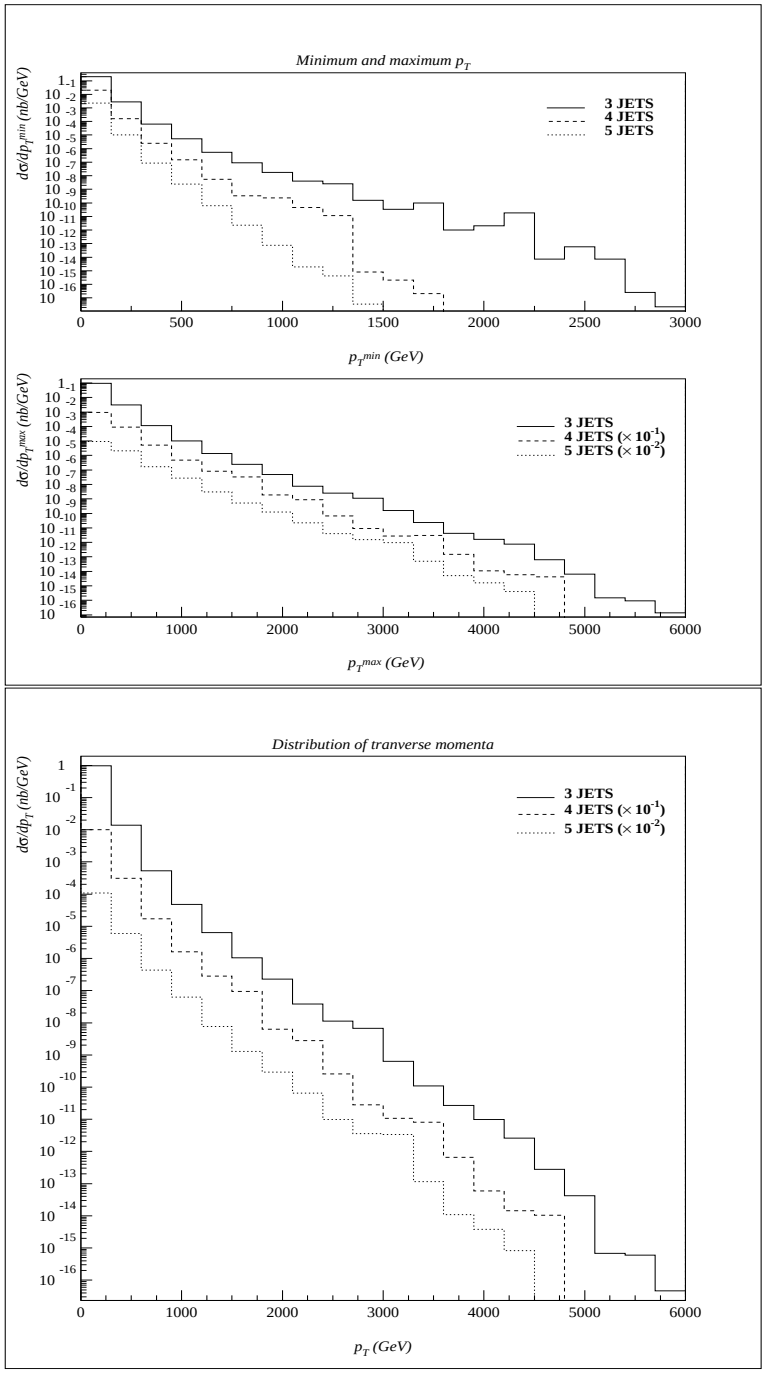

Figure 7.5: p_T distributions for 3,4 and 5 jet production

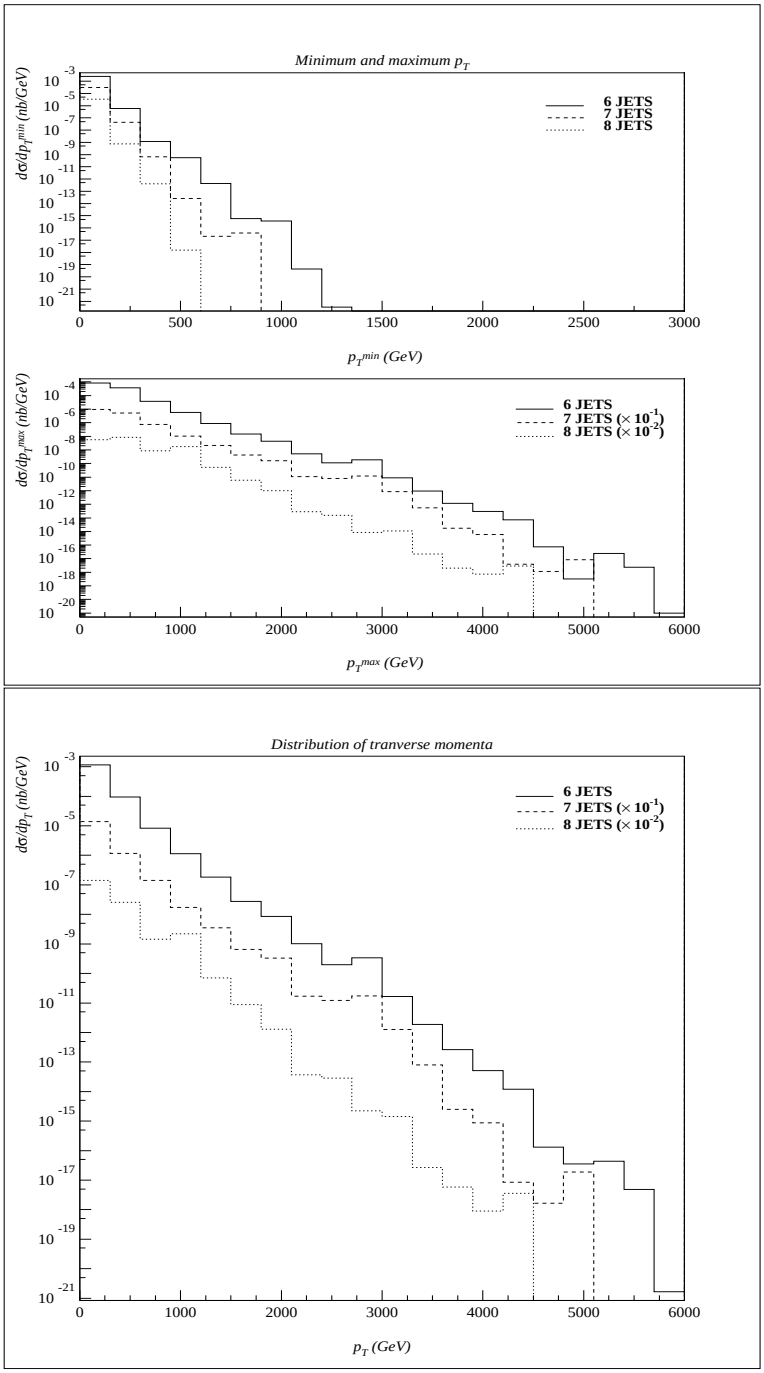

Figure 7.6: p_T distributions for 6,7 and 8 jet production

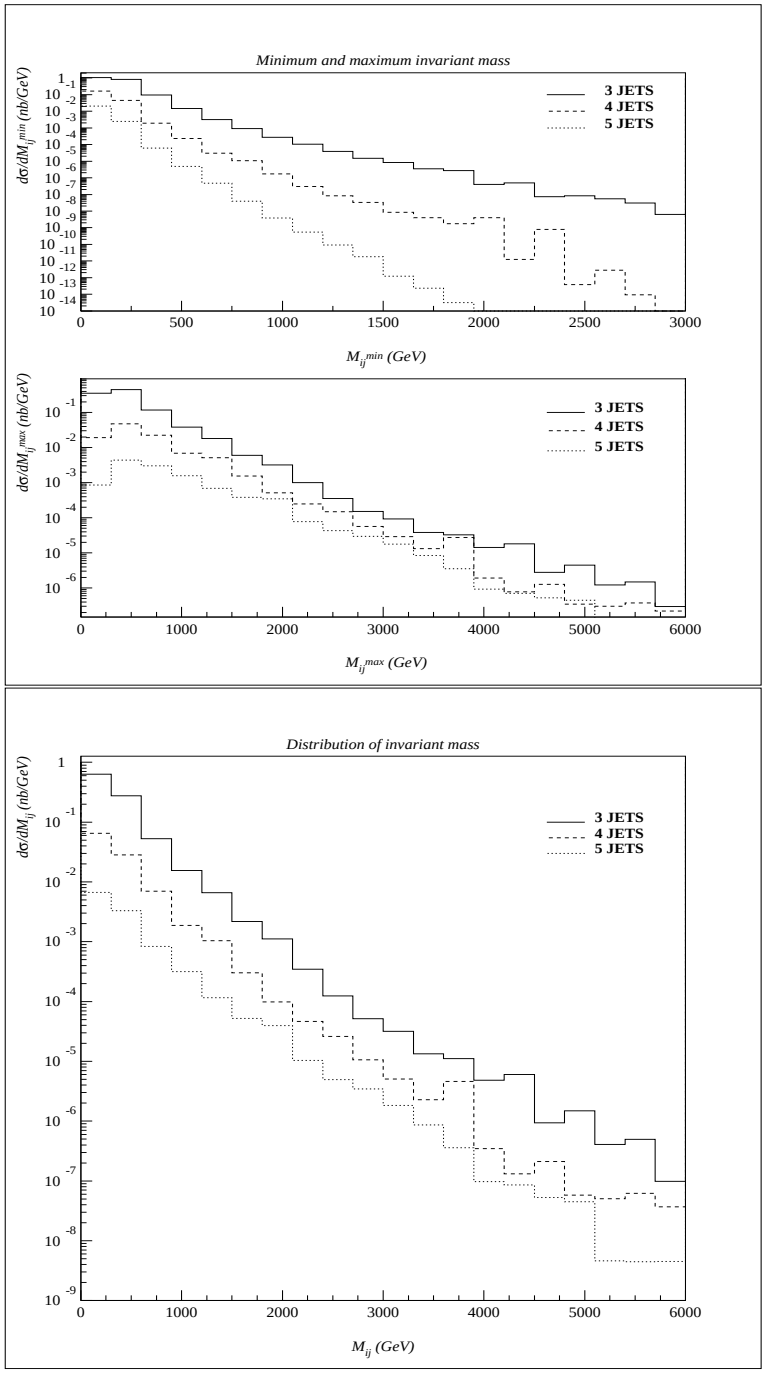

Figure 7.7: Invariant mass distributions for 3,4 and 5 jet production

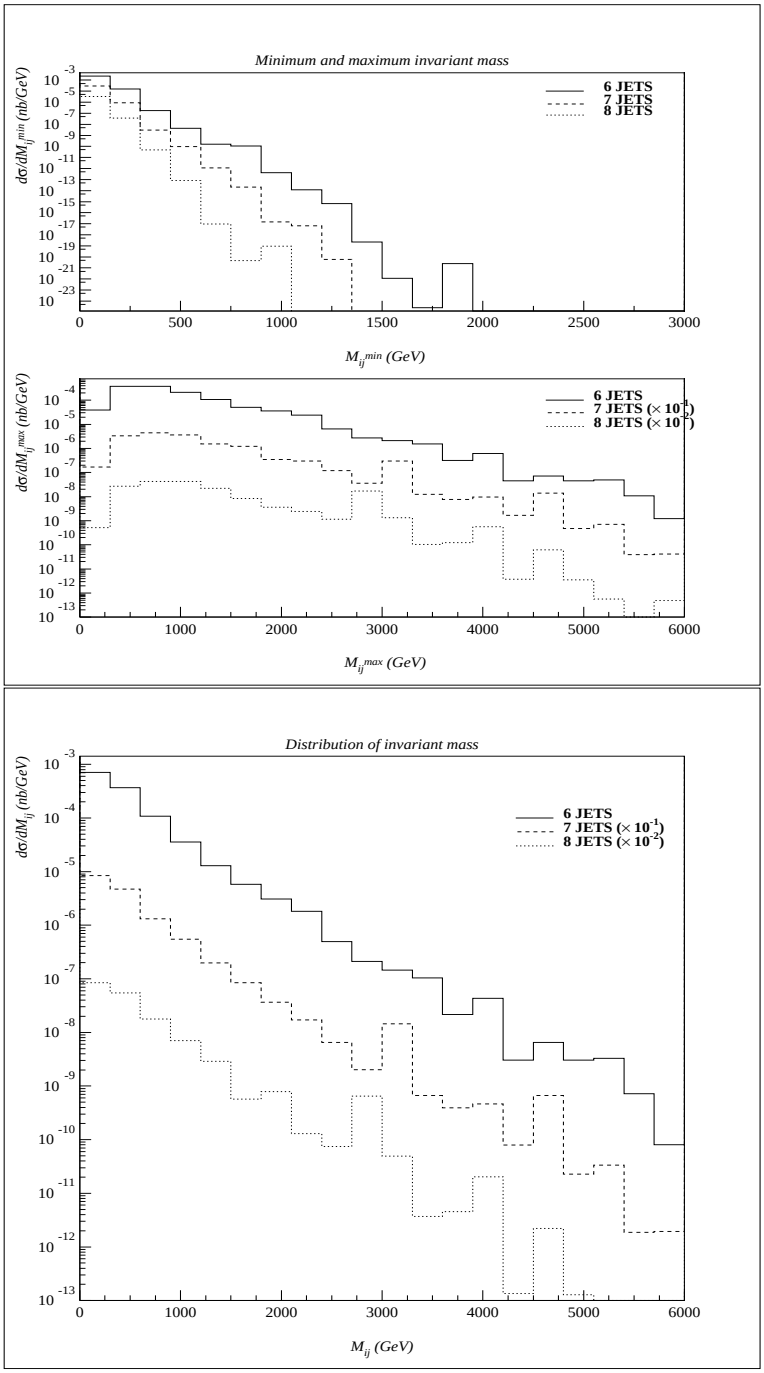

Figure 7.8: Invariant mass distributions for 6,7 and 8 jet production

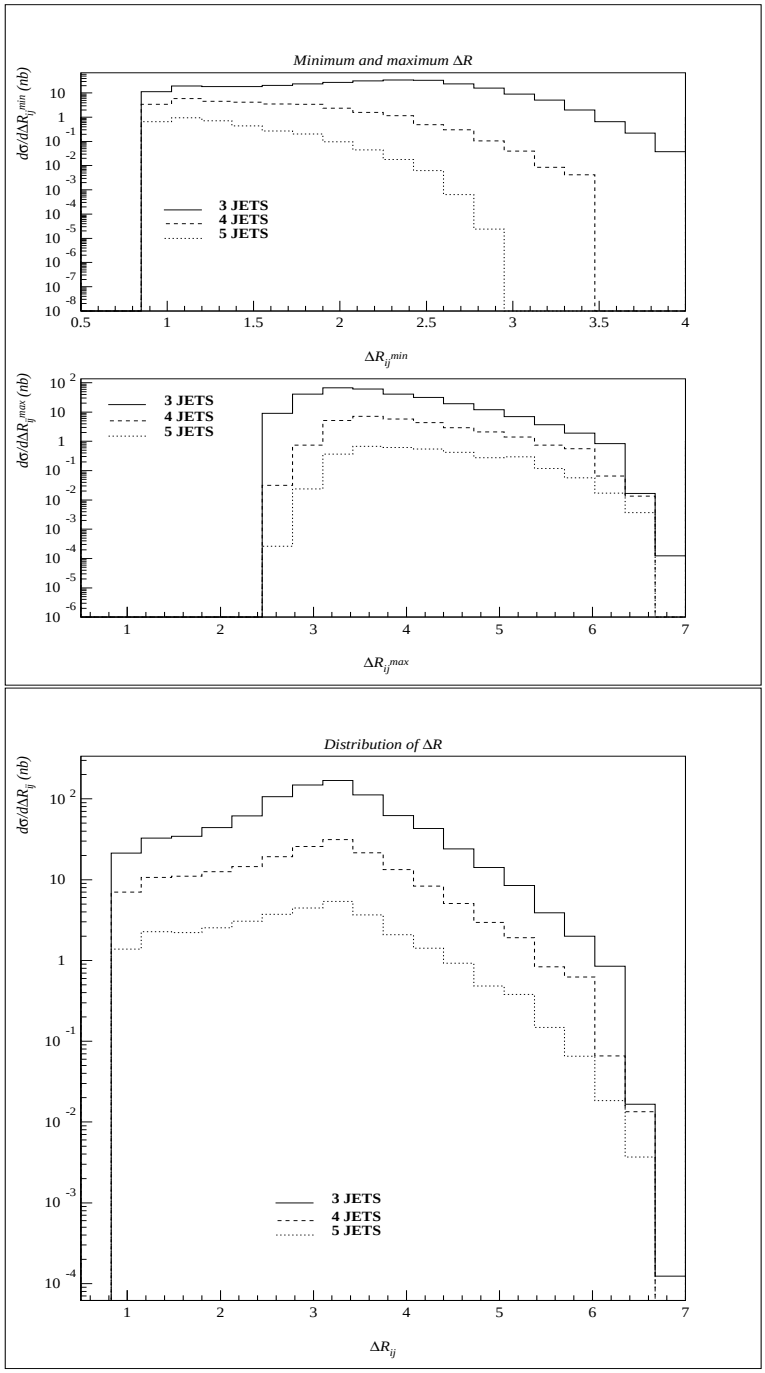

Figure 7.9: ΔR distributions (defined in the text) for 3,4 and 5 jet production

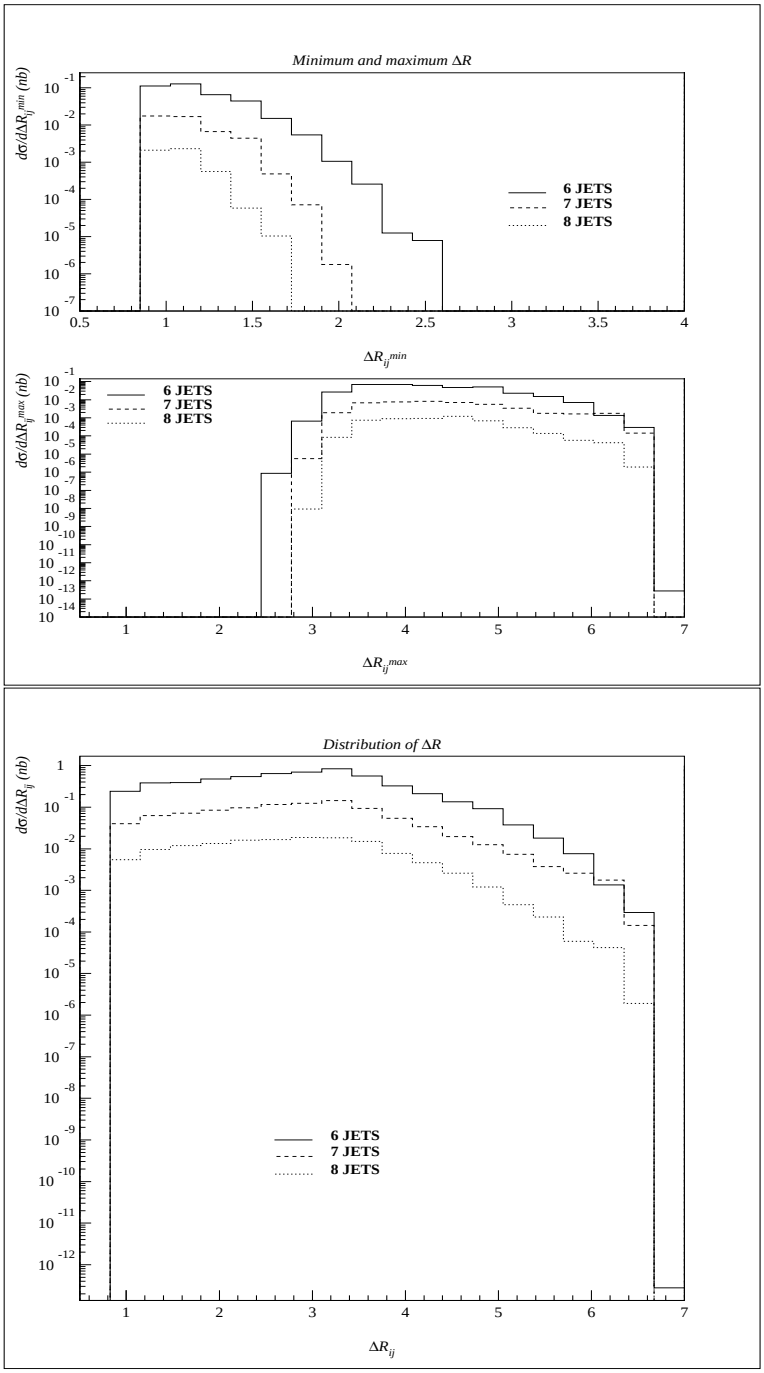

Figure 7.10: ΔR distributions (defined in the text) for 6,7 and 8 jet production

Bibliography

[Abramowitz and Stegun,] Abramowitz, M. and Stegun, I. *Handbook of Mathematical Functions*. Dover Publ., New York.

[Argyres et al., 1992] Argyres, E., Kleiss, R., and Papadopoulos, C. (1992). *CERN-TH.6496*, pages 1–14.

[Berends et al., 1990] Berends, F., Giele, W., and Kuijf, H. (1990). Exact and approximate expressions for multi-gluon scattering. *Nucl.Phys.*, B333:120.

[Caravaglios et al., 1999] Caravaglios, F., Mangano, M., Moretti, M., and Pittau, R. (1999). A new approach to multi-jet calculations in hadron collisions. *Nucl. Phys.*, B539:215–232.

[Caravaglios and Moretti, 1995] Caravaglios, F. and Moretti, M. (1995). An algorithm to compute Born scattering amplitudes without Feynman graphs. *Phys.Lett.*, B358:332–338.

[Corcella and et al., 2001] Corcella, G. and et al. (2001). HERWIG 6: an event generator for Hadron Emission Reactions With Interfering Gluons (including supersymmetric processes). *JHEP*, 0101:10.

[Draggiotis et al., 1998] Draggiotis, P., Kleiss, R., and Papadopoulos, C. (1998). On the computation of multigluon amplitudes. *Nucl. Phys.*, B439:157–164.

[Dyson, 1949] Dyson, F. (1949). *Phys. Rev.*, 75:1736.

[Ellis et al., 1996] Ellis, R., Stirling, W., and Webber, B. (1996). *QCD and Collider Physics*. Number 8 in Cambridge Monographs on Particle Physics, Nuclear Physics and Cosmology. Cambridge University Press.

[F.A.Berends and H.Kuijf, 1991] F.A.Berends and H.Kuijf (1991). Jets at the LHC. *Nucl.Phys.*, B353:59.

[Gianotti, 1999] Gianotti, F. (22 Aug.-4 Sep. 1999). Collider physics:LHC. In Olchevski, A., editor, *CERN 2000,Yellow Report*, volume 07. European School of High Energy Physics, Casta-Papiernicka, Slovak Rep.

[Giele, 1989] Giele, W. (1989). *Properties and calculations of multiparton processes*. PhD thesis, Leiden.

[Hardy and Wright, 1988] Hardy, G. and Wright, E. (1988). *An introduction to the theory of numbers*. Clarendon Press, Oxford.

[Kanaki and Papadopoulos, 2000] Kanaki, A. and Papadopoulos, C. (2000). HELAC: a package to compute electroweak helicity amplitudes. *Comput. Phys. Commun.*, 132:306–315.

[Kleiss, 2000] Kleiss, R. (20 Aug.-2 Sep. 2000). Field theory for the Standard Model. In Ellis, N; March-Russell, J., editor, *CERN 2000,Yellow Report*, volume 03. European School of High Energy Physics, Caramulo, Portugal.

[Kuijf, 1991] Kuijf, J. (1991). *Multiparton Production at Hadron Colliders*. PhD thesis, Leiden.

[Mangano, 1998] Mangano, M. L. (23 Aug.-5 Sep. 1998). Introduction to QCD. In Ellis, N; March-Russell, J., editor, *CERN 1999,Yellow Report*, volume 04. European School of High Energy Physics, St. Adrews, Scotland.

[Martin et al., 2000] Martin, A., Roberts, R., Stirling, W., and Thorne, R. (2000). Parton distributions and the lhc: W and z production. *Eur. Phys. J.*, C14:133–145.

[Schwinger, 1951] Schwinger, J. (1951). *Proc. Nat. Acad. Sci.*, 37:452.

[Stirling et al., 1986] Stirling, W., Kleiss, R., and Ellis, S. (1986). A new Monte Carlo treatment of multiparticle phase space at high energy. *Comp.Phys. Comm.*, 40:359.

[van Hameren, 2001] van Hameren, A. (2001). *Loaded dice in Monte-Carlo*. PhD thesis, Nijmegen.

[van Hameren and Kleiss, 2000a] van Hameren, A. and Kleiss, R. (2000a). A fast algorithm for generating a uniform distribution inside a high-dimensional polytope. *Comput.Phys.Commun.*, 133:1–5.

[van Hameren and Kleiss, 2000b] van Hameren, A. and Kleiss, R. (2000b). Generating QCD antennas. *Eur. Phys. J.*, C17:611–621.

[van Hameren et al., 2000] van Hameren, A., Kleiss, R., and Draggiotis, P. (2000). `SARGE`: An algorithm for generating QCD antennas. *Phys. Lett.*, B483:124–130.

[Voloshin, 1992] Voloshin, M. (1992). Multiparticle amplitudes at zero energy and momentum in scalar theory. *Nucl. Phys.*, B383:233.

List of publications

1. Petros D. Draggiotis, Ronald P. Kleiss, Costas G. Papadopoulos, *On the computation of multigluon amplitudes*, Phys. Lett. B439, 157-164, (1998) (hep-ph/9807207)

2. Petros D. Draggiotis, Andre van Hameren, Ronald P. Kleiss, *SARGE: An algorithm for generating QCD antennas*, Phys. Lett. B483, 124-130, (2000) (hep-ph/0004047)

3. Petros D. Draggiotis, Ronald P. Kleiss, *Parton counting: Physical and computational complexity of multijet production at hadron colliders*, Eur. Phys. J. C17, 437-445, (2000) (hep-ph/0006133)

4. Petros D. Draggiotis, Ronald P. Kleiss, Costas G. Papadopoulos, *Multiparton processes in QCD*, Published in 'Tampere 1999, High energy physics' 357-358 (1999)

5. Petros D. Draggiotis, Ronald P. Kleiss, *Counting tree diagrams: asymptotic results for QCD-like theories*, Eur. Phys. J. C23, 701-706, (2002) (hep-ph/0110225)

6. Chris Dams, Ronald P. Kleiss, Petros D. Draggiotis, Ernestos N. Argyres, Andre van Hameren, Costas G. Papadopoulos, *Recursive actions for scalar theories*, to appear in Eur. Phys. J. (2002) (hep-ph/0112258)

7. Petros D. Draggiotis, Ronald P. Kleiss, Costas G. Papadopoulos, *Multijet production in hadron collisions*, to appear in Eur. Phys. J. (2002) (hep-ph/0202201)